



UNIVERSITÀ
DEGLI STUDI
FIRENZE

Dottorato di Ricerca in Scienze Biomediche

Ciclo XXVIII

**Voltage gated K⁺ channels (Kv) and integrin receptors in
Pancreatic ductal adenocarcinoma (PDAC)**

Settore Scientifico Disciplinare: MED/04

Tutor
Prof.ssa ANNAROSA ARCANGELI

Dottorando
Dr. SAGAR SHASHIDHAR MANOLI

Coordinatore: Prof. Persio Dello Sbarba

Anni 2012/2015

This work is dedicated
TO MY BELOVED PARENTS

Acknowledgements

First and foremost I express my gratitude to my PhD supervisor and guide Professor Annarosa Arcangeli for giving me the opportunity to work in her laboratory. For all your guidance, discussions and encouragement to pursue my ideas and for being available whenever I needed, especially on weekends, I am immensely thankful to you.

During the three years of my work, I have worked in collaborations of with few people that has helped and contributed to my work and they rightly deserve to be acknowledged here. I am very fortunate to have worked closely with none other than my wife Nirmala K.R as a co-worker for 1.5 years of my PhD. She is been an immediate strength during the last 1.5 years and more so during the last stage of my work. Her constant support and patience with me both at work and home is something I am highly appreciative of. Dr Matteo Lulli has been extremely kind and available to me for all the innumerable number hours that he has spent for me for the confocal microscopy experiments. Thank you for your collaboration. I performed some part of my PhD work in Munster under the guidance of Professor Albrecht Schwab. Thank you for the opportunity and making me feel welcome in your laboratory. I would also like to thank Dr Stefano Coppola for the collaboration and contribution to the analysis of confocal and TIRF images.

I am thankful to all the present and past members of the group. Particularly, I am thankful to Dr. Olivia Crociani for helping me find my ways with the bureaucracy in the initial days of my stay and also teaching me some basic techniques in laboratory. Also, I am equally thankful to Dr. Serena Pillozzi and Dr Elena Lastraioli for always helping me with many things on day-to-day work. Dr Massimo D'Amico for all the patch-clamp experiments and hopefully I will one day learn from you. To all the past and present PhD students of the group, thank you very much for helping me in everything and I had a good time with you guys.

I would also like to express my gratitude to the European Marie Curie Initial Training Network for the fellowship during the three years. The funding helped me travel to attend many useful courses organized and establish a network among the fellows. I had a very good time with all the PhD fellows and I am thankful to all of them; especially Dr. Nikolaj Nielsen and Dr Otto Lindeman who also helped and made my stay at Munster a memorable.

Ultimately, my parents have been the greatest strength of my life and I am always blessed for all their love, guidance and teachings throughout my life. Like anything else in my life this PhD work is also dedicated to my beloved parents and my family members.

Abstract:

Most of the cancer cells and primary cancers show increased expression of various membrane proteins including ion channels, receptors like EGFR, integrin receptors etc. In this work we characterized the expression of potassium ion channels Kv11.1 (hERG1), EGFR and integrins in pancreatic ductal adenocarcinoma (PDAC). Firstly, our study shows that hERG1 specific blocking decreases the PDAC cell proliferation and anchorage independent colony formation. The study further demonstrates that blocking of hERG1 channels modulates the MAPK signaling pathway most likely mediated by EGFR receptors. In deed hERG1 makes complex formation with EGFR in both PDAC cell lines and primary samples. We then investigated the interactions between hERG1 and integrins. HERG1 and β 1 integrins complex formation requires both functional hERG1 channels and activated β 1 integrins. In other words, functional blocking of hERG1 channels or non-stimulated β 1 integrin or both would impair the complex formation between hERG1 and β 1. We further demonstrate, using model cell lines, that the interactions between hERG1 and β 1 could occur through transmembrane domains.

We further investigated the role of hERG1 channels in PDAC cell adhesion, migration and actin cytoskeleton organization. HERG1 specific blocking did not affect the integrin-mediated cell adhesion and focal adhesion formation on ECM proteins. However, when hERG1 was blocked we observed the alterations in filamentous actin organization mediated by β 1 integrins. HERG1 blocking specifically induced longer and finely organized f-actin in the cytoplasm, whereas over expression of hERG1 channels induced scattered shorter filaments. Next, we studied the role of hERG1 channels in cell migration and actin dynamics. For this purpose we challenged the role of hERG1 channels in multifactorial dynamic system that is similar to tumor microenvironment. PDAC cells were stimulated with conditioned media of hypoxia activated pancreatic stellate cells and, migration and actin dynamics were quantified. HERG1 blocking decreased the migration rate and interestingly, increased the actin flow (velocity). The increase in velocity was found to be due to increase in diffusion co-efficient of actin flow. Finally, we hypothesize that the hERG1 could mediate the actin dynamics and migration by altering the intracellular calcium concentration ($[Ca^{2+}]_i$). In fact hERG1 blocking decreased the $[Ca^{2+}]_i$ by more than two-fold.

CONTENTS

1. INTRODUCTION

1.1. Pancreatic Cancer and causes of pancreatic cancer	5
1.1.1. Pancreatic ductal adenocarcinoma (PDAC) and characteristics/progression of PDAC	6
1.1.2. PDAC tumor microenvironment (TME).....	9
1.1.2.1. Stromal fibroblasts-Pancreatic stellate cells (PSCs).....	10
1.1.2.2. Secreted proteins in TME	11
1.1.3. Immune/inflammatory cells.....	14
1.1.4. Ion channels and integrins in TME.....	15
1.2. Role of potassium ion channels in cellular physiology of cancer cells and cancer progression	16
1.2.1. Ion channels as biomarkers and prognostic markers in cancer	17
1.2.1.1. Ion channels as biomarkers in cancer diagnosis, prognosis and potential drug targets.....	17
1.2.1.2. Role of ion channels-mediated membrane potential in cell volume regulation, cell cycle progression/proliferation/migration.....	19
1.2.1.2.1. Ion channels in cell cycle progression	19
1.2.1.2.2. Ion channels in cell proliferation	21
1.2.1.2.3. Ion channels in cell Migration.....	22
1.2.2. Ion channels as potential therapeutic drug targets	24
1.3. Integrins structure, function, activation, signaling cascades in cancer	27
1.3.1. Integrins structure, function and activation.....	27
1.3.2. Outside-in signalling role of integrins	30
1.3.3. Integrins in cell adhesion signaling and migration	31
1.3.4. Integrins in cancer.....	35
1.3.4.1. Integrins expression: implications in pancreatic tumor progression	35
1.3.4.1.1. Beta (β) 1 integrins.....	35
1.3.4.1.2. AlphaVBeta3 (α V β 3) and alphaVbeta5 (α V β 5) integrins	36
2. AIMS OF THE THESIS.....	37

3. MATERIALS AND METHODS

3.1. <i>Cell lines</i>	39
3.1.1. Pancreatic ductal adenocarcinoma (PDAC)	39
3.1.2. Human pancreatic stellate cells.....	39
3.1.3. Model cell lines.....	39
3.2. <i>Materials</i>	39
3.2.1. Cell culture medium.....	39
3.2.2. Extracellular matrix (ECM) proteins	40
3.2.3. Antibodies.....	40
3.2.4. Drugs.....	42
3.2.5. Surface biotinylating agent	42
3.2.6. Buffer solutions	42
3.2.6.1. Phosphate buffered saline (PBS).....	42
3.2.6.2. Lysis buffer.....	42
3.2.6.3. Wash buffer.....	43
3.2.6.4. Running buffer (5X).....	43
3.2.6.5. Blotting buffer	43
3.2.6.6. Buffers in calcium measurement experiments	43
3.3. <i>Cell culture</i>	44
3.3.1. PDAC cells.....	44
3.3.2. Model cell lines-HEK293 and mouse fibroblast GD25	44
3.3.3. Human pancreatic stellate cells (hPSCs).....	44
3.3.4. Culture plate coating	45
3.4. <i>Transfection</i>	45
3.4.1. Transient transfection (plasmid DNA): DNA transfection	45
3.4.2. Stable transfection.....	45
3.5. <i>Cell proliferation assay</i>	46
3.6. <i>Soft agar colony formation assay</i>	46
3.7. <i>Cell adhesion assay</i>	46
3.8. <i>Cell migration assay</i>	47
3.8.1. Cell migration analysis.....	48

3.9. (Co)-Immunoprecipitation	49
3.9.1. Immunoprecipitation of surface biotinylation.....	50
3.10. Sodium dodecyl sulfate protein agarose gel electrophoresis (SDS-PAGE)	50
3.10.1. Western blot (WB).....	51
3.11. Fluorescence activated cell sorting (FACS) analysis	51
3.12. Immunofluorescence (IF)	52
3.13. Microscopy for image acquisition.....	52
3.13.1. Confocal microscopy and Image analysis using Fiji software.....	52
3.13.2. Image acquisition for actin dynamics study using Total internal reflection fluorescence (TIRF) microscope	53
3.14. Actin dynamics analysis using Spatio-temporal image correlation spectroscopy (STICS) method	53
3.15. Calcium measurement (by VisiView program)	54
3.16. Patch-clamp recording.....	54

4. RESULTS AND DISCUSSION

4.1. HERG1 channels are involved in PDAC cell proliferation and anchorage independent colony formation through MAPK/ERK signaling cascade	56
4.1.1. HERG1 channels are expressed differentially in PDAC cells	56
4.1.2. PDAC cell proliferation	57
4.1.3. PDAC soft agar colony formation	58
4.2. Characterization of surface expression of integrins in pancreatic ductal adenocarcinoma (PDAC) cell lines	60
4.3. HERG1 channels make macromolecular complex formation with EGFR and integrin subunits	63
4.3.1. The hERG1 intracellular domains are not necessary for hERG1/ β 1 interaction	68
4.3.2. The C-terminal (cytoplasmic) domain of β 1 integrin is not implicated in hERG1/ β 1 interaction	70
4.3.3. The hERG1/ β 1 complex assembly depends on the channel conformational state.	
71	

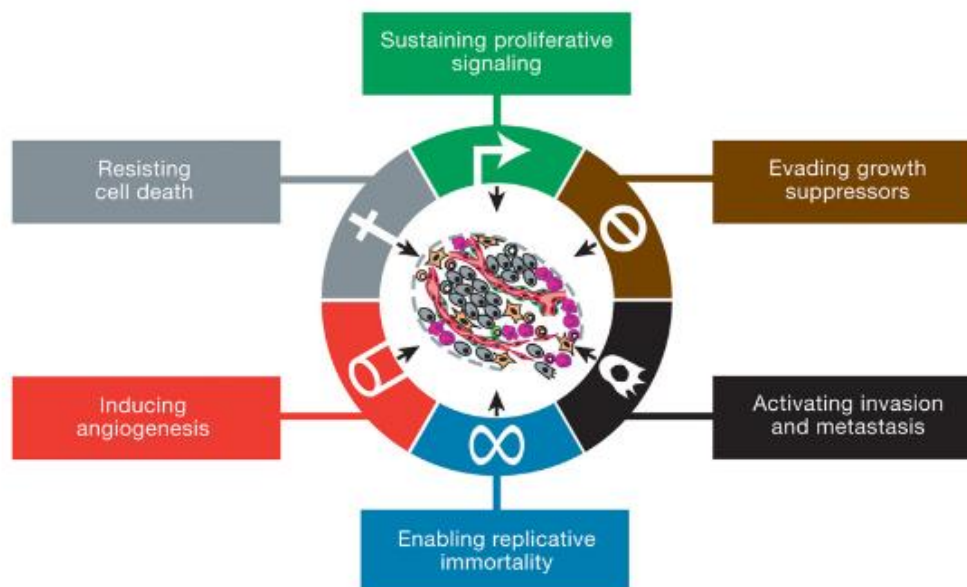
4.4. HERG1 channels are involved in integrin mediated PDAC cell migration and actin organization	74
4.4.1. HERG1 channels are involved in PDAC cell migration on basement membrane. 74	
4.4.2. HERG1 channels are not involved in cell adhesion on fibronectin.....	76
4.4.3. HERG1 channels make macromolecular complex formation with β 1 and FAK at the early stage of cell adhesion.	76
4.4.4. HERG1 channels are not involved in focal adhesions (FAs) and area of FAs of FAK and paxillin.	78
4.4.5. HERG1 channels are involved in altering actin cytoskeleton organization mediated by β 1 integrins	80
4.5. HERG1 channels in PDAC cell migration stimulated by activated PSC through actin dynamics and altered calcium concentration	86
4.5.1. Functional blocking of hHERG1 channels mitigate the PDAC cell migration through altered actin dynamics and decreased intracellular calcium concentration	86
4.5.2. HERG1 channel blocker E4031 decreases the Panc1 cells migration stimulated by hypoxia activated PSCs on desmoplastic matrix.	88
4.5.3. HERG1 channel blocker E4031 alters the actin dynamics of the migrating Panc1 cells stimulated by conditioned medium of hypoxically activated PSCs.	92
4.5.4. HERG1 channel blocker decreases the intracellular concentration of calcium and in Panc1 cells stimulated by PSC conditioned media.	94
5. CONCLUSION REMARKS.....	98
6. REFERENCES.....	104

1. INTRODUCTION

1.1. Pancreatic Cancer and causes of pancreatic cancer

Cancer, defined in the simplest form, is a disease stemmed from uncontrolled growth of cells. The history of cancer dates back to thousands of years. Greek physician Hippocrates, between 470-360 BC, coined the terms carcinos and carcinoma to describe non-ulcer and ulcer forming tumors. However, the documentation of cancer disease in humans and animals dates back further to around 3000 BC. Cancer (interchanged with the word tumor) is caused from wide array of factors like exposure to cancer causing agents (carcinogens), chronic infections (from for ex, hepatitis viruses, papilloma virus), life styles (eating, drinking, smoking habits, physical activities) and inherited genetic susceptibility to environment factors etc. (Ames and Gold, 1998).

From genetics point-of-view cancer is caused by accumulation of series of mutations either in oncogenes (tumor promoting) or tumor suppressor genes in normal cells over several years. This leads to severe alterations in both phenotypic as well as genotypic characteristics of transformed cells. During this transformation cells typically have to acquire certain set of capabilities that are ‘hallmarks of cancer’ to cause neoplastic disease. The seminal review paper by Hanahan and Weinberg categorizes the capabilities of diverse complex cancer tissue into six groups; sustaining proliferative signaling, evading growth suppressors, resisting cell death, enabling replicative immortality, inducing angiogenesis, and, activating invasion and metastasis (Hanahan and Weinberg, 2011).

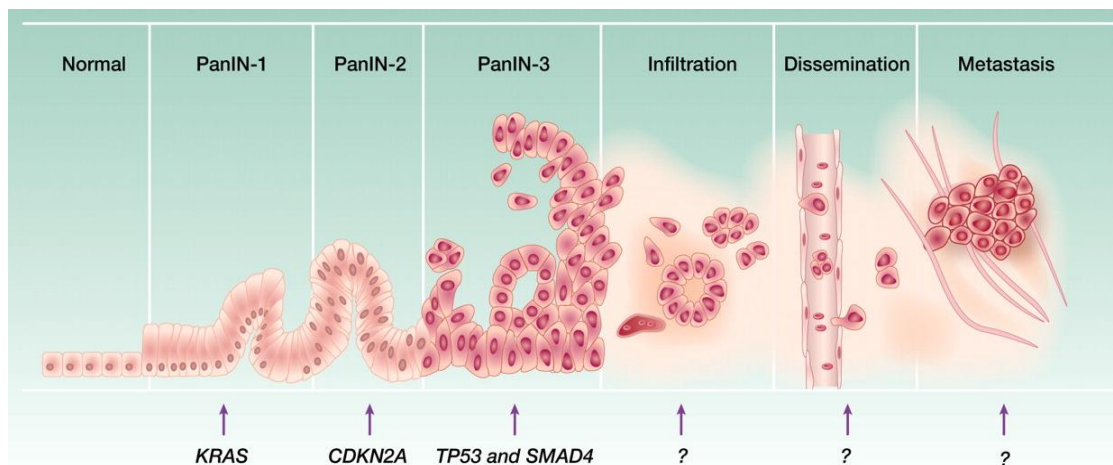


Scheme-1. Six hallmarks of cancer that is essential for the transformed cells to cause neoplastic disease (adapted from Hanahan and Weinberg, 2011).

1.1.1. Pancreatic ductal adenocarcinoma (PDAC) and characteristics/progression of PDAC

Tumors arising from the epithelium of exocrine pancreas are the most common type of pancreatic cancer that amount for over 95% of the pancreatic cancer. In this pancreatic adenocarcinoma (PDAC) is the most common type of exocrine pancreatic cancer that amount for more than 90% of the pancreatic cancer. Hence most of the time pancreatic cancer is generally referred to PDAC. PDAC is perhaps the most lethal form of cancer with five-year survival rate at dismal less than 5% and medial survival period is 6 months. PDAC arises from the ductal region of the pancreas and hence the term PDAC. Like any cancer the risk of acquiring PDAC is a multifactorial phenomenon; such as advanced age (>65), smoking (Fuchs et al., 1996), sex (male has 30% higher risk than female) and long standing chronic pancreatitis (Guerra et al., 2007) are the major risk factors followed obesity, diabetes and family history of PDAC patients (Hezel et al., 2006). These factors contribute to the series of accumulative genetic alterations such as point mutations, up regulation or down regulations of some key genes in normal ductal epithelial cells that

subsequently lead to transformed malignant cells as depicted in *scheme-2*. Studies show that this clonal evolution from non-invasive to invasive metastasized cells process takes around 10 years (Campbell et al., 2010; Yachida et al., 2010). This provides a window of opportunity for early detection and mapping of genetic changes that take place in transforming the ductal cells before they become invasive. Studies like whole genome sequencing and copy number variation (CNV) on PDAC patients have been performed to identify the key mutations in oncogenes, association of genomic instability with inactivation of DNA maintenance genes and mutational signatures in DNA damage repair deficiency (Waddell et al., 2015). There are, on average, as many as 63 gene alterations in PDAC but the four most commonly observed mutations include oncogene KRAS, and three tumor suppressor genes CDKN2A, TP53 and SMAD 54. PDAC patients possessing mutations in all four genes have lower survival rate compared to 1 or 2 mutations (Yachida et al., 2012). Studies reveal that twelve core signaling pathways including apoptosis, DNA damage control, KRAS, integrin signaling, adhesions etc are altered in more than two third of the cancer (Jones et al., 2008).



Scheme-2. Progression from normal pancreas to metastatic pancreatic cancer adapted from (Iacobuzio-Donahue et al., 2012).

1.1.1.1. Precursor lesions as indicators of future invasive PDAC

Pancreatic intraepithelial neoplasias (PanIN) are histologically distinct well-defined precursor lesions to invasive ductal adenocarcinoma that was first observed 40 years ago (Cubilla and Fitzgerald, 1976). PanIN lesions are characterized to be small and difficult to detect clinically and are commonly observed in elderly population. Genetic analyses of PanIN lesions demonstrate that almost 100% of even the lowest grade PanIN (PanIN-1) harbors some of the most prominent genetic alterations that are sustained till the cells become invasive (Kanda et al., 2012). For example telomere shortening and mutations in KRAS are among the earliest genetic alterations that occur since PanIN-1 (van Heek et al., 2002). These mutations are followed by mutations in tumor suppressors CDKN2A in mid-stage-PanIN-2 and, TP53 and SMAD4 in later stage-PanIN-3 (Iacobuzio-Donahue, 2012). This group of mutations, along with other, albeit less frequently occurring, mutations like BRCA1, MLL3 etc. may be considered to be initiating mutations that could drive the malignancy of cells. Hence the early detection of these genetic alterations and their downstream effects could represent an opportunity for probable cure of preinvasive neoplasia.

Intraductal Papillary Mucinous Neoplasms (IPMNs) are also precursor lesions to invasive PDAC and present a similar opportunity like PanIN towards early detection and curable neoplasia. IPMNs are large enough lesions that can be detected clinically and serves as an indication of pancreatic cancer. Studies show that >95% of IPMNs, particularly pancreatic cysts (fluid filled neoplasms in the pancreas) have shown to possess genetic mutations, for ex in KRAS and GNAS, that are associated with invasive PDAC (Wu et al., 2011). These evidences reinforce that IPMNs are bona fide precursor lesions progressing towards PDAC.

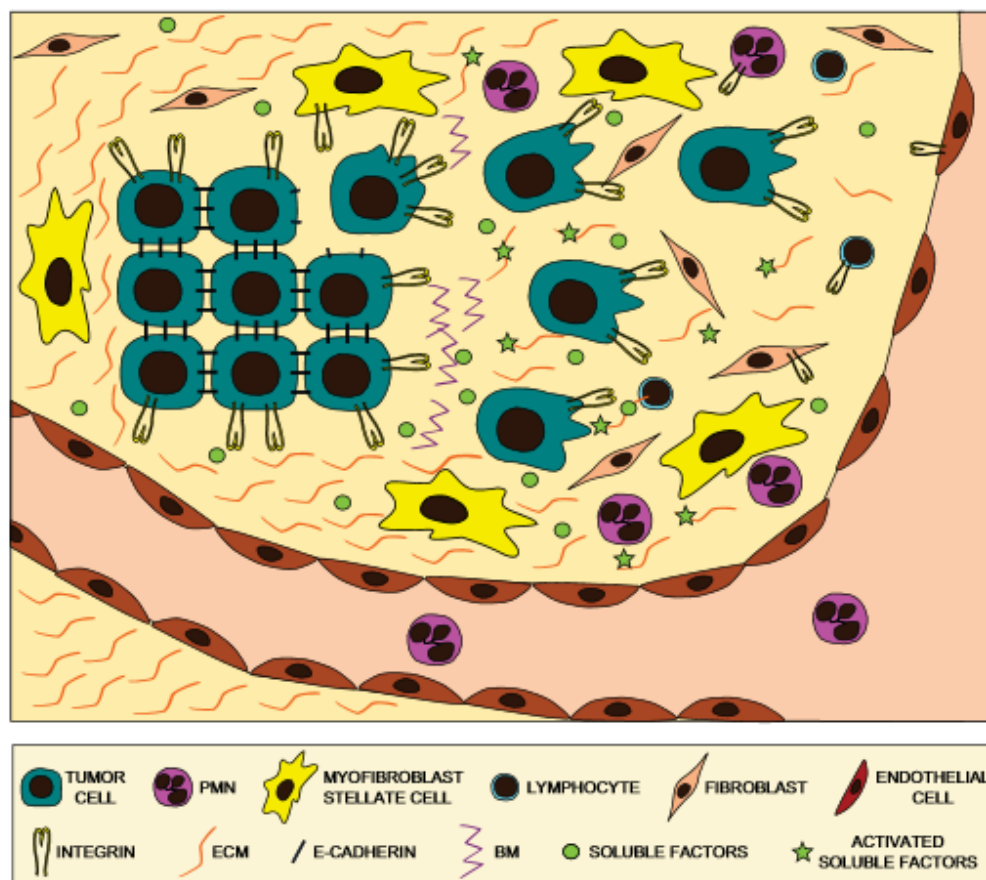
1.1.1.2. Metastasis of PDAC

When the non-invasive cells transform into malignant invasive cells they overgrow and eventually disseminate from primary site to distant organs causing secondary tumours called as metastasis. Most of the PDAC patients, at the time of

diagnosis, have metastatic stage and most often cancer related deaths are due to metastasis. As mentioned above, from an initiated pancreatic tumor cell, for ex in PanIN-1 stage, to disseminate and induce metastasis it takes longer than 10 years as estimated by mathematical model by Yachida et al (Yachida et al., 2010). Interestingly, in spite of such a long relatively slower progression of cancer, most of the genetic changes from the primary cancer were retained in metastases cancer. Another study involving larger group of patients show that 70% of the patients' death suffered from metastasis and 30% of deaths had locally destructive pancreatic cancer. The autopsy analyses indicate that only metastasis was closely correlated to the loss of tumor suppressor gene SMAD4 (Iacobuzio-Donahue et al., 2009). Another set of computational modelling of as large as 200 patients' samples (resected and autopsied combined) predicts that tumor growth of pancreatic cancer would exponential at the time of diagnosis prompting both early as well as timely diagnosis and treatment are quintessential for effective treatments (Haeno et al., 2012). However, larger role in tumor progression is played by the microenvironment of the tumor cells that include stromal cells, immune cells and their secreted proteins etc.

1.1.2. PDAC tumor microenvironment (TME)

PDAC is characterized to be highly dense and poorly vascularized stroma due to desmoplastic reaction. This PDAC stroma, collectively called as tumor microenvironment (TME), has a complex cellular compartment including tumor cells, immune cells, fibroblasts, inflammatory cells, endothelial cells etc. These individual cellular compartments interact with each other by secreting proteins like extracellular matrix (ECM), growth factors (GFs), cytokines, interleukins etc. and contribute to the overall progression of the tumor. A schematic representation of TME is shown below in *scheme-3*. Within the vastly heterogenic TME we limit our focus to pancreatic stellate cells (PSCs), key secretomes of PSCs and, ion channels and integrins.



Scheme-3. Schematic representation of TME and its key components adapted from (Arcangeli, 2011).

1.1.2.1. Stromal fibroblasts-Pancreatic stellate cells (PSCs)

Pancreatic stellate cells (PSCs) form one of the major components of TME. PSCs in healthy tissues exist in inactive quiescent state with large lipid storage rich in vitamin A as a characteristic feature. However, under chronic or acute pancreatitis (inflammation) PSCs are activated where they lose lipid storage and instead express alpha-smooth muscle actin (α -sma). Inflammation in pancreas like chronic pancreatitis is considered to be a major risk factor in developing PDAC and independent of sex, country and type of pancreatitis (Lowenfels et al., 1993). Activated PSCs show increased cell proliferation, migration to the wounded region and deposition of ECM proteins (fibrosis). In addition, activated PSCs secrete as many as 641 proteins while quiescent PSCs secrete a meagre 46 proteins. More than 35% of these secreted proteins were implicated, according to KEGG database, in

cellular processes, signaling pathways or human diseases (Wehr et al., 2011). PSCs and PDAC cells interact in a paracrine fashion that is, through secretion of signaling molecules that induce the changes in one another. Increasing evidence suggests that these activated PSCs, through secretion of various proteins, activate the PDAC cells and promote tumor progression. Notably, the secretion of ECM proteins like collagen-1, fibronectin and cytokines provide chemoresistance, GFs like PDGF, EGF, TGF β induce cell proliferation and migration, proteases like matrix metallo proteases (MMPs) in invasion of PDAC cells (Tang et al., 2013). The cross talks between PSC and PDAC are studied in monolayer or three-dimensional co-culture systems. The co-culturing has shown to increase the PDAC cell proliferation by the secretion of GFs and cytokines from PSCs. Interestingly, in co-culture as well as in mice, when quiescence of PSCs were induced by all-trans retinoic acid (ATRA) the proliferation of PDAC cells decreased, increased cell apoptosis and altered tumor morphology indicating that activated PSCs is essential for PDAC cell proliferation (Froeling et al., 2011). *In vivo* experiments also corroborate similar observations where co-injections of PDAC and PSC cells increase the tumor progression rate and metastasis (Hwang et al., 2008; Vonlaufen et al., 2008). The interaction between PDAC and PSCs are mutual beneficial in which they stimulate each other's growth and migration through the secreted proteins and thrive together. The conditioned media of activated PSCs when added to PDAC cells have shown to increase cell proliferation, migration and invasive capabilities and altered phenotype of PDAC cells (Lu et al., 2014). Similarly, the conditioned media of PDAC cells can further stimulate PSCs proliferation, activation, secretion of collagen-1 etc. (Apte et al., 2004). Hence it is increasingly perceived that activated PSCs can be a potential target to suppress the tumor protection and progression. Some of the key secreted proteins and their roles in TME are explained below.

1.1.2.2. Secreted proteins in TME

1.1.2.2.1. Extra cellular matrix (ECMs)

PDAC is characterized to be highly desmoplastic with large amounts of ECM proteins deposited around the tumor cells. PSCs are the chief source of ECM

consisting of collagen-1 (more than 90%), fibronectin, proteoglycans, hyaluronic acid and other ECMs. The constant accumulation of these ECMs distorts the normal architecture of the pancreas tissue and induces abnormal blood and lymphatic vessels as well as brings the ECMs and PSCs closer to cancer cells (Gnoni et al., 2013; Armstrong et al., 2004). In addition, ECM deposition around the tumor cells protects them against any therapeutic drugs and, also confines the tumor cells within the microenvironment. However, ECM turnover (synthesis, secretion and degradation) is critical in tissue remodeling in both normal as well as pathological processes. PSCs, when exposed to proinflammatory proteins like TGF-B, IL-6, secrete enzyme class matrix metalloproteinases (MMPs) that degrade ECM (Phillips et al., 2003). Cancer cells exploit this well-coordinated ECM turnover to migrate closer to blood vessels and further induce angiogenesis for eventual dissemination to distant organs.

1.1.2.2. Other proteins

TME is highly heterogenic and dynamic with rich source of proteins secreted by various types of cells. These proteins include GFs, cytokines, interleukins, proteases etc. specifically secreted by both PSC and PDAC cells. PDAC is also characterized to be hypoxic due to over growth of cancer cells. The GFs include EGF, VEGF, PDGF, IGF, TGF-B, FGF (fibroblast GF) that regulate wide range of signaling cascades in both normal as well as pathological process as reviewed in (Nandy and Mukhopadhyay, 2011).

- *Epidermal growth factor (EGF):*

EGF is a ligand that binds to EGF-receptors. EGFRs are one of the key receptors that are consistently up regulated in many tumors including PDAC. The EGF binding to EGFR leads to autophosphorylation of EGFR that in turn initiate cell proliferation signaling and thus excessive presence of EGF leads to increased proliferation. The EGF molecules are secreted by both PDAC and PSC cells and are involved in autocrine as well as paracrine function.

- Vascular endothelial growth factor (VEGF):

Both normal and pathogenic pancreas development involve angiogenesis- the process of new blood vessel formation. Many GFs like VEGF, PDGF, TGF- β , bFGF etc. are involved in angiogenesis, but VEGF is the most potent angiogenic factor that binds to VEGF-R and involved in every step of angiogenesis. Rapidly growing tumor cells need constant supply of nutrients through blood vessels. But because of the over growth of tumor and excess fibrosis the tumor cells are deprived of nutrients that are essential to support their growth rate. Hence these tumor cells secrete VEGFs that increase blood vessel formation and nutrient supply.

- Platelet derived growth factor (PDGF):

There are four PDGFs; PDGF-A, B, C and D that bind to either homo or heterodimer PDGF-receptors and modulate cell proliferation and migration signaling pathways detailed in review (Heldin, 2013). The PDGF and its receptors have important functions in regulation of growth and tissue repair; however, over expression and mutational activity of the PDGF-Rs drive the excessive cell growth and migration of both malignant and non-malignant cells. At the initial stage of pancreatitis macrophages and ductal cells are the main source of PDGFs that cause activation of fibroblast and proliferation. Over expression of PDGF-D has shown to increase the migration and invasion of PDAC cells and positively regulate activation of matrix metalloproteinase-9 (MMP-9) and VEGF (Wang et al., 2008).

- Matrix metalloproteinases (MMPs):

MMPs are calcium dependent zinc containing enzyme proteins that are capable of degrading ECMs. As mentioned above PDAC is characterized to be highly desmoplastic with excess accumulation of ECMs mainly collagen-1. Even though PDAC cells have shown to secrete MMPs it is PSCs that are the major source of MMPs that are involved in remodeling of fibrosis and ECM turnover (Schneiderhan et al., 2007). It is a necessary step for cells to degrade the ECMs in

order for the PDAC cells to migrate and invade to distant organs and, treating of MMP inhibitor has shown to reduce the invading cells (Ellenrieder et al., 2000).

- Cytokines:

Cytokines are another class of small molecule proteins that are secreted at higher levels in PDAC TME. Several types of cells within TME secrete both pro and anti-inflammatory cytokines that are involved in proliferation, migration, angiogenesis, EMT, poor prognosis etc. as summarized in review (Roshani et al., 2014). Clinical study of comparison between healthy and pancreatic cancer patients suggest that elevated expression of cytokines like interleukin-1 receptor antagonist (IL-1RA), IL-6 and IL10 expression had worse overall survival rate (Ebrahimi et al., 2005).

1.1.3. Immune/inflammatory cells

The TME has shown to be infiltrated by various inflammatory immune cells as an act of immune surveillance. This include cells of adaptive immunity like T lymphocytes, dendritic cells and occasionally B cells as well as cells of innate immunity like macrophages, natural killer (NK) cells etc. (Whiteside, 2008). The size of the infiltration of these cells could vary from tumor-to-tumor. Despite the recruitment of these immune cells as a defence mechanism against tumor cells, the tumor continues to grow: it could be because the adaptive immunity is weak and largely inefficient (Arcangeli, 2011). In addition, the cellular and molecular events in TME are often orchestrated and dominated by tumor cells in which tumor cells cause dysfunction and death of immune cells or worst cases immune cells are involved in promoting growth of tumor cells(Whiteside, 2008; Arcangeli, 2011). For example, tumor-infiltrating lymphocytes (TIL) obtained from tissue samples, the major component of immune infiltrates in tumor, showed inhibited proliferation in response to antigens, compromised signaling through T-cell receptor (TCR) and inability to induce cytotoxicity towards tumor cells. It is also shown that except for effector T cells, immunosuppressive cells like tumor-associated macrophages, myeloid derived suppressor cells (MDSC) and T regulatory cells (T_{reg}) except effector T cells are

recruited to the tumor site at the early stage and persist till the invasive cancer but tumor still grows. This suggests that effective immune defensive mechanism against tumor is undermined from the start (Clark et al., 2007). Recently, a comprehensive study identifies some of the key immune cells that, when recruited to TME in higher levels, are either associated with shorter or longer survival of PDAC patients (Ino et al., 2013).

1.1.4. Ion channels and integrins in TME

The TME, due to shift of cellular metabolism to towards excessive glycolysis, is characterized to be physiologically acidic and, also spatio-temporally dynamic as tumor growth continues (Dang, 2012). The secretome of the TME are involved in stimulating various receptor proteins as well as strategically placed other membrane proteins like ion transporters and channels of cells. Both ion channels and integrin receptors are ubiquitously expressed in all cells with varying degree that play key role in regulating normal as well as pathophysiology of cells that are explained in separate sections below. Integrins are adhesion molecules used by cells to anchor to its environment like ECMs (cell-matrix) or other cells (cell-cell interactions) and are involved in modulating broad cell signaling including adhesion, migration, and angiogenesis. Ion channels and transporters (ICTs) are also activated in the acidic TME where protons are exchanged between intracellular and extracellular space notably through sodium proton exchangers (NHE) (Andersen et al., 2014). It has been shown that ion channels and integrins (β 1) interact and modulate each other's function. One such example is activation of integrins through ECMs increased the ion conductance of potassium ion channels HERG1 (also called as hERG1) while functional blocking of channels interrupted integrin mediated signal (Cherubini et al., 2005). Also HERG1 channels make molecular complexes with EGFRs and other heterodimer integrins in PDAC cells that are involved tumor growth and angiogenesis. In the following sections below the detailed role of ion channels and integrins in cancer cell behaviour are mentioned.

1.2. Role of potassium ion channels in cellular physiology of cancer cells and cancer progression

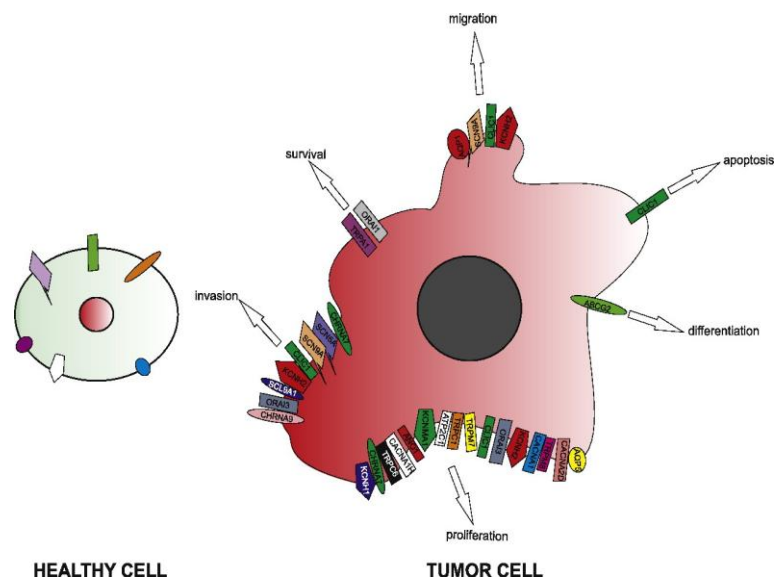
The development of noble prize-winning patch clamp method by Bert Sakmann and Erwin Neher led to tremendous breakthrough in ion channel research. Ion channels are the integral membrane proteins that regulate ion flow and thus voltage gradient across the membrane. The presence of ion channels and transporters at the plasma membrane allow the ions like Na^+ , K^+ , Ca^{2+} , Cl^- to pass across the membrane through specific ion channels. All cellular physiological processes depend on the flow of ions across the membrane barrier and this lead to the large electric potential difference between two sides of the membrane. The difference further leads to the switching of ion channels between conductance (open) and non-conductance (closed) state to restore the homeostasis of the membrane potential. The ion transport across the membrane barrier is characterized as ‘passive’ (i.e. without the need of energy) ion conductance driven by membrane potential (V_m). These ion channels play critical role in cellular physiology including cell volume, cell shape, cell cycle progression, cell proliferation, signaling, and apoptosis (programmed cell death) (Jehle et al., 2011) and thus any abnormalities in ion channel functioning will lead to pathophysiology (Kaczorowski et al., 2008). The list of pathophysiological diseases associated with ion channels has been discussed in the review articles (Jentsch et al., 2004; Hübner and Jentsch, 2002).

Over the last 15-20 years scientists have shown that ion channels are aberrantly expressed in many human cancers and they are involved in promoting hallmarks of cancer like continuous cell cycle progression, proliferation and migration. More importantly, because of the high expression of these ion channels at the early stage of tumor formation, they are considered to be effective biomarkers for early detection of cancer and perhaps as potential drug target for treatment of cancer. In the subsequent sections below, expression of ion channels in many human cancer tissues and cells and their functional of role in tumor cell progression, proliferation, migration as well as potential drug target are explained.

1.2.1. Ion channels as biomarkers and prognostic markers in cancer

1.2.1.1. Ion channels as biomarkers in cancer diagnosis, prognosis and potential drug targets.

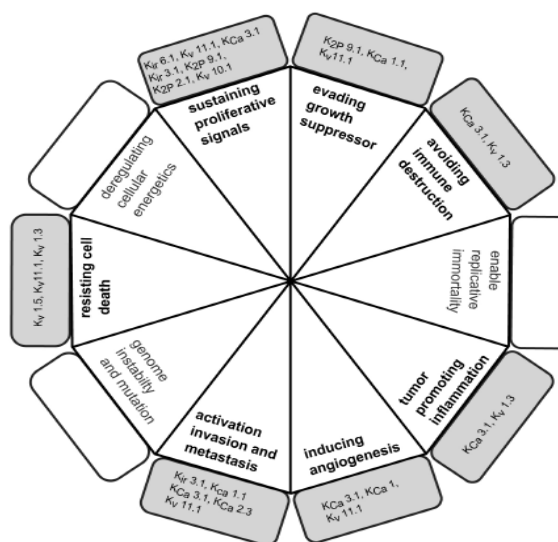
Although ion channels are one of the most indispensable membrane molecules for normal physiological processes of cells, some specific ion channels are explicitly implicated only under pathological conditions like cardiovascular disorders, neurological disorders, cancers etc. The group of pathological conditions are referred as ‘channelopathies’ (channels in pathology). The diseases are directly linked to stem from the dysfunction of ion channels due to mutations, altered membrane trafficking etc. (Dworakowska and Dołowy, 2000). The *scheme-4* below shows the differential expression of various ion channels in healthy and cancer cells and the implication of ion channels in promoting hallmarks of cancer. Cancer cells express vast number of ion channels that are typically absent in healthy cells.



Scheme-4. The differential expression of ion channels in healthy and tumor cell and their involvement in hallmarks of cancer (Lastraioli et al., 2015).

Over the last 30 years scientists have shown mounting evidence about the functional role of ion channels in life threatening diseases particularly in cancer and is consistently proven that ion channels are involved in regulating the hallmarks of cancer (Hanahan and Weinberg, 2011; Prevarskaya et al., 2010). Among many types

of ion channels such as voltage gate sodium channels (VGSCs), chloride (Cl-) channels, calcium activated potassium channels (KCa) etc. are involved in cancer, voltage gated potassium ion channels (Kv) are the most abundant ion channels coded by more than 70 human genes identified until now that are involved in cancer progression (<http://www.guidetopharmacology.org/GRAC/IonChannelListForward?class=VGIC>). The *scheme-5* below shows the involvement of various K⁺ channels in many hallmarks of cancer. As can be observed any ion channel can be involved in more than one hallmarks of cancer suggesting its importance in multistep process of cancer progression starting from hyperproliferation to invasion and metastasis. The detailed list of expression of vast number of ion channels in various cancer cells and tissues has been extensively reviewed in (Arcangeli et al., 2009; Bose et al., 2015).



Scheme-5. Potassium ion channels and their role in hallmarks of cancer (Prevarskaya et al., 2010)

Because of the involvement of these ion channels in multistep process of tumor progression they have been identified as prognostic markers in overall survival of many cancer patients. For instance, in breast cancer, large scale high-throughput expression profiling of 280 genes coding for ion channels that are in association with p53 mutation, estrogen receptor (ER) status and histological tumor grade predicts the overall clinical outcome (Ko et al., 2013). The ether-a-go-go (EAG) family of Kv10.1 ion channels have also been identified in several cancer cells, which are otherwise expressed only in brain tissue, and have been associated with poor prognosis.

Interestingly, over expression Kv10.1 was alone sufficient to increase cell proliferation and tumor progression in mouse models (Pardo et al., 1999). However, the pattern and expression level of ion channels in cancer is not always directly proportional, in all cancers, to its potential malignancy or overall survival rate. Because for ex, EAG related gene (ERG) family HERG1 was shown to be over expressed, including many tumor cells and tissues, in PDAC, acute myeloid leukemia (AML) and ovarian cancer cells and tissues. HERG1 expression level was in direct correlation to poor prognosis in both PDAC (Lastraioli et al., 2015; Pillozzi et al., 2007) and AML (Pillozzi et al., 2007), but in ovarian cancer there was no correlation with overall survival (Asher et al., 2010). In fact some ion channels have also shown to be down regulated in some highly malignant tumor like high-grade glioma where 16 out of 18 ion channels studied were down regulated (Wang et al., 2015). Similarly, low or dysfunctional expression of Kv7.1 and Kv1.1 is associated with hyper-proliferative, increased aggressiveness and low survival in patients with colorectal (Than et al., 2014) and breast cancer (Lallet-Daher et al., 2013) respectively indicating both these channels could act as a tumor suppressor. Hence it is consistently observed that there is differential expression of various ion channels across several tumor cells and tissues. Since last 30 years the role of ion channels in cancer cell cycle progression, proliferation, migration and invasion have been characterized across broad spectrum of cancer.

1.2.1.2. Role of ion channels-mediated membrane potential in cell volume regulation, cell cycle progression/proliferation/migration

1.2.1.2.1. Ion channels in cell cycle progression

The normal cell division process is divided into several phases; cell division starts with Gap (G1) phase, which separates previous cell division and DNA synthesis (S-phase) followed by second gap G2 phase and mitotic M phase. Further the cell can either proceed to next G1 phase for next cell division or G0 phase to attain quiescent state. After each phase cell has to undergo a checkpoint surveillance process to make sure the successful completion of previous phase. Hence these checkpoints are constitutive feedback pathways in safeguarding the key cell cycle

progression, which is however recognized to be defective in cancer cells (Urrego et al., 2014).

The membrane potential (V_m), largely modulated by K^+ ion channels, has been reported to be a key regulator of cell cycle progression. One of the well-established biophysical properties of cancer cells is they are more depolarized than their normal counterparts that favours increased cell proliferation and migration (Binggeli and Cameron, 1980; Blackiston et al., 2009; Yang and Brackenbury, 2013). This could also due to the differential expression of ion channels depending on cell cycle. Studies on various cancerous cells and tissues like breast cancer cells, hepatocytes, fibroblasts, ovarian and skin cancer tissues etc. shown to have depolarized membrane potential (V_m) while non-proliferating or terminally differentiated somatic cells show hyperpolarized V_m , indicating that V_m is functionally suggestive in cell development (Yang and Brackenbury, 2013). These depolarized cells had higher intracellular Na^+ concentrations than normal cells but K^+ concentrations were stable. However, this altered V_m is just an epiphenomenon of the transformation of normal cell to malignant.

The alternation in the V_m is imperative during the progression of cell cycle where V_m is hyperpolarized in G1/S phase through to G2 phase due to efflux of K^+ . Before cells enter M phase V_m is depolarized because of efflux of Cl^- and quiescent cells at G0 show mitotic activity when cells are depolarized (Cone and Cone, 1976). It is demonstrated that depolarization of cells initiate mitosis and DNA synthesis in both tumor and non-tumor cells. The number of studies has shown that by manipulating the V_m externally cell cycle progression could be altered. For ex, by hyperpolarizing the V_m , using extracellular ionic solution, of CHO cells at $-45mV$ mitotic arrest were induced and further at $-75mV$ the cell division was blocked. By depolarizing back at $-10mV$ the cell cycle was restored (Yang and Brackenbury, 2013). Although the fluctuation in the V_m throughout the cell cycle progression heavily depends on cell type, state of differentiation and density of cell monolayer in culture, it is consistently observed that the mean V_m of cancer cells is depolarized relative to non-transformed cells and could serves as a hallmark of cancer. Voltage

gated K⁺ ion channels (K_v) are the prominent ion channels that contribute to the overall V_m of the cell and thus an important regulator of cell cycle progression and proliferation.

1.2.1.2.2. Ion channels in cell proliferation

Cancer cells have a characteristic feature of having sustained cell proliferation signaling unlike non-cancer cells. Numerous K⁺ channels are aberrantly expressed in cancer tissues and cells most often with enhanced activity. These K⁺ channels could be activated by hyperpolarization of V_m , drug induced (Lansu and Gentile, 2013), membrane lipids like phosphatidylinositol 4, 5 bisphosphate (PIP₂), phosphatidylserine (PS) (Hansen, 2015; Zhou et al., 2015), integrin receptors (Levite et al., 2000; Cherubini et al., 2005) etc. A variety of ion channels have been linked to regulation of cell proliferation and pharmacological or genetic blocking of such ion channels has demonstrated to impede cell proliferation and in some cases even induce apoptosis.

Voltage gate potassium (K_v) ion channels are the most abundant as well as extensively studied ion channels that are implicated in cell proliferation and tumorigenesis. Most of these studies showed that blocking of K_v channels resulted in non-conductance of ions that lead to gradient in K⁺ ion concentrations. Because of the K⁺ gradient the influx of Ca²⁺ is inhibited which is crucial to trigger cell proliferation and maintenance of hyperpolarized V_m (Lang et al., 2005; 2007). However, cell cycle progression and proliferation is solely not determined by Ca²⁺ concentrations, because experimental observations show blockers or siRNA knockdown of specific type of K_v channels have shown to reduce the proliferation and arrested the cell cycle progression. For instance, K_v10.1 was blocked by specific single chain antibody fused to TNF-related apoptosis-inducing ligand (TRAIL). Only K_v10.1 expressing prostate cancer cells were targeted and induced apoptosis (Hartung et al., 2011). Another channels specific antibody as well as small molecule drug E4031 specific for HERG1 has shown to decrease the proliferation of pancreatic cancer cell line (Lastraioli et al., 2015). In E4031 specific blocking of HERG1 in K-

Ras mutated Panc1 cells led to ~50% reduction in mitogen-activated protein kinase (MAPK) signaling (Lastraioli et al., 2015). The simulated depolarization of V_m has also been shown to increase the nanoclustering of K-Ras at the membrane level and induce nanoscale reorganization of membrane lipids (Zhou et al., 2015). Interestingly Kv channels mutants for ion conductance, that is independent of ion permeation, have also shown to retain the influence of proliferation. It is plausible, under such scenario, that the impairment of ion conductance of specific channels could be compensated by expression of other channels. Hence the exact mechanism by which K^+ channels modulate cell proliferation is poorly understood. There are four proposed mechanism by which they could alter the proliferation and cell cycle progression. They are either by (i) setting up membrane potential, (ii) controlling cell volume dynamics, (iii) regulating calcium signaling or (iv) promoting malignant growth through non-canonical function, independent of ion permeation, where channel blocking could interfere with cell proliferation signaling cascade (Huang and Jan, 2014).

1.2.1.2.3. Ion channels in cell Migration

Most tumor cells, if not all of them, have a characteristic feature of invasion and metastatic in tumor progression; in which cell detach from primary tumor site and migrate to new position and form new attachment. The migrating cells exhibit a polarized feature where cell front and rear has differential polarity that is tightly governed, among many factors, by flow of ions and water molecules that also regulate cell volume, V_m and intra-and extra cellular pH. Likewise in cell cycle progression and proliferation intracellular concentration of Ca^{2+} plays a vital role in cell migration as well, perhaps through different mechanisms. Migration is a multifactorial phenomenon where cells make use of activated integrin receptors to move and most of the integrin function is calcium dependent. On the other hand ion channels mediated V_m determines the influx and efflux of Ca^{2+} and hence V_m could indirectly influence the cell migration. The intracellular calcium concentration ($[Ca^{2+}]_i$) has a great impact on cell migration because the migration machineries like focal adhesion kinase (FAK) (Giannone et al., 2002), myosin II (Betapudi et al., 2010), myosin light chain kinase (Tsai and Meyer, 2012), calpain, ion channels

(Schwab and Stock, 2014) etc. are calcium sensitive. The hyperpolarization of cells increases the intracellular concentration ($[Ca^{2+}]_i$) via transient receptor potential (TRP) channels or activates the voltage-gated Ca^{2+} channels to maintain depolarization (Schwab et al., 2012). Within the compartments of migrating cell, the $[Ca^{2+}]$ gradient is spatially and temporally regulated in which cell front has lowest $[Ca^{2+}]$ and cell rear has highest $[Ca^{2+}]$ (Brundage et al., 1991). The oscillations in $[Ca^{2+}]$ is observed within microdomains of the cell where $[Ca^{2+}]$ flickering occurs at highest level (flickering rate 4:1 front-to-rear) in lamellipodia at the cell front that could regulate the directionality of the migration (Wei et al., 2009). At the rear end of the cell Ca^{2+} contributes to the myosin-II dependent retraction force and disassembling of focal adhesion, and cytoskeleton reorganization (Brundage et al., 1991; Yang and Brackenbury, 2013).

As mentioned earlier migration is a multistep phenomenon that could be stimulated by V_m , GFs, integrin activation and other signaling molecules. For example depolarized V_m of epithelial kidney cells induces diphosphorylation of myosin light chain without altering the $[Ca^{2+}]$ but instead by activating on Rho-Rho (ROK) kinase pathway (Szász et al., 2005). Ion channels are also involved in crosstalk with integrin receptors and modulate integrin activation and signaling. For instance, depolarizing the T cells by increasing external $[K^+]$ increased the $\beta 1$ integrin activation which led to increased cell adhesion and migration (Levite et al., 2000), while blocking of Kv1.3 channels reduced proximity between Kv1.3 and $\beta 1$ integrins in malignant melanoma cells (Artym and Petty, 2002). A similar observations were made with HERG1 channels where both HERG1 and $\beta 1$ integrin reciprocally activate each other. On one hand functional blocking of HERG1 channel decreased the integrin-mediated activation of FAK while on the other hand integrin activation by fibronectin increased the HERG1 current density. Blocking of HERG1 indeed impaired both co-localization and co-immunoprecipitation of HERG1 and $\beta 1$ integrins (Cherubini et al., 2005). In colorectal cancer cells HERG1 channels have been shown to interact with $\beta 1$ integrin and modulate signaling pathway involved in angiogenesis. The functional blocking of channels abolishes the pro-angiogenesis signaling both in vivo

and in vitro (Crociani et al., 2013). Expression of HERG1 in pancreatic cancer patients serves as prognostic factor and blocking of HERG1 channel in pancreatic cancer cells has shown to decrease proliferation and migration (Lastraioli et al., 2015). The mounting evidences of involvement of many ion channels in cancer progression they are collectively viewed as potential drug targets in cancer.

1.2.2. Ion channels as potential therapeutic drug targets

Ion channels have long been the therapeutic targets in many pathophysiological conditions. There are many naturally occurring drugs or toxins that target ion channel with high affinity. The first synthetic ion channel modulator amylocaine a local anaesthetic was synthesized in 1903 that started a classic age of chemistry driven drug discovery and development. Ion channels are now the second most targeted class of proteins with ~ 13.4% of the marketed drugs targeting ion channels with worldwide annual sales worth \$12 billion. These small molecule drugs are used for wide range of physiological conditions such as local anaesthetic, anti-arrhythmic, anti-hypertensive, anticonvulsant, diuretic, stroke, diabetic, cystic fibrosis, neuromuscular blocker/muscle relaxants etc. (Clare, 2010). Despite the successful exploitation of ion channels, for their involvement in disease conditions, as potential drug targets, the currently targeted ion channels amount for only 20% of the 300 members of ion channels that are expressed in human (combined healthy and disease conditions). Moreover, the roles of ion channels in vast number of human cancer progression are very well documented and serve as huge potential targets. With recent advances in drug designing, structural biology of ion channels and high throughput patch clamp screening for effect of drugs on ion channel modulation has increased the pace of drug discovery against non-targeted ion channels.

The role of ion channels in vast number of human cancer has been studied since last 20-30 years. In most cancers ion channels are over or aberrantly expressed indicating their role in enhancing the tumor malignancy. Hence the over expressed ion channels are increasingly viewed as biomarkers for possible early diagnosis as well as oncogenes for potential drug targets. For efficient targeting of these ion

channels various drug-designing strategies have been employed namely small molecule drugs to block the ion permeation, full-length antibodies to target extracellular epitope or loop of the ion channels (Xu et al., 2005), fusion proteins consisting of single chain antibody fused to TRAIL ligand to induce cancer cell specific apoptosis, overexpression of ion channel targeting microRNAs (Feng et al., 2014) etc. Plethora of evidence suggest that functional impairment of over expressed ion channels in cancer by blocking the channels with specific small molecule drugs, antibody targeting or silencing the channel expression by siRNA have remarkably decreased the tumor cell proliferation, migration, invasion in both *in vitro* and *in vivo* animal models.

The **table 1** below shows the summary of aberrant expression of only K⁺ ion channels with focus limited only to pancreatic cancer tissues and cells. Because of both the peculiar expression pattern of ion channels under pathological conditions as well as membrane expression make them easy to detect valuable biomarkers particularly for early diagnosis and perhaps also as potential drug targets as therapeutic strategy.

Table 1. K⁺ ion channels expression in pancreatic cancer cells and their mode of action in promoting malignant features.

Hallmarks of cancer	Ion channel type	Expression level	Modulators	Mode of action
Cell proliferation	HERG1	Up regulated	E4031	E4031 decreased pMAPK cell signaling in K-Ras(mut) cell line (Lastraioli et al., 2015)
			miR-96	Micro-RNA (miR-96) expression down regulates HERG1 (Feng et al., 2014a)
	Kv10.1	Up regulated	Bifunctional scFv Ab	Fusion protein targeting extracellular epitope of Kv10.1 and TRAIL that induces death of Kv10.1 (Hartung et al., 2011)

	KCa3.1	Up regulated	Clotrimazole and TRAM-34	Decreases cell proliferation in expression dependent manner (Jäger et al., 2004)
	Kv 1.5, 1.1 and 1.3			
Cell migration /metastasis	HERG1		E4031	Decreases the PDAC cell migration stimulated by pancreatic stellate cells and alters the actin dynamics through interaction with B1 integrin.
			miR-96	miR-96 expression directly target HERG1 and decreases cell migration of HERG1 in vitro and tumorigenicity, metastasis and HERG1 expression <i>in vivo</i> models (Feng et al., 2014b)
Apoptosis	HERG1		siRNAs	Silencing of HERG1 expression increases the (%) cells that enter apoptosis (Feng et al., 2014b).
	Kv10.1		Bifunctional Ab	Antibody fusion protein containing extracellular epitope recognizing of Kv10.1 (scFv) and TRAIL that induces death of Kv10.1 expressing tumor cells (Hartung et al., 2011).
Prognosis	HERG1			HERG1 expression in PDAC tumor show poor prognosis (Lastraioli et al., 2015).

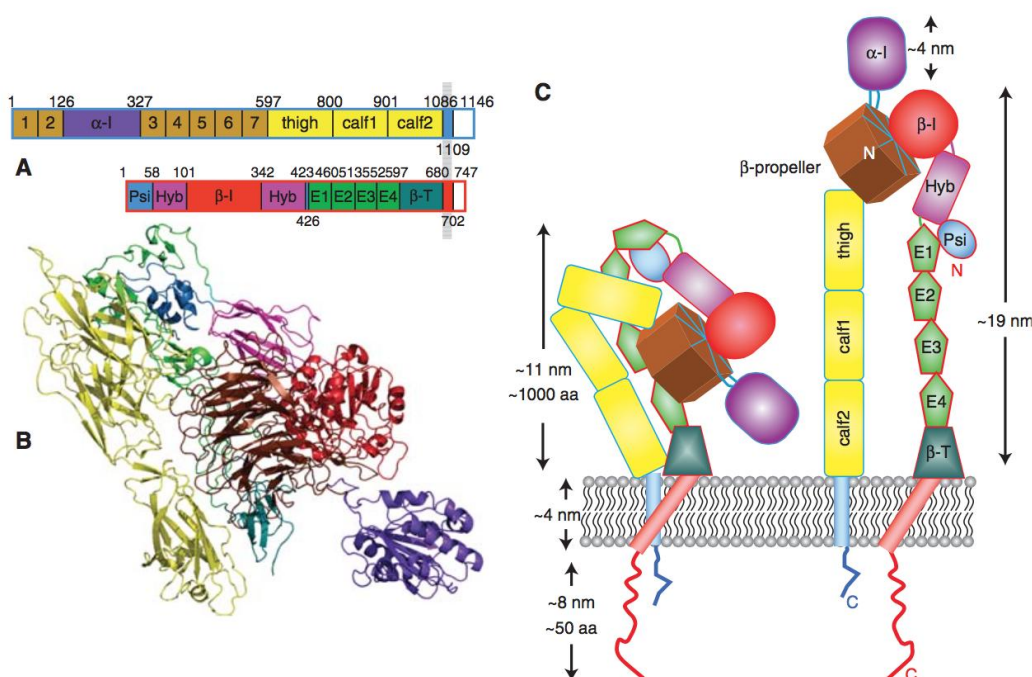
1.3. Integrins structure, function, activation, signaling cascades in cancer

1.3.1. Integrins structure, function and activation

Mammalian cells express wide range of cell adhesion molecules (CAMs) that aid anchorage of the cells either to ECM or to neighbouring cells. These CAM proteins are divided into calcium dependent or independent. Integrins are major class of CAMs that are calcium dependent. Integrins are large heterodimer transmembrane cellular receptor proteins made of alpha (α) and beta (β) subunits. In vertebrates there are 16 α and 8 β subunits that made up to 24 combinations of non-covalent heterodimer integrin receptors (Calderwood, 2004). Each integrin heterodimer is distinct in property of binding affinity and tissue distribution. The large extra cellular domain of each subunit is made up of many smaller domains called as ‘ectodomains’ that are held together by flexible linkers. The transmembrane domain is a single membrane spanning helix while the cytoplasmic domain of integrin is a small-unstructured domain (Campbell and Humphries, 2011; Calderwood et al., 2013). The detailed structure of ectodomains of the integrins is reviewed by Campbell ID and Humphries MJ (Campbell and Humphries, 2011), below only the brief introduction of each of the domain will be explained.

Although the entire crystal structure of integrin molecule is not solved yet, the breakthrough in the structure of integrins came when crystal structure of ectodomains of $\alpha V\beta 3$ integrins was deciphered by Xiong et.al in 2001(Xiong et al., 2001)Currently, the crystal structures of $\alpha V\beta 3$, $\alpha I\text{Ib}\beta 3$ and $\alpha X\beta 2$ are available. Below is the representation of $\alpha X\beta 2$ integrin that has inserted α -I domain. The integrins are transmembrane proteins with large portion in extracellular domain and two smaller portions in transmembrane and cytoplasmic domain. (a) **Extracellular domain:** As shown in above *scheme-6* of $\alpha X\beta 2$ there are four-five ectodomains in alpha monomer: seven bladed β -propeller, a thigh and two calf domains in-that-order and the fifth domain, inserted between blade two and three of β propeller, is α -I domain present in only nine out of 18 α chains. The last three or four blades of β propeller binds Ca^{2+}

ions and influence the ligand binding. There are two main flexible regions in the ectodomains; one between the flexible linker is between β propeller and thigh and, the other is between thigh and calf1 domain. The α I domain is inserted in β propeller with linkers and shows higher flexibility in contrast to other domains and regulates the binding affinity. The β monomer chain of integrin however, on the other hand consists of more complex flexible and interactions. It consists of β -I domain, hybrid domain, plexin-semaphorin-integrin (PSI) domain, and four cysteine rich *epidermal growth factor* (EGF) domains (EGF1, EGF2, EGF3 and EGF4) followed by β tail domain closest to plasma membrane as shown in scheme 6. The β -I domain is homologues to α -I domain and inserted into the hybrid domain. The hybrid domain is in turn inserted in PSI domain that is split into two portions. A disulphide bond at Cys13 and Cys 435 connects the two portions of PSI domain.



Scheme-6. Adapted from Integrin Structure, Activation, and Interactions (Xie et al., 2010; Campbell and Humphries, 2011). The structure of α X β 2 integrin (Xie et al. 2009).

The EGF domains, in α V β 3, consist of even number of eight cysteines, bonded in C1-C5, C2-C4, C3-C6 and C7-C8 except in EGF1, while in α IIB β 3 all 56 cysteines were disulfide bonded in β 3 subunit. Overall, it was observed that the β subunit was more flexible than α subunit. The cations are very essential for integrin

binding to ligands. The ectodomains of both α and β at the outer most domains consist of cation binding sites. The ligands bind to the crevice of the $\alpha\beta$ interface (α -I and β -I domain). In the absence of α -I in integrins, ligand binding occurs between β -propeller and β -I interface and the binding are dependent on cations like Mg^{2+} , Mn^{2+} and Ca^{2+} . However, in presence of α -I domain integrin ligand binding involves Mg^{2+} ion, a metal ion dependent adhesion site (MIDAS) (Shattil et al., 2010; Campbell and Humphries, 2011) (b) **Transmembrane (TM) domain**: TM domains were significantly smaller domains of integrins with single spanning structures of ~25-29 amino acid that form α -helix. There are no currently available high-resolution crystal structure TM domains of any integrin and most of the structural data are from NMR analysis. The α and β subunits in TM are tightly packed through glycine-glycine interactions (Kim et al., 2011; Srichai M.B and Zent R, 2010). Studies involving electron microscopy (EM), disulfide cross-linking, activating mutations and FRET suggest that α and β subunits are associated in TM domain in inactive or bent conformation. Both the separate structures of α Ib and β 3 subunits and complex structures solved by NMR both and in complex and, disulfide cross-linking of intact α Ib β 3 show similar structure. The α Ib helix is perpendicular to the membrane while β 3 makes slightly tilted angle. (c) **Cytoplasmic domain**: Likewise with TM domain there are no high-resolution crystal structures available for the cytoplasmic domain. The cytoplasmic domain of the integrins are also relatively short with ~10-70 amino acid (except β 4 with >1000 a.a). The cytoplasmic domain of β 3 is highly homologous while the α Ib is highly divergent subunit (Srichai M.B and Zent R, 2010). The β subunit within cytoplasmic domain has two motifs; membrane proximal and membrane distal motif that serve as binding sites for integrin binding proteins like talin, kindlins etc which are critical for integrin activation from inside the cell.

Integrins are the bridging molecules between extracellular environment (especially matrix proteins) and intracellular cytoskeleton. When integrins interact with specific sequences on the matrix proteins their conformation changes are induced along the length of the integrin. At the extracellular domain, the bent conformation of the integrin is changed to extended conformation, at the TM domain the α and β subunits are dissociated and lastly at the cytoplasmic domain the

conformational changes include unmasking of the protein binding sites, which are involved in either intracellular signalling or intermediate proteins to link integrins to actin. Integrins are linked to actin cytoskeleton through a complex hierarchy of proteins that form into a globular structure termed as adhesome. There are as many as 180 protein-protein interaction nodes in this structure defining the complexity and connectivity of the network (Parsons et al., 2010).

Integrin activation: Firstly, the integrins are essentially expressed at the membrane in an inactive conformation. Integrins are not just receptor molecules but when activated they are also involved in both outside in and inside out signalling. However, because integrin lack tyrosine kinase activity the intracellular signalling occurs through the recruitment of non-receptor tyrosine kinase proteins to its cytoplasmic protein binding sites. Integrin is activated from both extracellular ligand binding in ectodomains (outside-to-in signalling) and intracellular integrin binding proteins at the cytoplasmic tail (inside-to-out signalling). Both outside-in and inside-out signalling are dynamic spatial and temporal regulation of assembly and disassembly of multiprotein complexes that form at the cytoplasmic tail of integrins (Harburger and Calderwood, 2009). This integrin activation leads to a conformational change from bent to the extended heterodimer and dissociation of α and β subunits at the TM domain, a required conformational change shown for α IIb β 3 (Zhu et al., 2007).

1.3.2. Outside-in signalling role of integrins

The extra cellular matrix (ECM) proteins bind to the α and β interface and the conformational changes are conveyed through TM domain to cytoplasmic domains where further conformational changes lead to integrin clustering and formation of focal adhesion sites. This outside-to-in signalling modulates wide range of signalling cascade that are involved in cell adhesion, proliferation, migration, cytoskeleton organization of actin, paxillin etc. Intriguingly, the involvement of integrin activation in these physiological processes is highly temporal dependent (Legate et al., 2009). For example when the integrins initiate the engagement with matrix, the integrins

recruitment of phospho tyrosine kinases like FAK, Src, RACK1 and paxillin to its nascent adhesion site is an early event (typically 0-10minutes of engagement), even upstream of integrin activators like talin. But when adhesion is more matured the talin is more engaged with integrins (Serrels and Frame, 2012). The subsequent effect of integrin engagement with matrix leading to actin cytoskeleton organization, spreading, cell polarity occurs typically in 10-60 mins while effects on gene expression, cell survival and differentiation is a long term effect (Legate et al., 2009).

1.3.3. Integrins in cell adhesion signaling and migration

1.3.3.1. Integrins in cell adhesion and signaling

In cell adhesion, cells anchor to either the neighbouring cells or to ECM ligand with the help of cell adhesion molecules (CAMs) like integrins, cadherins and selectins. Integrins are the central part of the cell-matrix adhesion that is essential for normal physiological processes like embryonic development, wound repair, as well as during disease progression such as cancer. On the other hand ECM are large proteins and composite of various matrix molecules like glycoproteins fibronectin, collagen, laminin etc and non-matrix secreted cellular components like growth factors. Interestingly, within the ECM integrins recognize short peptide sequence residues, typically RGD (arginine-glycine and aspartic acid). However, not all RGD comprised peptide sequence can induce cell attachment; in fact out 2600 proteins sequences including fibrinogen, vitronectin, von Willebrand factor etc that have RGD peptide only a minority of them do so. This may be due to RGD sequence is not always presented on the surface or not compatible for the integrins to bind (Ruoslahti, 1996). Interestingly, it is the residues that are outside RGD motifs that provide the high affinity and specificity for ligand-integrin pair and these secondary sites are assumed to interact with the alpha subunit of the integrins while RGD peptide interacts with β subunit (Takagi, 2004). For example, $\alpha 5 \beta 1$ preferentially binds to RGD sequence when RGD is flanked by GW amino acid but $\alpha V \beta 1$ has broader specificity (Mould et al., 2000) while some amino acids like proline if present outside RGD can inhibit the cell attachment (Ruoslahti, 1996).

Cell matrix adhesions are highly dynamic structures that are organized around cytoplasmic tail of clustered integrins. At the early stage of integrin activation by ligands, the FAK is recruited to the integrins at the FA by talin, an integrin activator (Serrels and Frame, 2012). FAK is one of the most significant integrin signaling molecules because it harbours multiple activation sites and interacts with various proteins. At N-terminus it has FERM domain (binding of protein 4.1, ezrin, radixin and moesin homology), kinase domain (for multiple autophosphorylation sites) and FAT domain at C-terminus. FAK is recruited at the nascent adhesion (early stage of the adhesion) and auto-phosphorylated firstly at 397 a.a that leads the creation of the binding site for Src-homology2 (SH2) of Src. This binding in turn lead to cascade of phosphorylation, mainly initiated by SH2 domain of Src, along the FAK and interactions of FAK with other proteins that are essential in adhesion-dependent signalling (Kumar, 1998; Mitra et al., 2005; Huveneers and Danen, 2009). The FAK-Src active complex phosphorylates other FAK associated proteins like paxillin, p130Cas and tensin (Kumar, 1998). At C-terminus FAK interacts with paxillin. During the course of adhesion maturation, however, the FAK is folded back and integrin is more associated with talin for stronger adhesion structures (Lawson et al., 2012). To this end actin binding proteins like vinculin and α -actinin bind to talin and connect the ECM and cytoskeleton organization through integrins.

In addition to FAK modulation, Rho family of GTPases (RhoA, Rac1 and Cdc42) are also regulated in integrin-mediated adhesion. RhoA, Rac1 and Cdc42 are the most thoroughly studied members of Rho family. RhoA when activated induces FAs and bundle of contractile actin and myosins called as stress fibers: while Rac1 and Cdc42 stimulate the formation of two types of protrusions lamellipodia and filopodia (Kumar, 1998; Arthur and Burridge, 2001; Huveneers and Danen, 2009). That is to suggest that, Rac1 and Cdc42 are localized at the cell front but with distinct spatial and temporal sites while RhoA is prominently active in cell rear of the migrating cell. In the initial phase of adhesion and spreading (10-30mins) the active RhoA (GTP bound RhoA) level is transiently reduced and the levels of Rac1 and Cdc42 are elevated. At more mature stage of adhesion (45-90mins) the RhoA-GTP

level increases whereas the Rac1 and Cdc42 levels are decreased (Arthur and Burridge, 2001; Huvneers and Danen, 2009). There is also evidence of hierarchical interconnections within these family members where Cdc42 regulates Rac and, Rac in turn regulates Rho proteins (Kumar, 1998).

1.3.3.2. Integrins in cell migration

Integrins are hands and feet of the cell to grasp its extracellular environment and move along it. Cell migration is highly dynamic multifaceted phenomenon that requires that interaction between cell and substratum on which cell is attached and migrates. The migration can be either single cell or collective cell migration and unidirectional or random. In collective cell migration, the intercellular interactions and co-ordinations are retained. The single cell migration is further categorized into mesenchymal and amoeboid, though there are conflicting evidences that suggest nonmesenchymal cells well as amoeba-like dictyostellium can have mesenchymal like migration (Huttenlocher and Horwitz, 2011). Mesenchymal migration (for ex fibroblasts, cancer cells) involves cell polarization to form actin-rich protrusions at the leading edge, adhesion formation and maturation, cell body translocation and detachment of cell rear. This multifaceted dynamics involve strong interactions of integrins with substratum. Whereas, amoeboid like migration involve gliding and rapid migration (for ex neutrophils, dendritic cells, lymphocytes) and exhibit weak or no integrin mediated traction forces. Thus the level of expressions of integrins and ligands, their binding affinity, cytoskeleton association etc. regulates the migration rate and direction of migration. In general, the optimum migrations of cells in both 2-D and 3-D occur at intermediate levels of expression of integrins like $\alpha 5\beta 1$, $\alpha 2\beta 1$ and ligands like fibronectin and collagen (Huttenlocher et al., 1996; Huttenlocher and Horwitz, 2011).

The structure of a typical migrating cell can be divided into three compartments; leading edge (consisting of lamellipodium, FA complexes, actin filaments), cell body and rear or trailing edge (consisting of actomyosin filaments). The FA complexes are formed when cells grasp to the ECMs and generate forces for the cells to move forward. At the leading edge the stabilization of nascent adhesion

leads to the activation of Rac and Cdc42 that in turn reinforce the actin polymerization at the leading edge and subsequent protrusion. When cells grasp to the ECM, the FA complexes are formed that lead to the stabilization of nascent adhesion and activation of Rac and Cdc42 that in turn reinforce the actin polymerization at the leading edge and subsequent protrusion. This step generates necessary force to pull the cells body forward at the leading edge (Nagano et al., 2012). The cell movement is accompanied by the release of FA complexes, a process of disassembly, from the ECM and perhaps also internalization of integrins. As the lamellipodium moves forward the nascent adhesion has to disassemble. However, when nascent adhesions are connected with actomyosin in lamellum they mature and form larger focal adhesions that are accompanied by the localized activation of Rho (Parsons et al., 2010; Huttenlocher and Horwitz, 2011).

When the integrins are clustered upon activation it recruits wide array of intracellular proteins to its cytoplasmic tail that link integrins to actin cytoskeleton. Although several molecules are implicated to link integrins and actin, most likely candidates that are involved in bridging are talin, vinculin and α -actinin. The linkage stabilizes the adhesion and disruption of any molecular linkers compromises the integrity of adhesions and lead to the disassembly. For example, talin is required for integrin activation and linking integrin with actin and stabilizing the adhesion. However, when a protease calpain binds to talin or talin knockout cell show unstable adhesions. Similarly, vinculin gene, which is involved in mature and stable adhesions, deletion increases cell migration. Finally, integrins with their unique ability to tune their affinity to ligands regulate the stability of adhesions (Vicente-Manzanares et al., 2009).

However, inside-out signalling is initiated by the dissociation of non-covalently linked α and β subunits. Also several mutational studies to disrupt α and β subunits, which otherwise would have held both the subunits through salt bridge, have shown to activate integrin (Shen et al., 2012). There are various proteins that bind to the integrin and increase its affinity for ECM binding. Talin is a major integrin activating homodimer ~270kDa protein that bind to cytoplasmic tail of

integrin. Like integrin, talin is shown to be essential for normal development in mice, *drosophila* and *c.elegans*. Talin can strongly bind, its head domain, and activate broad range of β subunits like $\beta 1A$, $\beta 1D$, $\beta 2$, $\beta 3$, and $\beta 5$ and increase its affinity to ECM proteins (Calderwood, 2004a). The activation of integrins from inside as well as outside governs some of the key cellular processes. They include cell adhesion, cell-cell interactions, cell-substratum interactions, cell proliferation, differentiation, migration and apoptosis. Within this broad range of cellular processes that involve integrins we mainly focus on cell adhesion, migration and cell signalling pathways in below section.

1.3.4. Integrins in cancer

Similar to ion channels mentioned in previous section, integrin expression patterns can vary considerably between normal and tumor tissues. Many integrins are up regulated in cancers that contribute to tumor progression by mediating migration, proliferation and survival of tumor cells summarized in review (Mizejewski, 1999). There are some integrins like $\alpha 2\beta 1$ that are down regulated for ex in breast cancer and, over expression of $\alpha 2\beta 1$ alleviates tumor growth (Zutter et al., 1995). Similarly, over expression of laminin-5 receptor, $\alpha 3\beta 1$ integrin in skin carcinoma cells showed decreased tumor growth rate (Owens and Watt, 2001). Among 24 different heterodimer combinations of integrins, the most widely studied integrins that are associated with disease progression are $\alpha V\beta 3$, $\alpha V\beta 5$, $\alpha 5\beta 1$, $\alpha 6\beta 4$, $\alpha 4\beta 1$ and $\alpha V\beta 6$ (Desgrosellier and Cheresch, 2010). The integrins however are not oncogenes *per se* as they do not have the capabilities of transforming the cells, but they cross talk with oncogenes and receptor kinases to enhance tumor promoting signaling cascade.

1.3.4.1. Integrins expression: implications in pancreatic tumor progression

1.3.4.1.1. Beta (β) 1 integrins

The $\beta 1$ subunit is the most extensively studied integrin subunit for its role as receptor signaling molecule in both normal and neoplastic cells. The $\beta 1$ subunit makes heterodimer complex with the as many as 12 different α subunits and thus can

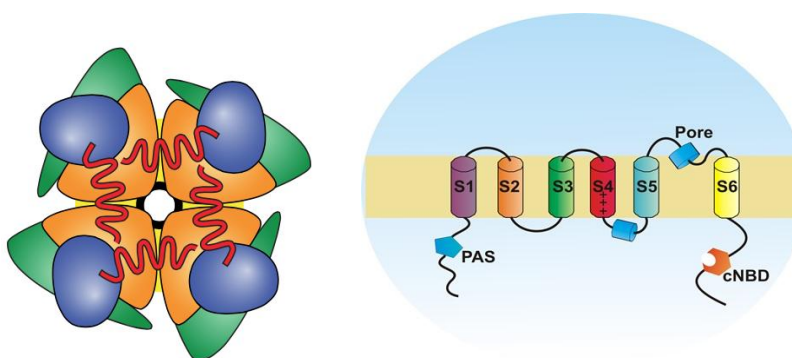
interact with most of the ECM ligands depending at varying affinity depending on the α subunit partner. Because various ECMs and $\beta 1$ integrin expressions are up regulated in most of the pancreatic cancer tissue and cell lines their interactions are crucial for the progression of tumor at various stages (Grzesiak et al., 2007; Hall et al., 1991). The integrin $\beta 1$ and ECM collagen are predominantly expressed in PDAC and PDAC cells. The characterization of integrin-ECMs interactions in several pancreatic cancer cells shows that collagen promotes maximal PDAC cell adhesion, proliferation and migration through $\alpha 2\beta 1$ integrins (Grzesiak and Bouvet, 2006). Another study by the same group shows that the knockdown of $\beta 1$ integrin in pancreatic cancer cell model decreased cell proliferation and migration *in vitro* and, primary tumor size and completely abrogated metastasis *in vivo*. Interestingly, $\beta 1$ knock down also reduced surface expression of its α subunit partners like $\alpha 1$, 2, 3, 5 and V subunits (Grzesiak et al., 2011). Pancreatic stellate cells (PSCs) play a major role in both increasing the malignancy of tumor cells. The supernatant of PSCs stimulate $\alpha 2\beta 1$ mediated PDAC cell migration, adhesion and activated FAK signaling. Both the anti- $\alpha 2\beta 1$ antibody and inhibition of FAK diminished the effect of the PSCs (Lu et al., 2014; Mantoni et al., 2011).

1.3.4.1.2. AlphaVBeta3 ($\alpha V\beta 3$) and alphaVbeta5 ($\alpha V\beta 5$) integrins

Integrins autonomously regulate diverse signaling cascades in the cells. In addition, there is growing body of evidence that integrins and growth factor receptors interact at membrane-proximal level and regulate cell-signaling pathways involved in cancer cell adhesion, proliferation, migration and metastasis. For ex integrin $\alpha V\beta 5$ and EGFR cross talk enhances invasion and metastasis of pancreatic cancer cells through Src kinase dependent activation (Ricono et al., 2009). In another example, exogenous expression of $\beta 3$ integrin in pancreatic cancer cell model lead to increased tumor growth and metastasis compared to cells lacking $\beta 3$ expression. The study further reveals that $\beta 3$ integrin is involved in enhanced anchorage-independent cell survival through $\alpha V\beta 3/c$ -Src oncogenic unit activation (Desgrosellier et al., 2009)

2. AIMS OF THE PHD STUDY

Scientists have been providing ever-growing evidence about the implications of ion channels and transporters in many pathological conditions including cancer. The group of pathological conditions that are due to impaired functioning of ion channels are termed as channelopathies. More often than not, most of the ion channels are aberrantly expressed in primary cancer and cancer cell lines but not in normal counter parts. In addition the expression of these ion channels are retained at various stages of cancer progression. Hence it is imperative to characterize their roles in diseases and progression of diseases. Evidence suggests that the membrane potential of most of the cancer cells are altered to more depolarized V_m . Potassium ion channels are the largest family of ion channels expressed in both normal and cancer cells and therefore could play vital role in regulating the cellular physiological process including cell proliferation, migration and cell-volume. Within the large class of potassium ion channels, human ether-a-go-go related gene 1 (HERG1) is a voltage-gated potassium ion channels $K_v11.1$ that is coded by gene *KCNH2*. The schematic representation of hERG1 channels is shown below. These hERG1 channels are normally expressed in heart. In heart, hERG1 channels are best known to be responsible for repolarizing the rapid delayed rectifier current (I_{Kr}) in cardiac action potential. Below is the schematic representation of hERG1 channels



Scheme 7: HERG1 channels are made of four identical alpha subunits (left panel- intracellular view), each with six transmembrane alpha helices (S1-S6) and cytoplasmic N and C terminus (right panel). The S4 helix is the voltage sensor and K^+ ions are conducted through it.

However, hERG1 channels are also expressed in many tumor tissues and cell lines including PDAC cells but not in normal counter parts. Hence we aimed to study the following roles of hERG1 channels in PDAC cells.

- Functional role of hERG1 channels in PDAC cell proliferation and the mechanism of modulating cell proliferation.
- Interactions of hERG1 channels with other membrane proteins like EGFR and integrins.
- Functional role of hERG1 channels in PDAC cell migration and its role in modulating cytoskeleton organization through interactions with integrins.

3. MATERIALS AND METHODS

3.1. Cell lines

3.1.1. Pancreatic ductal adenocarcinoma (PDAC)

PDAC cells included Panc1, MiaPaca2 and BxPC3 cells. The Panc1 and MiaPaca2 cells harbor mutation in KRAS and TP53, homozygous deletion (HD) in CDKN2A/p16 and wild type (WT) SMAD4, while BxPC3 cells harbor mutation in TP53, HD in SMAD4 and WT KRAS (Deer et al., 2010).

3.1.2. Human pancreatic stellate cells

Immortalized human pancreatic stellate cells (hPSCs or RLT-PSCs) were a kind gift from Dr Ralf Jesenofsky of Universitätsmedizin Mannheim, Germany.

3.1.3. Model cell lines

HEK293 and mouse fibroblast GD25 cells were used for the exogenous expression of hERG1 channels as model cell lines. Three GD25 cells; GD25WT, GD25 β 1A (stably transfected with β 1A integrin) and GD25 β 1Tr (expressing β 1 integrin truncated at cytoplasmic tail) were used as model cell lines.

3.2. Materials

3.2.1. Cell culture medium

Cell culture media used to grow various cells was dupleco's minimum essential medium (DMEM) (Euroclone), RPMI 1640 (Euroclone) and DMEM-F12 (Sigma Aldrich) medium supplemented with 10% fetal bovine serum. DMEM media was supplemented with 4mM of l-glutamine and RPMI with 2mM. RLT-PSC cells were cultured in DMEM-F12 medium with 10% FCS. The culture media were also sometimes supplemented with penicillin/streptomycin (penstrep) antibiotic and fungizone.

3.2.2. Extracellular matrix (ECM) proteins

ECM proteins fibronectin and laminin were purchased from Sigma Aldrich, collagen-1 was purchased from Millipore, collagen-III and IV from BD bioscience.

3.2.3. Antibodies

Following table below shows the antibodies that were used in various applications with dilutions and companies from which they are purchased.

3.2.3.1. Primary antibodies

Table 2. List of primary antibodies used in the study

Antibodies name	Expt	Mol Wt (kDa)	Company	Source	Diln.	Clonal
Anti-Phospho-MAPK	WB	42/44	Cell Signaling Technology	Rabbit	1:500	Poly
Anti-ERK1	WB	42/44	Santa Cruz	Rabbit	1:500	Poly
Anti- α -tubulin	WB	55		mouse	1:500	
Anti-Phos-AKT1/2/3	WB	62/56/62	Santa Cruz	rabbit	1:500	Poly
Anti-P85 of PI3K	WB	85				
Anti-Phospho-Tyr(Py20)	WB	Total p-tyr proteins	Santa Cruz	mouse		
Anti-hERG1 mAb	IP		In house	mouse	5 μ g/mg protein	mono
Anti-hERG1-alexa 488	IF				1:1000 dil.	
Anti-EGFR	IP		Santa Cruz	rabbit	4 μ g/mg protein	Poly
Anti-EGFR	WB	170	Santa Cruz	Rabbit	1:500	Poly
C54 (Anti-hERG1)	WB	135/155	In house	Rabbit	1:1000	Poly

RM-12 (anti-Beta1A)	WB	~110	Immunological Sciences	Rabbit	1:1000	Poly
TS2/16 (anti-B1)	IP		Biolegend	Mouse	5µg/mg protein	mono
	IF				5ug/ml	
	FACS					
Anti-αVβ5 (P1F6)	IP		Abcam	Mouse	3.75µg/mg protein	mono
	IF				1:1000	
	WB				1:1000	
	FACS					
Anti-αV(L230)	WB			Mouse	1:1000	mono
	FACS					
Anti-FAK	WB	125	Santa Cruz	Rabbit	1:1000	
Anti-pFAK Y397	WB	125	Cell Signaling Technology	Rabbit	1:500	
Anti-Paxillin	IF			mouse	1:1000	

WB → western blot, IP → immunoprecipitation, IF → immunofluorescence, FACS → fluorescence-activated cell sorting

3.2.3.2. Secondary Abs

Source Rabbit- 1:10000 dilutions anti-α rabbit-peroxidase in 0.1% Tween-PBS (T-PBS).

Source mouse- 1:5000 dilution anti- α-mouse peroxidase.

HRP-conjugated streptavidin- 1:10000 dilutions.

3.2.3.3. Secondary Abs with fluorescent dyes

Source Rabbit: Cy-3 conjugated rabbit 2nd antibody 1:1000 diltion in 10% PBS-BSA.

Source Mouse: Alexa-488 conjugate mouse 2nd antibody 1:1000 diltion in 10% PBS-BSA.

3.2.4. Drugs

HERG1 channel blocker E4031 and activator NS1643 were purchased from sigma and Enzo life sciences respectively.

3.2.5. Surface biotinylating agent

Hundred milligrams (in powder form) of Ez-link Sulfo-NHS-LC-Biotin was purchased from ThermoFisher. The powder was always freshly dissolved in ultrapure dd. H₂O at 0.5mg/ml before use.

3.2.6. Buffer solutions

All the components of the buffer solutions were prepared in ddH₂O unless mentioned otherwise.

3.2.6.1. Phosphate buffered saline (PBS)

PBS solution composition (1X) includes NaCl-8g, KCl-0.2g, Na₂HPO₄·2H₂O-1.44g and KH₂PO₄-0.2g in 1L dd.H₂O

3.2.6.2. Lysis buffer

Following table below shows the components of lysis buffer

Table 3. Components of lysis buffer

Ingredients	Mol wt	Quantity (vol)	Final conc.
NP40 10% in H ₂ O	617	1ml	150mM
NaCl 1.5M (10X)	58.44	1ml	150mM
Tris pH 8 (1M)	121.14	0.5ml	50mM
EDTA 100mM pH 8.0	292.24	0.5ml	5mM
NaF 100mM	41.99	1ml	10mM
Na ₄ P ₂ O ₇ 100mM	265.90	1ml	10mM
Na ₃ VO ₄ 200mM	183.91	20µl	0.4mM
H ₂ O		5ml	
Total		10ml	

3.2.6.3. Wash buffer

Following table shows the components of wash buffer

Table 4. Components of lysis buffer

Ingredient	Mol wt	Quantity (vol)	Final conc.
NP40 10% in H ₂ O	617	1ml	150mM
NaCl 1.5M (10X)	58.44	1ml	150mM
Tris pH 8 (1M)	121.14	0.5ml	50mM
EDTA 100mM pH 8.0	292.24	0.5ml	5mM
Na ₄ P ₂ O ₇ 100mM	265.90	1ml	10mM
H ₂ O		6ml	
Total		10ml	

3.2.6.4. Running buffer (5X)

Tris 15g, glycine 72g and SDS 5g were dissolved in 1L of dd.H₂O and stored in 4-8C.

3.2.6.5. Blotting buffer

Blotting buffer includes 3g of Tris and 14.4g of glycine in 800ml of ddH₂O and 200ml of methanol.

3.2.6.6. Buffers in calcium measurement experiments

HEPES ringer Buffer 1.2mM Ca²⁺ (for 1L): Set pH at room temperature (25⁰C) 7.568 that corresponds to pH~ 7.4 (at 37⁰C).

Table 5. Components of HEPES ringer buffer

Compound	Stock Conc. (M)	Volume (ml)	Final Conc. (mM)
NaCl	3	40.8	122.5
KCl	1	5.4	5.4
CaCl ₂	0.1	12	1.2
MgCl ₂	0.1	8	0.8
HEPES	2.38gm	-	10
Glucose	1.09gm	-	5.5

3.2.6.6.1. Calibration buffers

- a. 5mM Calcium buffer (for 500ml)

Table 6. Components of 5mM Calcium buffer

Compound	Stock Conc. (M)	Volume (ml)	Final Conc. (mM)
NaCl	3	20.4	122.5
KCl	1	2.7	5.4
CaCl ₂	0.1	0.277gm	5
MgCl ₂	0.1	4	0.8
HEPES	2.38gm	1.19	10

- b. 0mM Calcium buffer (for 500ml)

Table 7. Components of 5mM Calcium buffer

Compound	Stock Conc. (M)	Volume (ml)	Final Conc. (mM)
NaCl	3	20.4	122.5
KCl	1	2.7	5.4
EGTA	0.95gm	-	5
MgCl ₂	0.1	4	0.8
HEPES	2.38gm	1.19	10

3.3. Cell culture**3.3.1. PDAC cells**

PDAC cells Panc1 and MiaPaca2 were cultured in DMEM media freshly supplemented with 4mM l-glutamine and BxPC3 cells in RPMI media with 2mM glutamine. All the cell culture media were supplemented with 10% fetal bovine serum (FBS) and cultured at 37C and 5% CO₂ unless mentioned otherwise.

3.3.2. Model cell lines-HEK293 and mouse fibroblast GD25

The HEK293 and three GD25 cell lines (GD25WT, GD25B1A and GD25B1Tr) were culture as PDAC cells.

3.3.3. Human pancreatic stellate cells (hPSCs)

Immortalized hPSCs were cultured in DMEM-F12 media pre-supplemented with l-glutamine. The medium was freshly supplemented with 10% FBS. For hypoxic stimulation or activation, semi-to-fully confluent hPSCs were incubated at 37C in

serum-free DMEM media in hypoxic incubator (1% O₂, 5%CO₂) for not more than 18h.

3.3.4. Culture plate coating

Culture plates were coated with extracellular matrix (ECM) proteins like fibronectin (FN), collagen-1 (col-1), poly-l-lysine (PLL) and bovine serum albumin (BSA). FN and col-1 were coated at final concentrations of 5µg/cm² and 10µg/cm² (of surface area) respectively as per manufacturer's instructions. PLL at 20 µg/ml and BSA at 0.25mg/ml. All the coating substrates were diluted in serum-free media and plated to cover the entire growth surface followed by incubation at 37C for 1h (BSA for 30mins). Cells were seeded on to the coated surface for various time periods (described below).

3.4. Transfection

3.4.1. Transient transfection (plasmid DNA): DNA transfection

Panc1 cells were transfected with LifeAct-GFP plasmid using lipofectamine2000 as per the protocol. LifeAct-GFP plasmid besides coding for GFP protein also codes for a 17 amino acid peptide, at C-terminus of GFP, which binds to filament-actin. The transfected cells (GFP positive) were visualized for actin filaments using TIRF microscopy.

3.4.2. Stable transfection

HEK293 cells were transfected with pcDNA3.1 plasmid harboring genes coding for hERG1 potassium channel and antibiotic resistance gene against geneticin (G418). The transfection was performed by lipofecatamine 2000 as per Invitrogen protocol and cells were cultured under selection pressure by supplementing the culture media with G418 at 0.8mg/ml.

3.5. Cell proliferation assay

The PDAC cell lines; Panc1, MiaPaca2 and BxPC3 cells were cultured in respective media as mentioned above. For cell proliferation assay, ~ 90% confluent cells were serum starved for 18-20hr to synchronize the cells in G0/G1 phase. On the day of assay, cells were detached by trypsinization and pre-treated with hERG1 blocker at 40 μ M for 30mins at 37⁰C. The excess E4031 was removed by centrifugation and cells were freshly resuspended in complete medium. The cell density was estimated by trypan blue manual counting. Ten thousand cells were seeded in to each well of 96 wells plate in 200 μ l of final volume with E4031 and incubated for the duration of experiments. The cell proliferation and viability was estimated by trypsinizing the cells every 24hrs and manual counting using trypan blue exclusion method.

3.6. Soft agar colony formation assay

The clonogenic potential of cells was determined in soft agar assays. Cells were suspended in 2,5 ml of 0.35 % agar low melting point (Sigma) in DMEM medium containing 10% fetal bovine serum and plated on top of 3,5 ml of 0,5 % agar low melting point, in the same medium, in 60 mm culture dishes (1500 cells/dish). Wherever necessary, E-4031 (40 μ M) and hERG1-mAb (50-100 μ g/ml) were added to the medium. Cells were then incubated fourteen days at 37⁰C in a CO₂ humidified incubator. Colonies were visualized by staining with 2% methyele blue in 50% ET-OH, images of the stained colonies were acquired and counted with ImageJ software.

3.7. Cell adhesion assay

The 96 wells plate was coated with 1 μ g of FN per well. For cell adhesion experiments on ECM proteins cells were detached by PBS-EDTA (5mM), pelleted and resuspended in serum-free DMEM medium. Ten thousand cells were seeded on it to study the time course of cell adhesion and the effect of functional blocking of hERG1 channel by E4031 on cell adhesion. During the time-course of adhesion, unattached cells were washed away with PBS and attached cells were fixed using 4%

para-formaldehyde (PFA) for 15' at RT, washed three times of PBS. Fixed cells were stained by toulidine-blue at final concentration of 0.5% in PFA for 10' at RT. Excess toulidine blue was washed way with PBS (at least 3 times) and stained cells were treated with 5% SDS for 10' to recover the toulidine-blue. The absorbance was measured at 595nm and percentage of cell adhesion was estimated.

3.8. Cell migration assay

The cell migration work was performed as Secondment in collaboration with Prof. Albrect Schwab, University of Munster, Germany. The PSCs were hypoxically activated for not more than 18h in serum-free DMEM media. During the activation PSCs secrete large number of proteins like GFs, cytokines, col-1 and MMPs etc that stimulate Panc1 cell migration. In parallel, 12 cm² T-flasks were coated with 'desmoplastic matrix cocktail' (see table below) at incubated at 37C for polymerization. One milliliter of matrix cocktail was used to coat six T-flasks. Twenty five thousand Panc1 cells were resuspended in serum-free media, seeded on the coating and allowed to spread (1-2hr). The Panc1 cell migration was stimulated by replacing serum-free medium with conditioned medium of hypoxically activated PSCs. The cells were immediately treated with hERG1 blocker E4031 at final concentration of 40μM and time-lapse images were acquired using bright field microscope for 6hr with interval of 5mins. For the analysis of cell migration every second image (10minutes interval) of last 4 hours was considered. To track the cell migration path total of 25 images of each cell were painted using the software program Amira.

Table 8. Composition of despmoplastic matrix

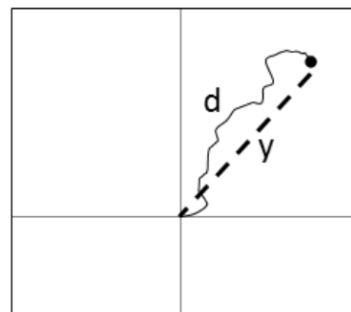
Composition	Concentration	Volume	Final concentration	Percentage of matrix (%)
RPMI 5x	52 g/L	200 μL	10.4 g/L	
HEPES 10x	100 mmol/L	100 μL	10 mmol/L	
NaOH	1 mol/L	4.8 μL	4.8mmol/L	
H ₂ O	-	397 μL	-	
Laminin	1 mg/mL	40 μL	40 μg/mL	4.46 %

Fibronectin	1 mg/mL	40 μ L	40 μ g/mL	4.46 %
Collagen IV	0.9 mg/mL	6 μ L	5.4 μ g/mL	0.602 %
Collagen III	1.0 mg/mL	12 μ L	12 μ g/mL	1.34 %
Collagen I	4 mg/mL	200 μ L	800 μ g/mL	89.15 %
		1000 μl	Total conc. 897.4 μg/ml	100%

3.8.1. Cell migration analysis

For quantification and tracking of 2D migration the Amira Imaging Software was used to label the circumferences of the cells as previously described (Fabian et al., 2012; Fabian et al., 2008). The individual cell contours were manually determined frame-by-frame over the entire migration movie, which then served as the basis for further analysis. Every other image of the time-lapse video was selected for analysis giving intervals of 10 min duration. The duration of the migration movie analyzed was between 2-6h. Using a Java-based Plugin for ImageJ individual data files could be obtained for each segmented mPSC. This data file was then imported into Microsoft Excel and the following parameters were determined:

Cell migration tracking and calculations of speed, distance, directionality,



$$\text{Directionality} = y/d$$

Definitions of Directionality. The directionality of migration is calculated by the translocation from start to end (y) divided by the total distance covered (d). Changes in the directionality can point toward difficulties in the cells steering capabilities.

1) Migration velocity [μ m/min]: Calculated from the movement of the cell center per unit time.

- 2) Translocation [μm]: Defined by the distance from start to end position.
- 3) Total path length [μm]: Defined by the total distance covered (from start to end position) during the migration movie. Calculated from mean velocity multiplied with the duration of the movie in minutes.
- 4) Directionality: The ability of the cell to move in a direct line from A to B. Calculated by the translocation (start to end point) (y) divided by the total path length (d). Cells moving in a direct line give values close to “1”, whereas cells changing direction give lower values.
- 5) Cell Area [μm^2]: Defined by the projected area covered by the cell. Not applicable to cells followed/marked only with a dot (cell center).
- 6) Structure Index [SI]: The structure index defines cell morphology. Spherical cell shape structures give values close to “1”, whereas values closer to “0” indicate a more star-shape and extended structure/morphology. SI was calculated as follows:

$$SI = (4 * \pi * A) / p^2$$

“A” is the area covered by the cell and p is the perimeter of A.

3.9. (Co)-Immunoprecipitation

For all the (co)-immunoprecipitation experiments cells were seeded on the culture plates coated with substrates like ECM proteins, PLL or BSA (as mentioned above) and incubated for a mentioned duration of time. After the desired time period of incubation for cell attachment on substrates cells were gently collected by mild scraping and resuspended in ice cold PBS. Further cell pellet was gently resuspended in lysis buffer to lyse the cell membrane without lysing the nuclear membrane and incubated for 15-20mins on ice. Cell lysate was centrifuged at maximum speed for 10mins at 4C and supernatant was collected. Total protein concentration was quantified using Bradford assay and 2mg of total lysate was considered for (co)-immunoprecipitation step. Two mg of total lysate was subjected to pre-cleaning step by adding 25 μl protein A/G agarose beads and incubated for at least 1.5h at 4C to

capture IgG type antibodies from the total lysates. The supernatant was collected and further subjected to overnight immunoprecipitation (IP) by specific antibodies against protein-of-interest. After overnight incubation the immuno-complex was captured by 30µl of protein A/G agarose beads for 2hr. The agarose beads were washed for 3 times in ice-cold wash buffer and 3 times in ice cold PBS followed by addition of 2 X lameli buffer (14µl) and boiled for 5mins at 95C. The supernatant was subjected to sodium dodecyl sulfate-protein agarose gel electrophoresis (SDS-PAGE) for desired period of time.

3.9.1. Immunoprecipitation of surface biotinylation

For biotinylation of surface proteins cells seeded on ECM etc were collected and washed in PBS as above. Cells were resuspended in sulfo-NHS-LC-Biotin (Thermo fisher) at 0.5mg/ml and gently agitated at room temperature (RT) for 30mins. Excess biotinylating agent was removed and cells were washed 3 times with ice cold PBS. Cells were then lysed for 20mins on ice using lysis buffer (Tris-HCl 20mM, pH 7.4, NaCl 150 mM, glycerol 10%, Triton X-100 1%, phenylmethanesulfonyl fluoride (PMSF) 1 mM, aprotinin 0.15 units/ml, leupeptin 10mg/ml, NaF 100 mM, Na vanadate 2 mM). The total protein concentration estimation and subsequent steps of IP was followed as mentioned above.

3.10. Sodium dodecyl sulfate protein agarose gel electrophoresis (SDS-PAGE)

All the protein samples were loaded onto 7.5% SDS gel and subjected to SDS-PAGE for desired time period. Below is the composition of resolving gel and stacking gel. The protein electrophoresis was run in 1X running buffer of 650ml.

Table 9. Composition of resolving and stacking gel

Resolving gel		Stacking gel	
<i>Components</i>	<i>1 gel</i>	<i>Components</i>	<i>1 gel</i>
dd. H2O	3.4 ml	dd. H2O	2.41 ml
1.5M TRIS-HCL	1.75 ml	0.5M TRIS-HCL	1 ml

pH8.8		pH 6.8	
10% SDS	70 μ l	10% SDS	40 μ l
Acrilamide/bis	1.75 ml	Acrilamide/bis	530 μ l
10% APS	35 (70 μ l)	10% APS	20 (40 μ l)
TEMED	3.5 (7 μ l)	TEMED	4 (8 μ l)
Total volume	7 ml	Total volume	4 ml

3.10.1. Western blot (WB)

After protein electrophoresis the proteins in the gel were transferred onto PVDF membrane in blotting buffer under cold condition for 1hr at 100V. The PVDF membrane was then blocked with 5% BSA in T-PBS solution for 3hr at RT to cover the unspecific antibody binding sites on the membrane. The membrane was incubated ON with antibody of interest. The following day the membrane was washed with T-PBS (15mins X 3 times) and appropriate secondary antibody conjugated with peroxidase enzyme was dissolved in 5% BSA in T-PBS for at least 45mins and washing steps were repeated as before. The membrane was then illuminated with ECL solution in dark room to reveal the protein bands transferred on the blotting paper. Re-blotting on the same membrane was performed after stripping the membrane with stripping solution (mild or strong stripping solution depending on the signal), blocking again with 5% BSA in T-PBS for 30' and ON incubation of primary Ab.

3.11. Fluorescence activated cell sorting (FACS) analysis

FACS was employed to study the surface expression of integrin subunits like β 1, β 3 and α V β 5 integrins. Firstly, integrins were stimulated by seeding the cells on ECM proteins till cell spreading and cells were collected, washed with ice cold PBS three times and primary antibody against integrins were added for 30-45mins at RT. Excess/unbound antibody was removed, washed as above and secondary antibody was added for 30mins and washing step was performed again. The cells were then resuspended in PBS and subjected to FACS analysis for quantifying the % of cells expressing integrins at the membrane level.

3.12. Immunofluorescence (IF)

Thin glass cover slips were ethanol and flame sterilized and coated with fibronectin (FN). The cells were seeded on the glass cover slips for the desired time period. The unattached cells were washed away with PBS and cells were fixed with 4% methanol-free para-formaldehyde (PFA) for 15' at RT. The excess PFA was removed and washed three more times with PBS. For staining the membrane proteins, cells were incubated with appropriate antibodies specific for membrane proteins of interest overnight at 4C or 1-2h at RT followed by incubation with secondary antibodies conjugated with fluorescent dye-Alexa488 or Cy-3 (see the table-2 list of antibodies and secondary antibodies and their dilution). For intracellular staining, cells were permeabilized with 0.01% Triton-X for 5' at RT, washed with PBS. Cells were then blocked with 5-10% BSA in PBS solution for at least 90' at RT, washed and incubated with appropriate antibodies or rhodamine conjugated phalloidin (for actin). Cells were mounted in mounting solution containing DAPI for nucleus staining.

3.13. Microscopy for image acquisition

3.13.1. Confocal microscopy and Image analysis using Fiji software

The fluorescent labelled cells were examined under confocal microscope Nikon Eclipse TE2000-U (Nikon). The images were captured at 512X512 pixels; objective used was 60X and numerical aperture 1.4.

Fiji software was used to (i) study co-localization between hERG1 and Beta1 integrins. The images acquired using multi fluorescence channel confocal microscope was processed using built-in plugin coloc2, with default settings, to study the degree of co-localization between hERG1 and Beta1 integrins. (ii) The Fiji software was also used to estimate the number of focal adhesions of FAK and paxillin and their area (Horzum U et al., 2014).

3.13.2. Image acquisition for actin dynamics study using Total internal reflection fluorescence (TIRF) microscope

Panc1 cells were transfected with lifeAct-GFP that binds the f-actin filaments without interfering with the dynamics of actin (Riedl et al., 2008). The inverted microscope was equipped with digital camera (Visitron), TIRF slider (TILL Photonics) and a 100x 1.45 oil immersion objective. The TIRF microscope was used to acquire images of cells stained for actin with lifeAct-GFP. The image acquisition was controlled by MetaVue program and time-lapse images were acquired every 1second for two minutes (Nechyporuk Z.V et al., 2008).

3.14. Actin dynamics analysis using Spatio-temporal image correlation spectroscopy (STICS) method

To assess the actin dynamics, the time series of images (acquired by TIRF microscope) were analysed using the spatio-temporal image correlation spectroscopy method (Hebert B et al., 2005). Each image (1024x1024 pixels) has been divided into smaller non-overlapping regions of interest (ROIs) of 16x16 pixels. An immobile filtering method has been performed to delete the contribution of fluorescent immobile structures (same Hebert citation above). Frames t apart in time was then spatially correlated to obtain 2D Gaussian-like spatio-temporal correlation functions (CFs). By means of a non-linear least squares (asymmetric) 2D Gaussian fitting, we obtained the temporal evolution of the Gaussian peak position and width. If flow is present in the ROI, the displacement of the peak over time is directly related to the velocity (i.e. $x_p = -v_x t$ and $y_p = -v_y t$). The diffusion coefficient is instead obtained from the increase of the Gaussian width over time (i.e. $w = w_0 + 4Dt$). To determine the minimum velocity that the method is able to detect, we simulated movies (120 frames at 1Hz) of only diffusing particles (i.e. no flow) in 16x16 pixels frames, setting all the parameters according to the analysis of real data (i.e. the diffusion coefficient D was set $0.25 \text{ pixels}^2/\text{frame}$ and noise has been added to obtain a signal-to-noise-ratio (SNR) of ~ 8). The STICS analysis have been performed on these simulated data and the resulting detected velocity was $v_{\min} = 0.004 \pm 0.002 \text{ } \mu\text{m/s}$. All the obtained

velocities were then cleaned according to the threshold and used to build flow maps superimposed on the fluorescent images

3.15. Calcium measurement (by VisiView program)

The intracellular free calcium level was measured by treating the cells with free calcium binding dye Fura2 in 1ml (final conc. 3 μ M). Fura2 was mixed in either PSC conditioned medium or serum free DMEM medium and incubated for 30mins at 37C. The excess Fura2 was removed and replaced with HEPES ringer buffer (containing 1.2mM CaCl₂). The images were acquired for every 10 seconds during the entire course of the measurement. Intracellular calcium intensity was measured at 340nm wavelength for Fura2 dye. The measurement was done in pre-warmed constant perfusion of HEPES ringer buffer. When the intensity (and ratio of 340/380nm) was stabilized the perfusion was stopped and cells were treated with E4031 in HEPES ringer buffer for at least 10mins and the intensity was measured. When the intensity was stabilized then the perfusion was again started with 0mM Ca²⁺ calibration buffer supplemented with 20ul ionomycin until the Fura2 intensity was stabilized. Then the perfusion was switched to 5mM Ca²⁺ calibration buffer supplemented with 20ul ionomycin and intensity was measured till stabilization.

3.16. Patch-clamp recording

Membrane currents were recorded in the whole-cell configuration of the patch-clamp technique, at room temperature (about 25°C), by using a Multiclamp 700A amplifier (Molecular Devices). Micropipettes (3-5 M Ω) were pulled from borosilicate glass capillaries (Harvard Apparatus), with a PC-10 pipette puller (Narishige). Series resistance was always compensated (up to approximately 80%). Currents were low-pass filtered at 2 kHz and digitized online at 10 kHz, with Digidata 1322A and pClamp 8.2 (Molecular Devices). Data were analyzed off-line with pClamp 8.2 and OriginPro 8.0 (Microcal Inc.). Pipette contained (in mM): K⁺ aspartate 130, NaCl 10, MgCl₂ 2, CaCl₂ 2, HEPES 10, EGTA 10, titrated to pH 7.3 with KOH. During the experiments, cells were perfused with an extracellular solution

containing (in mM): NaCl 130, KCl 5, CaCl₂ 2, MgCl₂ 2, HEPES 10, Glucose 5, adjusted to pH 7.4 with NaOH. In this case, the K⁺ equilibrium potential (E_K) was -80 mV. When necessary, a high extracellular [K⁺] was applied to increase the amplitude of the currents measured at -120 mV. In this case, the NaCl and KCl concentrations were, respectively, 95 and 40 mM ($E_K = -30$ mV). The activation curves for hERG1, hERG1 Δ 2-370, hERG1 Δ C+RD and G628S were determined from peak tail currents (I_{tail}) at -120 mV (for 1.1 s), following 15 s conditioning potentials from 0 mV to -70 mV (10 mV steps). The time between consecutive trials in the same stimulating protocol was 4 s. The holding potential (V_H) was 0 mV. The activation curves for hERG1, hERG1-K525C and hERG1-R531C were obtained following a stimulation protocol similar to the one used by Zhang et al. From a negative holding potential (V_H -80 to -120 mV), we applied 1 s test voltages (in 10 mV increments) every 15 s. The test voltages (V_t) varied from -60 to +40 mV, from -70 to +50 mV and from -30 to +70 mV, respectively for hERG1, hERG1-K525C and hERG1-R531C. To elicit I_{tail} the test voltages were followed by repolarisation to -50 mV. Currents were registered in the presence of 5 mM-extracellular K⁺. For each cell the peak amplitude of I_{tail} obtained at the different test voltages was normalized to the maximum tail current (I_{max}). The relationship between normalized tail currents (I_{tail}/I_{max}) and V_t was fit to a Boltzmann function.

4. Results and Discussion

4.1. HERG1 channels are involved in PDAC cell proliferation and anchorage independent colony formation through MAPK/ERK signaling cascade

4.1.1. HERG1 channels are expressed differentially in PDAC cells

The three PDAC cells Panc1, MiaPaCa2 and BxPC3 cells were firstly characterized for the expression of hERG1 channels. The hERG1 expression was analysed for the mRNA levels by qPCR (figure 1a), protein levels by immunoprecipitation (IP) of total lysate (figure 1b), surface expression of the hERG1 channels by immunofluorescence (IF) (figure 1c) and hERG1 current by whole cell patch clamp (figure 1d). The Panc1 and MiaPaCa2 cells show several fold higher expression of hERG1 channels compared to BxPC3 cells (Lastraioli et al, 2014).

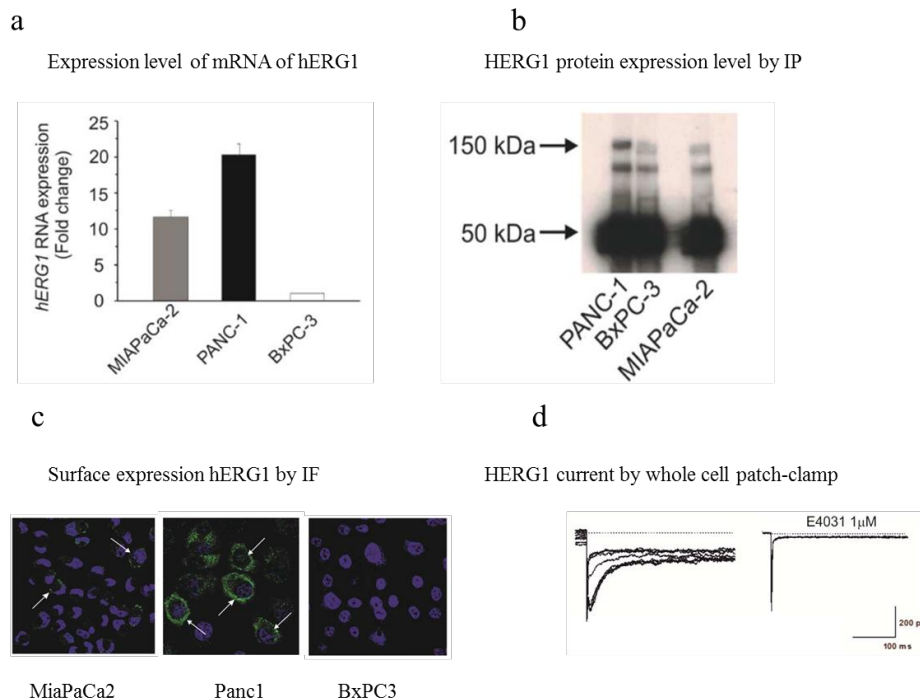


Figure 1. The characterization of hERG1 expression in PDAC cells. Panc1 cells show highest expression of hERG1, MiaPaca2 shows intermediate and BxPC3 cells show lowest expression of hERG1 channels. (Note: These data was taken from Lastraioli et al 2015 in which I am a co-author).

4.1.2. PDAC cell proliferation

All three PDAC cell lines Panc1, MiaPaca2 and BxPC3 were used for studying the role of hERG1 channels in cell proliferation. The cell lines were serum starved for at least 18h to synchronize the cells in G0/G1 phase. Ten thousand cells were seeded per well in 96-well plate and treated with hERG1 channel specific blocker E4031 at 10 μ M, 20 μ M and 40 μ M concentrations. The cell proliferation was estimated every 24h by trypan blue exclusion assay as described in material and methods section. The effect of E4031 on cell proliferation was observed to be dose dependent and was also in direct co relation to the amount of hERG1 expressed by cells. The highest effect of E4031 was observed in Panc1 and MiaPaca2 cells at 72h at concentration of 40 μ M (figure 2). Hence in all subsequent experiments we used E4031 at 40 μ M concentrations unless mentioned otherwise.

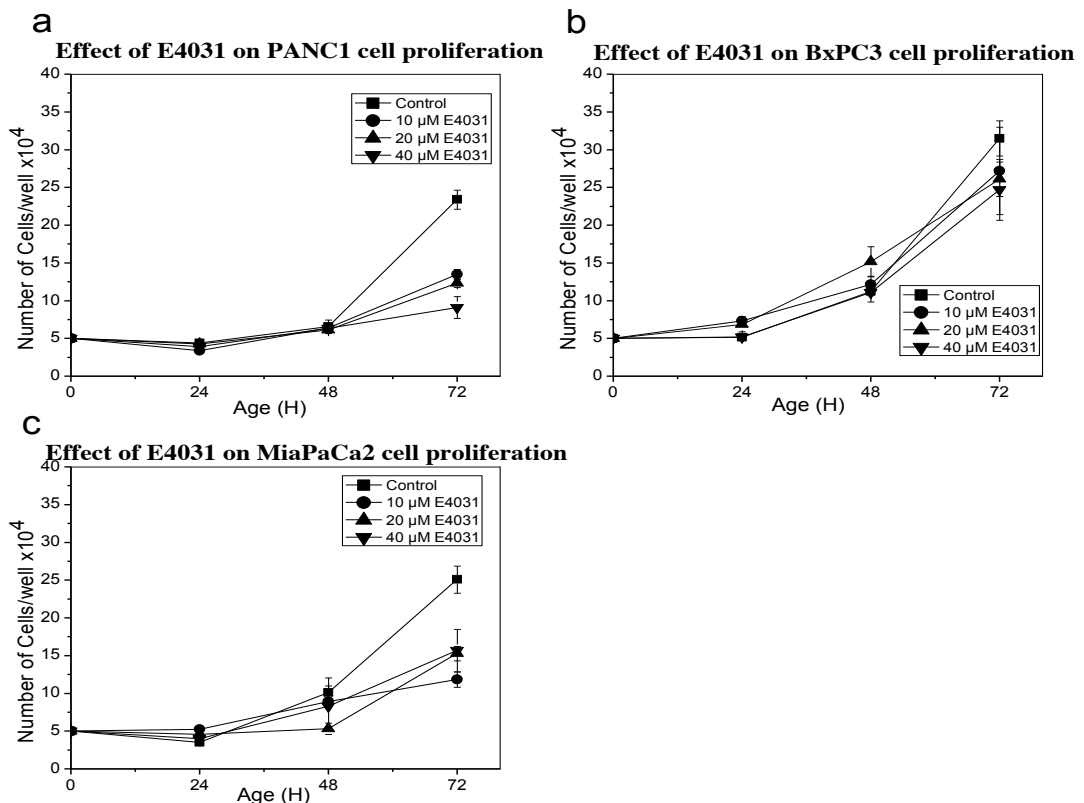


Figure2. All three PDAC cells were treated with hERG1 channel specific blocker E4031 at different concentrations and cell proliferation was estimated by trypan blue method. The E4031 at final concentration of 40 μ M showed the highest decrease in proliferation of all three-cell lines.

4.1.3. PDAC soft agar colony formation

We further studied the ability of these cell lines in colony formation in anchorage independent manner. Invasive cancer cells have the ability to survive and grow in anchorage independent manner during invasion. The role of hERG1 channels in aiding such process was tested in soft agar colony formation assay. Both Panc1 and MiaPaca2 cells were seeded at both 1500 and 3000 cells per 60mm dish and treated with E4031 (40 μ M). The cells were grown for two weeks and the effect of E4031 on colony formation was estimated by difference in number colonies formed. BxPC3 cells, however, did not form any colonies at 1500 and 3000 cells/dish but when seeded at 10,000 cells/dish they formed colonies much fewer than Panc1 and MiaPaCa2 cells. Similar to the effect observed on cell proliferation, E4031 treatment significantly decreased the number colonies of formed in Panc1 and MiaPaCa2 cells but not in BxPC3 cells (figure 3).

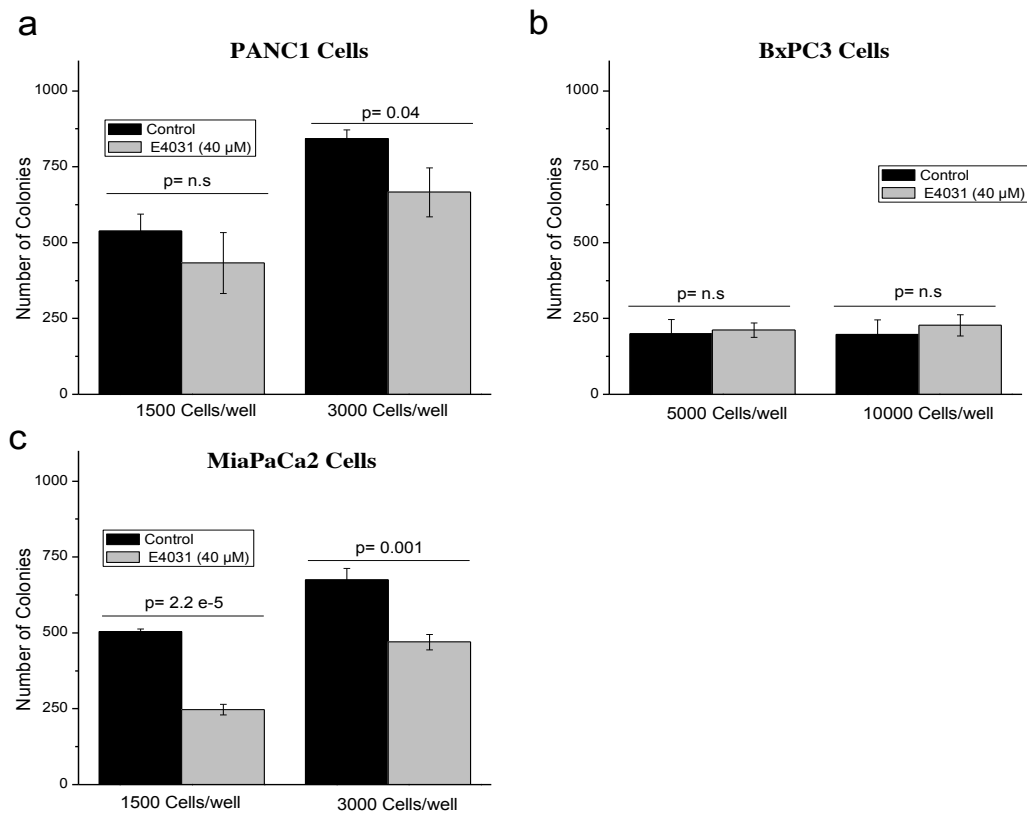


Figure3. All three-cell lines were treated with hERG1 channel specific blocker E4031 during the

course of the experiments (2 weeks). The E4031 treatment significantly decreased the number of colonies formed by *Panc1* and *MiaPaCa2* cells (a and c).

The cell proliferation and growth involves wide array of signaling cascades including KRAS/MAPK and AKT pathways that are reviewed extensively in (Durino RJ and Xiong Y, 2013). Interestingly, hERG1 channel coding gene *KCNH2* is clustered in the signaling network together with *KRAS* and *TP53* that is related to tumor growth and metastasis of pancreatic cancer (Zhou B et al., 2012). So we studied whether hERG1 channel was involved in MAPK/ERK and ATK signaling pathways in tumor cell growth. All three cells were treated with E4031 for three-hour in complete medium, total lysate was extracted and 15µg of total lysate was separated in SDS-PAGE. The E4031 treatment decreased the activation of MAPK/ERK pathway in accordance with cell proliferation. The significant decrease in MAPK/ERK pathway was observed only in *Panc1* cells and pAKT pathway was not affected in any cells (figure3).

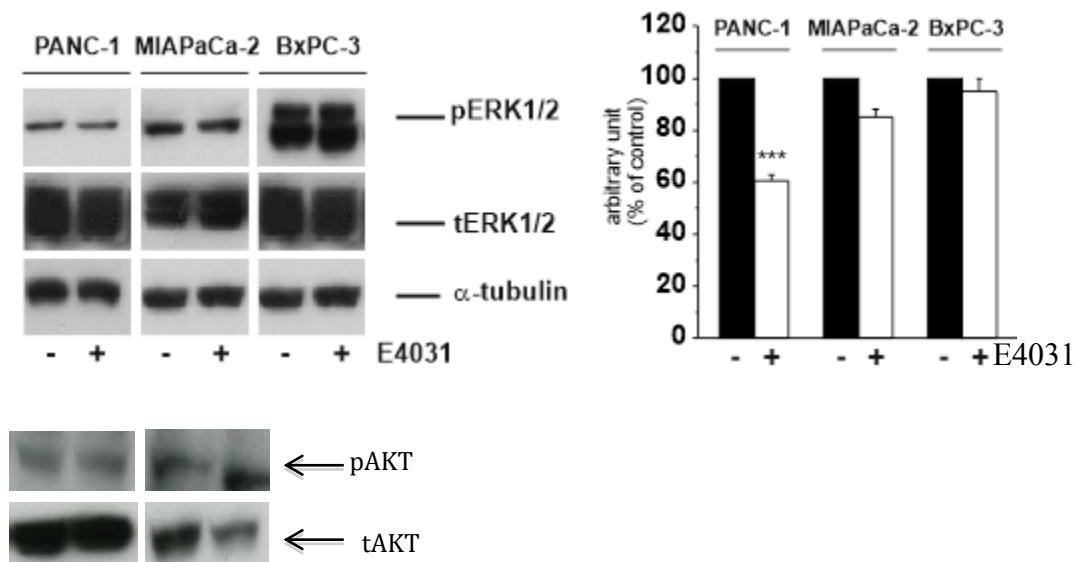


Figure 4. All cell lines were treated with E4031 to study the effect on MAPK and AKT pathways. Western blot images (right) show the decrease in MAPK pathway only in *Panc1* cells that is also represented as blot intensity (on left). AKT pathway was not affected in these cells.

4.2. Characterization of surface expression of integrins in pancreatic ductal adenocarcinoma (PDAC) cell lines

There is growing evidence that several integrin expressions are up regulated (and some are also down-regulated) in most of the primary tumours and tumor cell lines. These integrins are involved in various steps of tumor progression and thus they are perceived to be potential drug targets (Desgrosseillier J.S and Cheresh D.A, 2010). The tumor cells switch the expression of several integrins during tumor progression and retain some integrins, due to the selection pressure exerted by the host on the genetically unstable cancer cells. For ex, neoplastic cells lose some of the integrins that secure the adhesion and retain the integrins that are involved in cell survival, migration and proliferation (Guo W and Giancotti F.G, 2004).

So we aimed to characterize the surface expression of $\beta 1$ and $\alpha V\beta 5$ integrins in Panc1 and BxPC3 cells seeded on various ECM. All the confocal images presented henceforth were taken with the collaboration of Dr Matteo Lulli, University of Florence. The study of surface expression of these integrins was performed by fluorescent assisted cell sorting (FACS) analysis, immunofluorescence and IP of surface biotinylated proteins. The cells were seeded on ECM coated dishes until cells were attached and spread. In the FACS analysis, cells were stained for specific anti-integrin antibodies at room temperature (RT) followed by secondary antibody. The cells were then subjected to FACS and mean fluorescence intensity (MFI) for each integrin was quantified against only secondary antibody stained cells. Figure shows the MFI of $\beta 1$ and $\alpha V\beta 5$ integrins in Panc1 and BxPC3 cells seeded on ECMs. To our surprise, we observed (i) lower MFI for $\beta 1$ and $\alpha V\beta 5$ integrins in Panc1 cells and (ii) higher MFI for $\alpha V\beta 5$ integrins in BxPC3 cells. Because, researchers have shown that $\beta 1$ and $\alpha V\beta 5$ integrins are highly expressed in Panc1 cells and $\alpha V\beta 5$ is poorly or not expressed in BxPC3 cells (Grzesiak J.J and Bouvet M, 2006).

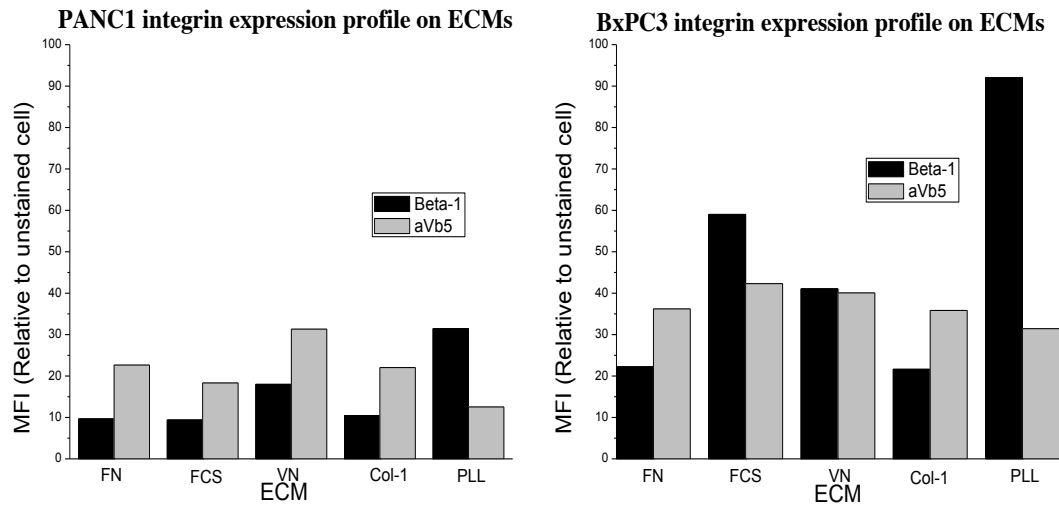


Figure 5. The surface expression of β 1 and α V β 5 integrins was quantified by FACS analysis in Panc1 and BxPC3 cells seeded on various ECM.

To confirm the above observation on MFI of integrins in Panc1 and BxPC3 cells we performed immunofluorescence experiments on Panc1 and BxPC3 cells and observed differential expression of various integrins as above. Both Panc1 and BxPC3 cells showed strong surface expression of β 1 integrins whereas α V β 5 integrins were moderately stained in Panc1 cells and very poorly stained in BxPC3 cells. The fluorescence intensity of integrins showed more diffused signal when cells were seeded on FN due to the largely spread cell surface area compared to round cells on PLL where the signals were more concentrated (figure 6A). So we quantified the corrected total cell fluorescence (CTCF) signal considering the surface area of the cells. The CTCF values demonstrate that integrin activation by FN leads to highly increased membrane trafficking of integrins compared to PLL (figure 6b). We further biotinylated the surface proteins and immunoprecipitated with appropriate antibodies against integrins. Panc1 cells showed similar enhanced level of surface expression in β 1 but surprisingly we observed an enhanced surface expression of α V β 5 when seeded on FN in contrast to PLL (figure 6c). The discrepancies we observed in the surface expression of integrins, in spite of employing same anti-integrin antibodies, could be because of the experimental protocol dependent for ex, staining of fixed cells (for IF) and staining the detached cells in suspension (FACS). So conclude that

at the total protein level $\beta 1$ was highly expressed in both Panc1 and BxPC3 cells and $\alpha V\beta 5$ only in Panc1.

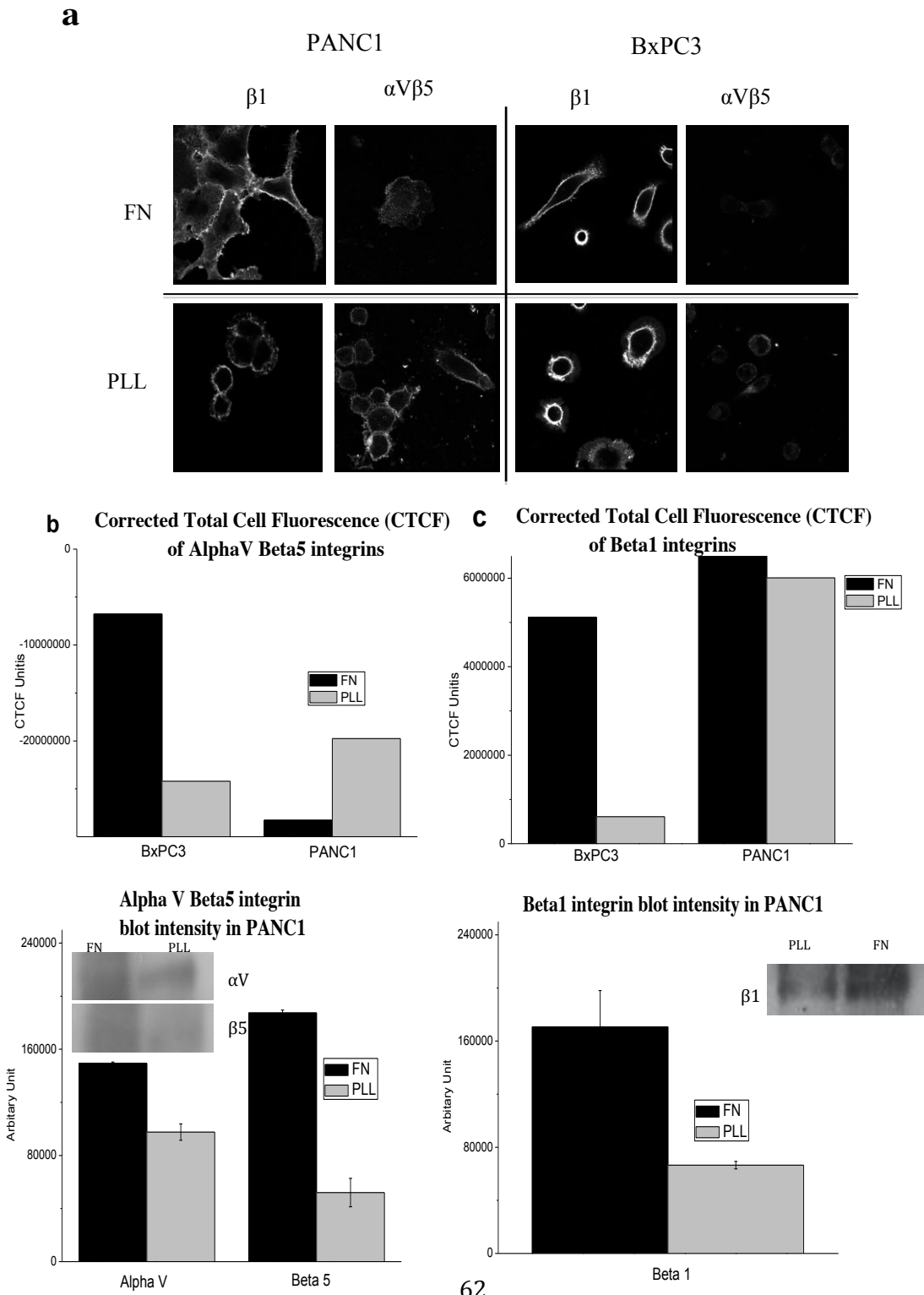


Figure 6. Characterization of surface expression of integrins $\beta 1$ and $\alpha V\beta 5$ in Panc1 and BxPC3 cells. The surface expression of these integrins was greatly enhanced when cells were seeded on fibronectin in contrast to cells seeded on PLL. The immunofluorescence images of cells stained for $\beta 1$ and $\alpha V\beta 5$ integrins (a) were used to quantify the corrected total cell fluorescence (CTCF) for each of the integrins (b). The IP experiments of surface biotinylated proteins in Panc1 cells also showed enhanced localization of surface integrins when cells were on FN (c).

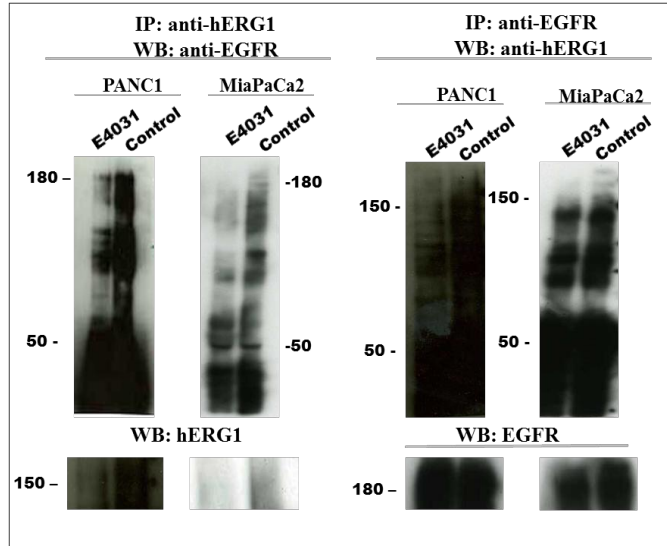
4.3. HERG1 channels make macromolecular complex formation with EGFR and integrin subunits

We further aimed to study the interactions between hERG1 channels and membrane receptors like integrins and EGFRs. In almost all cancers it is well established that there is an up-regulation of wide range of membrane proteins like ion channels, growth factor receptors and integrin receptors that play a role in promoting tumor growth. Ion channels are transmembrane proteins that form the pores on the cell membrane for the easy passage of ions across the membrane. Due to the strategically membrane localization of these channels and ability to conduct ions across the membrane they are implicated to play key role in wide range of cellular activity including tumor promoting cell signaling pathways in proliferation, invasion, angiogenesis, migration, invasion and metastasis in addition to cellular physiology. These activities are more often carried out through the interactions with other membrane proteins like growth factor receptors (Rosen L.B and Greenberg M.E, 1996; Pillozzi S et al., 2007), G-protein coupled receptors (Altier C and Zamponi C, 2011), integrins (Pillozzi et al., 2007; Crociani O et al., 2013) etc. For example, hERG1 channels interact with $\beta 1$ integrins and promote the signaling cascade in angiogenesis in colorectal cancer (Crociani et al. 2013). Similarly EGFR has been shown to interact with $\beta 1$ integrin and $\alpha V\beta 5$ integrins to promote tumorigenic properties in lung (Morello V et al., 2011) and pancreatic cancer cells (Ricono J. M et al., 2009) respectively. In the above studies we have shown the hERG1 channels modulate MAPK pathway, perhaps through interactions with EGFR. So firstly, we investigated the complex formation between hERG1 and EGFR in PDAC cells in

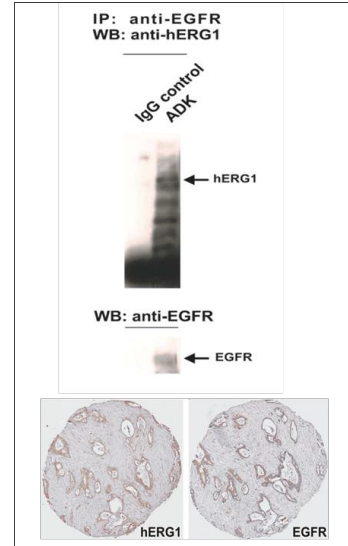
10%FCS supplemented medium. In the PDAC cells Panc1 and MiaPaca2, hERG1 channels co-immunoprecipitate (co-IP) with EGFR (figure 7a). Similar complex formation was also observed when co-IP was performed on three different primary PDAC samples (figure 7b). In addition, immunohistochemistry (IHC) on the same primary PDAC tissue sections reveals the co-expression of hERG1 and EGFR (figure 7b right panel). We further tested the role of E4031 in hERG1-EGFR complex formation and observed that E4031 did not interfere with complex formation (data not shown).

Secondly, we investigated whether hERG1 channels make complex with integrin subunits. As described in above section, we characterized the expression of various integrins in PDAC cells and observed that $\beta 1$ and $\alpha V\beta 5$ integrins are highly expressed in Panc1 cells while BxPC3 cells do not express high $\alpha V\beta 5$ and hERG1 channels. So for further experiments we considered only Panc1 cells (and BxPC3 cells wherever necessary as a negative control). The co-IP experiments included the stimulation of integrins by appropriate ECM like fibronectin, collagen-1, vitronectin and non-stimulant coating of poly-l-lysine (PLL as a non-integrin mediated adhesion). Cells were seeded on these matrix proteins till cells showed spread morphology (typically 60mins). The co-IP experiments were performed using appropriate antibodies as explained in methods section. HERG1 was observed to co-IP with $\beta 1$ integrins in all stimulation conditions including serum medium, but interestingly, under non-stimulating conditions like PLL hERG1 did not co-IP with $\beta 1$ integrin (figure 7c). In addition, hERG1 also makes complex formation with $\alpha V\beta 5$ in both stimulation and non-stimulation conditions (figure 7d). Thus in summary hERG1 channels make macro molecular complex with EGFR, $\beta 1$ and $\alpha V\beta 5$ integrins. However, hERG1/ $\beta 1$ complex formation occurs only when $\beta 1$ integrins is stimulated by ECM proteins as shown in scheme 8.

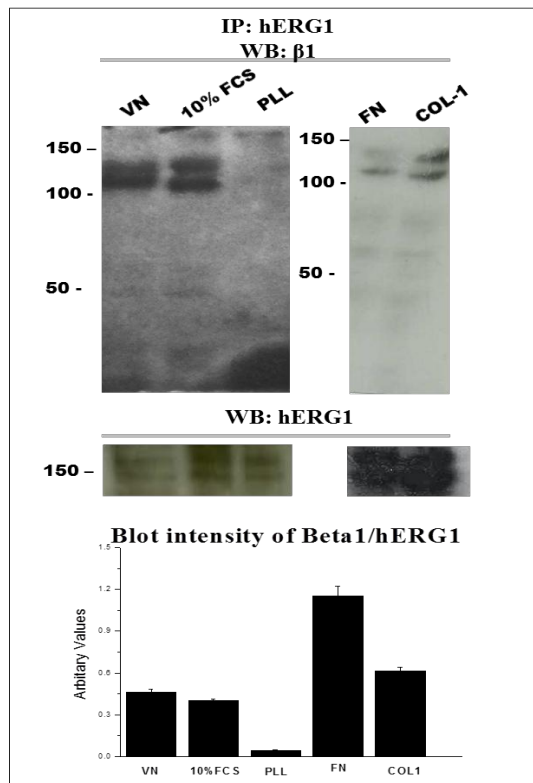
a



b



c



d

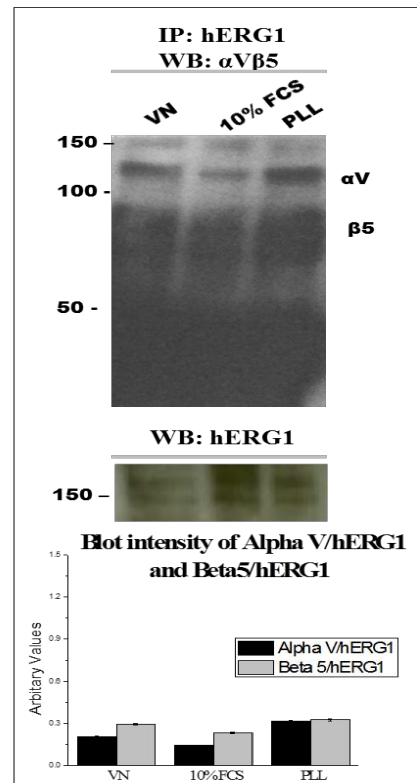
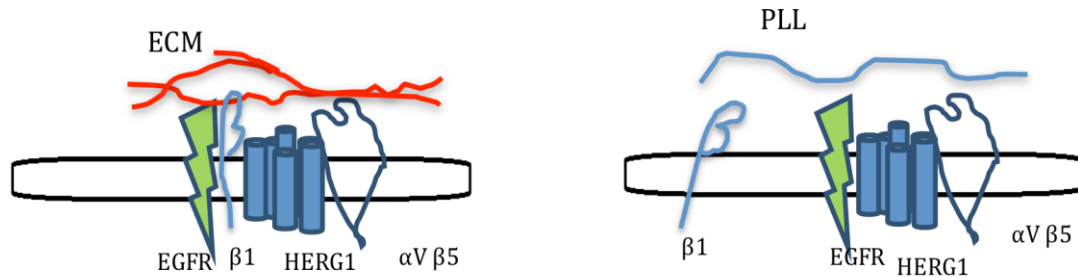


Figure 7. Co-immunoprecipitation of hERG1 with EGFR in PDAC cell lines (a) and PDAC primary cells and tissue samples (b). hERG1 channels also co-IP with $\beta 1$ (c) and $\alpha V \beta 5$ integrin (d).



Scheme 8. Summary of the macro molecular complex formation of hERG1 channel with EGFR and integrins under activation (left panel) and non-activation conditions (right panel).

We further pursued our interests in characterising the interactions between hERG1 and $\beta 1$ integrins in Panc1 cells. Cherubini et al have shown that hERG1 and $\beta 1$ integrin interactions is two-fold; integrin activation increases the conductance of hERG1 channels while the functional blocking of the channel has shown to mitigate the integrin mediated signaling, namely activation of FAK in hERG1 transfected HEK293 cells (Cherubini et al 2005). With this observation we aimed to study the membrane co-localization of the hERG1 and $\beta 1$ integrin in Panc1 cells seeded on fibronectin and poly-l-lysine (PLL) and treated the cells with hERG1 specific blocker E4031. Panc1 cells adhered on fibronectin and assumed spread morphology through the engagement of integrins while on PLL cells were attached with round shape. The immunofluorescence (IF) was performed to observe the co-localization of hERG1/ $\beta 1$ in Panc1 cells. The $\beta 1$ integrin stimulation by fibronectin showed strong co-localization between hERG1 and $\beta 1$ integrins (figure 8a) but functional blocking of hERG1 channels with E4031 treatment for 24hrs hERG1/ $\beta 1$ co-localization was significantly diminished (figure 8b). Similarly when $\beta 1$ integrins were not stimulated on PLL we observed diminished-to-poor co-localization in both untreated (figure 8c) and E4031 treated cells (figure 8d).

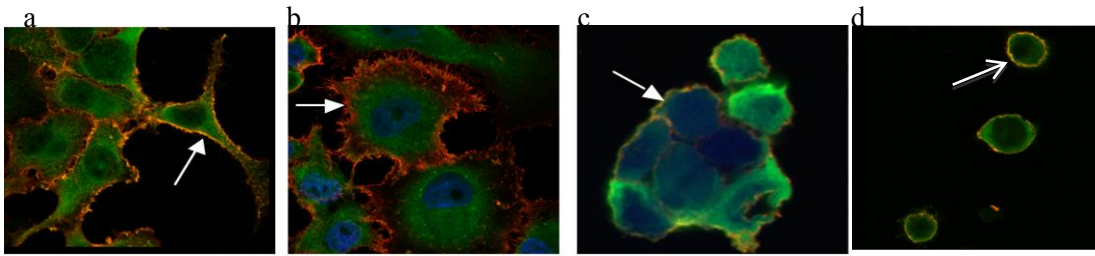


Figure 8. *HERG1* and $\beta 1$ co-localization in *Panc1* cells seeded on fibronectin without *hERG1* blocker treatment (a), treated with *hERG1* blocker (b) and on PLL, without blocker (c) and with blocker (d).

The degree of co-localization of hERG1/ $\beta 1$ was further quantified using Fiji software with built-in plugins. The analysis provides Pearson and Manders' co-localization values shown in table below. The values represented are the average values of at least 10 cells from three independent images. Manders' values tM1 and tM2 with threshold shows that hERG1/ $\beta 1$ co-localization was strongest in *Panc1* cells that were not treated with E4031 (control) and seeded on FN (control). The E4031 treatment as well as cells on PLL showed drastic decrease in co-localization.

Table 10. The Pearson and Manders' co-localization R-values in hERG1- $\beta 1$ co-localization

		FN-control	FN+E4031	PLL-control	PLL+E4031
Pearson R value (above threshold)		0.43±0.070	-0.09±0.111	0.19±0.025	0.363±0.089
Manders' value					
Without thresholds	M1 ($\beta 1$)	0.997	1.000	1.000	0.999
	M2 (hERG1)	0.979±0.006	0.976±0.010	0.938±0.031	0.748±0.036
With thresholds	tM1 ($\beta 1$)	0.972±0.005	0.581±0.203	0.562±0.142	0.549±0.079
	tM2 (hERG1)	0.960±0.012	0.499±0.180	0.384±0.053	0.199±0.039

4.3.1. The hERG1 intracellular domains are not necessary for hERG1/ β 1 interaction

After studying the functional role of hERG1 channels and activation of β 1 integrins in the complex formation, we investigated the molecular domains within these proteins that could be involved in the complex formation. To this purpose, we used three variants of hERG1 channels; WT hERG1, N-terminus deleted hERG1 (hERG1 Δ 2-370) and C-terminus deleted hERG1 (hERG1 Δ C+RD). The hERG1 Δ 2-370 lacks the entire N-terminus domain while hERG1 Δ C+RD lacks c-terminus except for the Recapitulation Domain (RD) that allows the hERG1 channels insertion into the plasma membrane. All three variants were stably transfected in HEK293 cells and hERG1 current was measured.

Figure 9A shows representative currents expressed by the two mutants. As a control, we used HEK-hERG1 cells, as indicated. In agreement with previous reports, hERG1 Δ 2-370 displayed the typical faster deactivation conferred by N-terminus deletion (Villoria C.G et al., 2000), whereas hERG1 Δ C+RD generally expressed current amplitudes considerably smaller than the controls' (Kupersmidt S et al., 1998). Cells expressing either hERG1 or hERG1 Δ 2-370 were immunoprecipitated with either anti- β 1 antibody (figure 9B, left), or the anti-hERG1 monoclonal antibody (figure 9B, middle). Cells expressing hERG1 Δ C+RD were instead only immunoprecipitated with the anti-hERG1 monoclonal antibody (figure 9B, right). Both the N-deleted and the C-deleted hERG1 associated with β 1 integrin to the same extent as hERG1. The average densitometric results are shown in figure 9C. These results suggest that the cytoplasmic hERG1 domain is not critical for assembly with β 1.

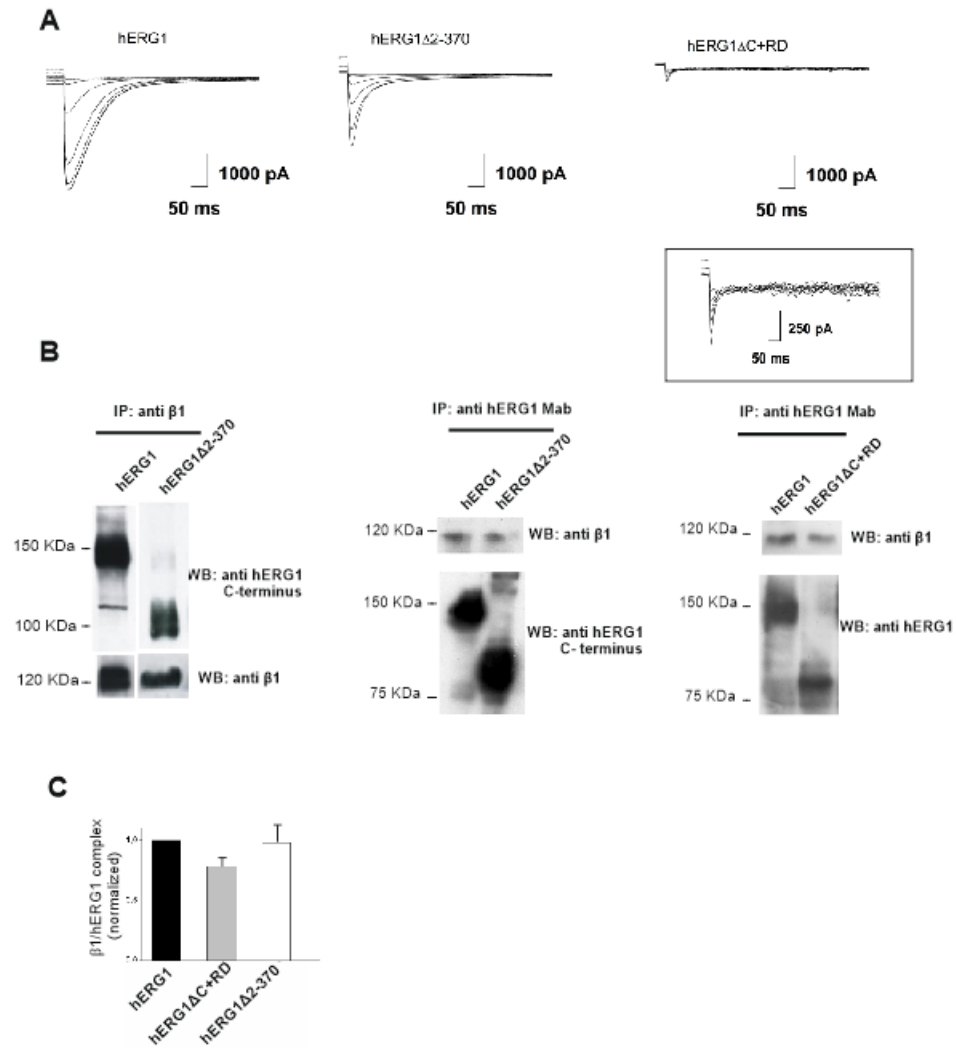


Figure 9. *HERG1* currents measured in HEK-*hERG1* cells stably transfected with the indicated constructs. **(B)** Representative co-IP results for *hERG1* and β 1, in HEK-*hERG1*, HEK-*hERG1* Δ 2-370 and HEK-*hERG1* Δ C+RD cells, obtained by using the indicated antibodies. The average densitometric values obtained from 4 independent experiments are shown in the right panel. For each condition, the intensity of the band relative to co-IP *hERG1* or β 1 was, respectively, normalized to the intensity of the band corresponding to immunoprecipitated β 1 or *hERG1*. For easier inspection, the value obtained on HEK-*hERG1* cells was set to 1. (Note: This work has been submitted for publication in *Science signaling*, Becchetti A et al., in which I am a co-author)

4.3.2. The C-terminal (cytoplasmic) domain of $\beta 1$ integrin is not implicated in hERG1/ $\beta 1$ interaction

To study whether the $\beta 1$ intracellular domain (i.e. the C-terminus) is directly implicated in the interaction with hERG1, we used the following constructs (Fig. 11A): i) wild type $\beta 1$ ($\beta 1$), ii) $\beta 1$ lacking the C-terminus ($\beta 1$ -extra) and iii) the $\beta 1$ C-terminus linked to the transmembrane and extracellular portions of the interleukin-2 receptor ($\beta 1$ -cyto). These constructs were labelled with YFP, and transfected into GD25 cells, which almost lack $\alpha 1$ integrins (Fässler R et al., 1995). The efficiency of transfection was evaluated by WB with anti-YFP antibodies (figure 11B). Cells were then transiently co-transfected with hERG1 and co-IP was performed with the anti-hERG1 monoclonal antibody. Figure 11C shows that both WT $\beta 1$ and $\beta 1$ -extra integrin co-immunoprecipitated with hERG1, whereas $\beta 1$ -cyto did not. We conclude that the cytoplasmic $\beta 1$ integrin domain is not necessary for the complex with hERG1 to form, and the interaction between hERG1 and $\beta 1$ likely takes place between their transmembrane domains.

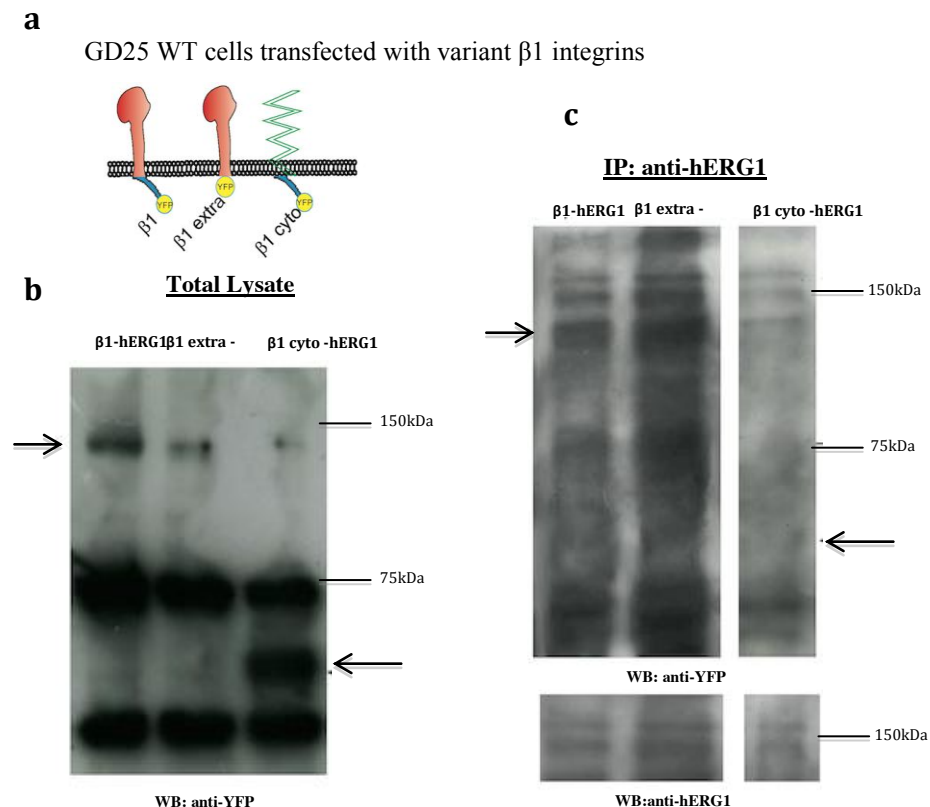


Figure 10 (A) Scheme of the $\beta 1$ constructs used in these experiments: $\beta 1$, $\beta 1$ -extra, and $\beta 1$ -cyto (defined in the main text). (B) WBs of total cellular lysates from GD25 cells transfected with the three constructs, and decorated with anti-YFP antibodies. The upper arrow indicates the expected molecular weight of YFP-conjugated $\beta 1$ and $\beta 1$ -extra (approximately 127 KDa). The lower arrow indicates the expected molecular weight of $\beta 1$ -cyto (67 KDa). The band around 75 KDa and the thin bands between 130 and 150 KDa can be attributed to non-specific signal. (C) Co-IP of hERG1 and $\beta 1$ in GD25 cells transfected with the three constructs and transiently co-transfected with hERG1. The anti hERG1 Mab was used for immunoprecipitation, and WB was revealed with the anti-YFP antibody. Membrane was reprobed with the anti C-terminus hERG1 polyclonal antibody. The upper arrow on the left indicates the bands of $\beta 1$ and $\beta 1$ -extra (lanes 1 and 2). In lane 3 (relative to $\beta 1$ -cyto-transfected GD25 cells) no 67 KDa band is visible (dotted arrow). The IgG bands (50 KDa) are evident in all lanes, although at different intensities. Blots are representative of three independent experiments.

4.3.3. The hERG1/ $\beta 1$ complex assembly depends on the channel conformational state.

We tested the macromolecular complex formation by using two voltage sensor (S4 domain) hERG1 mutants (K525C and R531C) with different steady state activation properties. Representative current traces recorded from hERG1-K525C channels are shown in figure 11A (left panel). Compared to hERG1 wild-type (WT), the amount of hERG1-K525C protein expressed onto the plasma membrane and the maximal current density were generally lower (figure 11B), while the activation curve was strongly shifted to more negative V_m (figure 11C). In agreement with literature (43), the estimated $V_{1/2}$ was -55 mV, and the measured resting V_m was -56 ± 1.5 mV ($n=9$). This suggests that, at the steady state, hERG1-K525C channels spend approximately 50% of the time in the open state. The same analysis was carried out for hERG1-R531C. Typical current traces are shown in (figure 11A) and the maximal current density of hERG1-R531C was similar to the WT's (figure 11B). The activation curve was dramatically shifted to positive V_m (figure 11C), with an estimated $V_{1/2}$ of +35 mV. The corresponding resting V_m was -42 ± 2.6 mV ($n=15$), implying that hERG1-R531C channels essentially reside in the closed state in HEK-hERG1-R531C cells.

Figure 11D shows a representative co-IP test of the above channel types with $\beta 1$ integrin. The densitometric analysis of four similar experiments is reported in the histogram of figure 11E (grey bars). Assembly with $\beta 1$ was facilitated in hERG1-R531C, compared to hERG1, whereas the opposite applies to hERG1-K525C. These results suggest that the $\beta 1$ /hERG1 complex formation is favoured when the channel spends most of the time in the closed state. To confirm this hypothesis we measured the amount of hERG1 co-immunoprecipitating with $\beta 1$ in cells seeded onto FN in low extracellular K^+ (control) and high (130 mM) extracellular K^+ . In the latter condition, the measured resting V_m was $+19.6 \pm 1.1$ mV (n=9), at which WT channels are substantially removed from the closed state. Figure 11F shows representative co-IP tests in these conditions. The corresponding densitometric analysis is shown in figure 11G. Complex assembly in the presence of high extracellular K^+ was significantly lower than observed in standard low K^+ medium. From this study on characterization of hERG1/ $\beta 1$ complex formation we conclude that hERG1 and $\beta 1$ interaction (i) depends on the activation of $\beta 1$ integrins on FN (ii) is impaired when the hERG1 channels are blocked (iii) do not occur through cytoplasmic domain but through transmembrane domain and (iv) depends on the channels' conformational state.

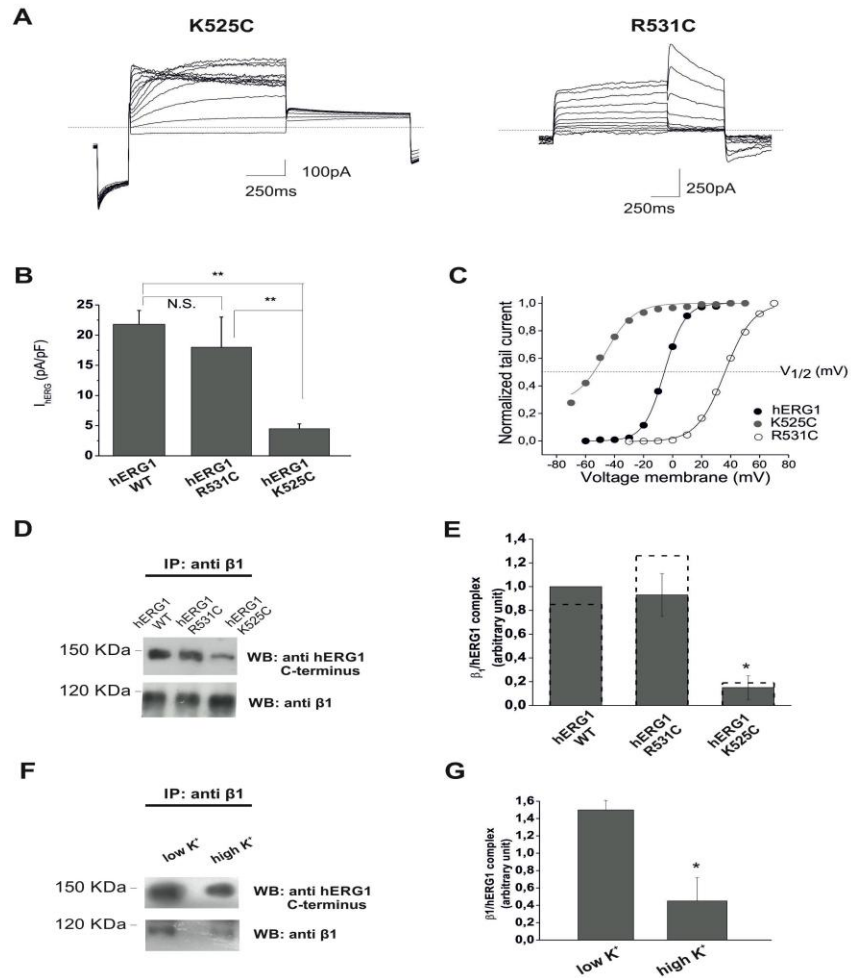


Figure 11. Analysis of the hERG1/ $\beta 1$ complex formation in S4 hERG1 mutants. (A) Typical whole-cell current traces elicited in HEK cells stably transfected with either hERG1-K525C or hERG1-R531C. Currents were recorded in 5 mM extracellular $[K^+]$. (B) Comparison of the maximal current densities of hERG1, hERG1-K525C and hERG1-R531C cells. Data are average peak tail current densities calculated from at least 5 cells. (C) Activation curves of hERG1, hERG1-K525C, and hERG1-R531C cells. Data points are normalized peak tail currents calculated from experiments as in A). (D) Co-IP of $\beta 1$ and hERG1 in cells expressing hERG1, hERG1-K525C, hERG1-R531C and seeded onto FN for 90 min. The experimental procedure was as described in the legend to Fig. 6) Grey bars summarize densitometric results obtained in three independent experiments. (F) Co-IP of $\beta 1$ and hERG1 in HEK-hERG1 cells laid onto FN for 45 min in two different Tyrode solutions containing BSA (250 μ g/ml): 1) low extracellular K^+ (5 mM); 2) high extracellular K^+ (130 mM, substituting the Na^+). Immunoprecipitation was performed as described in the legend to Fig. 6. (G) Bars summarize densitometric analysis corresponding to the low and high K^+ conditions, obtained in three independent experiments. The band intensities were normalized to the intensity of the band corresponding to

immunoprecipitated β 1-integrin. (Note: This work has been submitted for publication in Science signaling, Becchetti A et al., in which I am a co-author).

4.4. HERG1 channels are involved in integrin mediated PDAC cell migration and actin organization

4.4.1. HERG1 channels are involved in PDAC cell migration on basement membrane.

After characterizing the interactions between hERG1 channels and β 1 integrins we aimed to study the role of hERG1 channels in integrin mediated cell migration, adhesion and cytoskeleton organization. The potential of any transformed cells to become malignant and invasive is their ability to dissociate from the confined region within the basement membrane (BM). The BM is a thin dynamic structure composed of ~50 glycoproteins including ECM like collagen-iv, laminin and fibronectin produced jointly by epithelial, endothelial and stromal cells to separate epithelium or endothelium from stroma and stromal cells secreted interstitial matrix (Lu P et al., 2012). The invasive cells show the ability to migrate along the BM, remodel or degrade the structure through enzymatic degradation and escape to the more dynamic tumor microenvironment (TME), where the tumor progression is regulated by non-cell autonomous processes regulated by paracrine or juxtacrine interactions from the TME (Watnick R.S, 2012). We tested whether hERG1 channels are involved in PDAC cell migration on BM. The hERG1 channels blocking by E4031 decreased the cell migration of Panc1 cells significantly ($p < 0.05$) compared to statistically less significant in MiaPaCa2 ($p < 0.02$) and BxPC3 cells ($p < 0.01$) (Figure 12 Lastraioli et al. 2015).

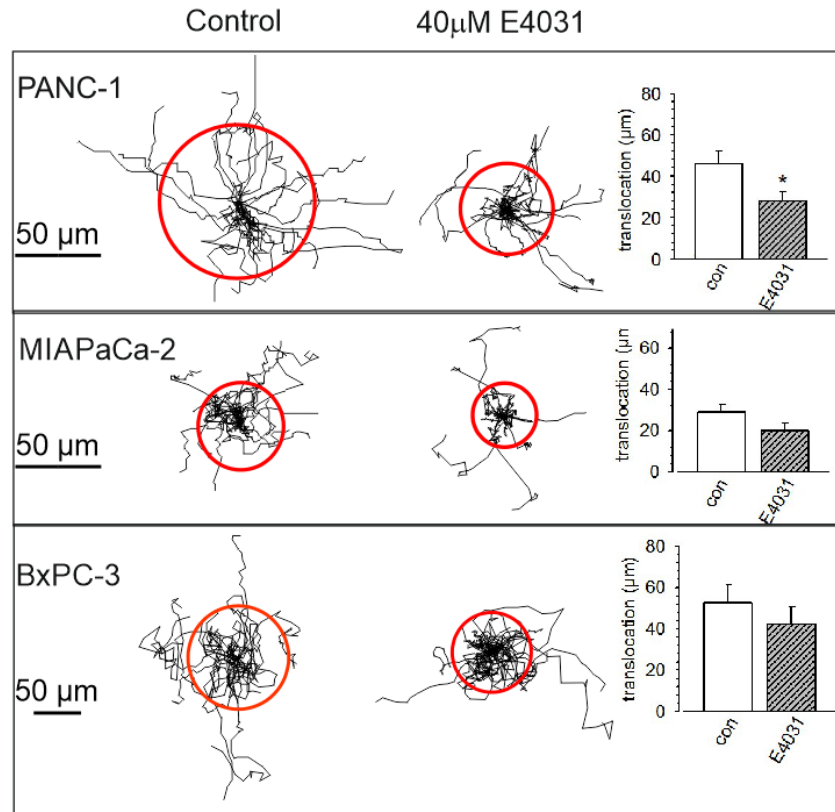


Figure 12. All three PDAC cells were tested for the effect of E4031 on cell migration. E4031 treatment showed significant inhibition of cell migration only in Panc1 cells. (Note: This data was taken from Lastraioli E et al, 2015, in which I am a co-author).

Cell migration is a five-step phenomenon that has been summarized as (i) extension of the leading edge, (ii) cell adhesion to the ECM, (iii) contraction of the cytoplasm (iv) release from the focal adhesion sites and (v) recycling of the membrane receptors (like integrins) from the rear to the front of the cell (Sheetz M.P et al., 1999). These steps involve tightly coordinated interactions between ECMs, integrins and the cytoskeleton proteins. In the subsequent studies we aim to investigate the role of hERG1 channels in modulating cell adhesion, adhesion dependent interactions with integrins and signaling pathways and actin cytoskeleton organization and finally calcium signaling that regulate the components of cytoskeleton among many other proteins.

4.4.2. HERG1 channels are not involved in cell adhesion on fibronectin

Integrins are one of the most prominent receptor molecules that aid the cells to adhere to its extracellular ligands. We investigated whether hERG1 channels interaction with $\beta 1$ integrins can influence the cell adhesion on fibronectin. Endogenous hERG1 expressing PDAC cells as well as stably transfected hERG1 in HEK cells were used for this study. The time course of adhesion of these cell lines show that the percentage of cells attached on fibronectin was not different between the cells that were treated with or without hERG1 blocker. Similar observation was also made between hERG1 expressing and non-hERG1 expressing HEK cells (figure 13).

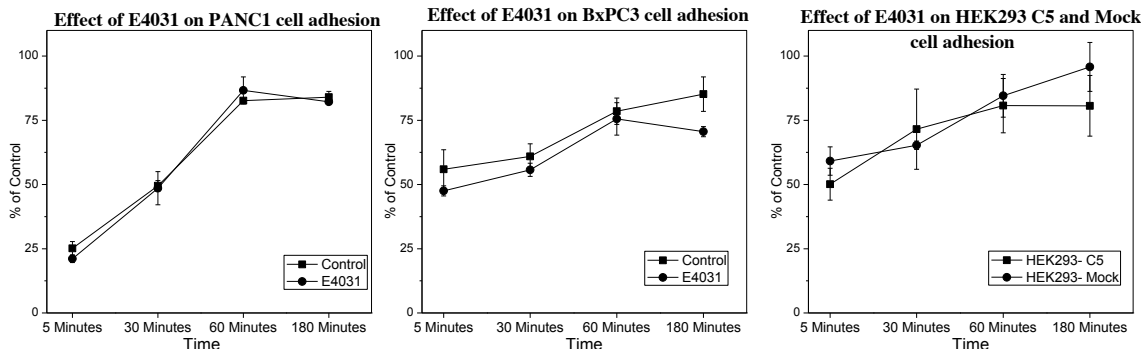
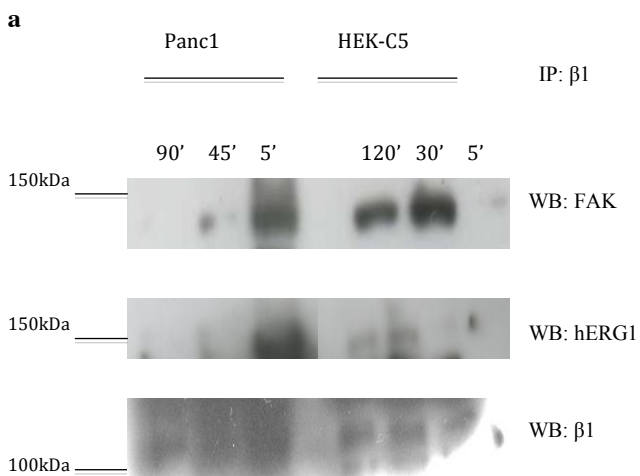


Figure 13: Cells were seeded onto fibronectin for the mentioned time points, fixed and stained with toluidine- blue as mentioned in methods section. The attached cells were quantified as % of control cells. The hERG1 blocking by E4031 treatment in PDAC cells and over expression of hERG1 in HEK293 cells did impact the cell adhesion.

4.4.3. HERG1 channels make macromolecular complex formation with $\beta 1$ and FAK at the early stage of cell adhesion.

Integrins, when engaged with ECM, are in principle involved in two sets of functions; (i) the wide array of signaling cascades that are associated with cell proliferation, gene expression, survival etc. and (ii) assembling the cytoskeleton remodelling that include actin and actin binding proteins that bridge actin and integrins (Ross R.S, 2004). Since integrins do not possess the enzymatic activities the signaling is mainly carried through focal adhesion kinase (FAK). Upon integrin

engagement with ECM FAK is auto-phosphorylated first at 397th amino acid residue tyrosine and this leads to the cascade of phosphorylation along the FAK and other adhesion dependent protein interactions (Kumar CC, 1998). FAK is also one of the first proteins that are recruited to the cytoplasmic tails of integrins during the nascent adhesion. However, as adhesion matures the FAK rolls back and is no longer engaged with integrins. In fact integrin has been shown to co-immunoprecipitate with integrin-linked kinase (ILK) instead of FAK at later stages of adhesion (Hannigan G.E et al., 1996). This observation prompted us to perform the time course of co-IP between β 1/FAK and β 1/hERG1 in Panc1 and HEK293-C5 cells seeded on FN. The time requirement for the FAK recruitment to the cytoplasmic tail of the β 1 integrin after activation was distinctive between HEK293-C5 and Panc1 cells. The β 1-FAK complex formation was at the peak only after 5mins of stimulation with FN in Panc1 cells while in HEK293-C5 cells it was at 30mins. The association between β 1/FAK at later intervals decreased significantly (figure 14). Interestingly, the β 1/hERG1 complex formation also followed a similar trend for both the cells suggesting that β 1/FAK/hERG1 complex formation is an early event that could depend on the cell lines and its integrins expression profile.



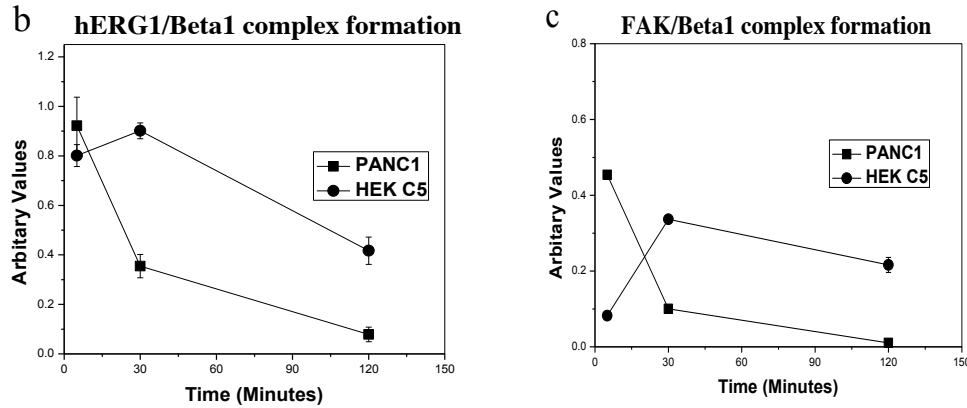


Figure 14. The time-course of co-IP between β 1/FAK and β 1/hERG1 channels in Panc1 and hERG1 expressing HEK-C5 cells. (This observation is a representative of only one experiment).

We further investigated the role of activation of FAK especially autophosphorylation of FAK (pFAK) at 397th amino acid residue tyrosine in Panc1 cells. We observed that pFAK at the basal level when cells were seeded on non-stimulating PLL. The pFAK was increased on FN and blocking of hERG1 channels decreased the pFAK. Insert hERG1 effect on pFAK.

4.4.4. HERG1 channels are not involved in focal adhesions (FAs) and area of FAs of FAK and paxillin.

We further pursued our interests in understanding the role of hERG1, if any, on focal adhesions and area of focal adhesions. Panc1 and BxPC3 cells were seeded on FN and treated with E4031 for the above mentioned time intervals. The cells were fixed, permeabilized and stained for cytoskeleton proteins FAK and paxillin. The number of focal adhesions of FAK and paxillin were quantified using the imageJ software according to Horzum et al., 2014. The cells showed increased number of FAs of both FAK and paxillin with time while the area of each of their FA decreased with time (figure 15).

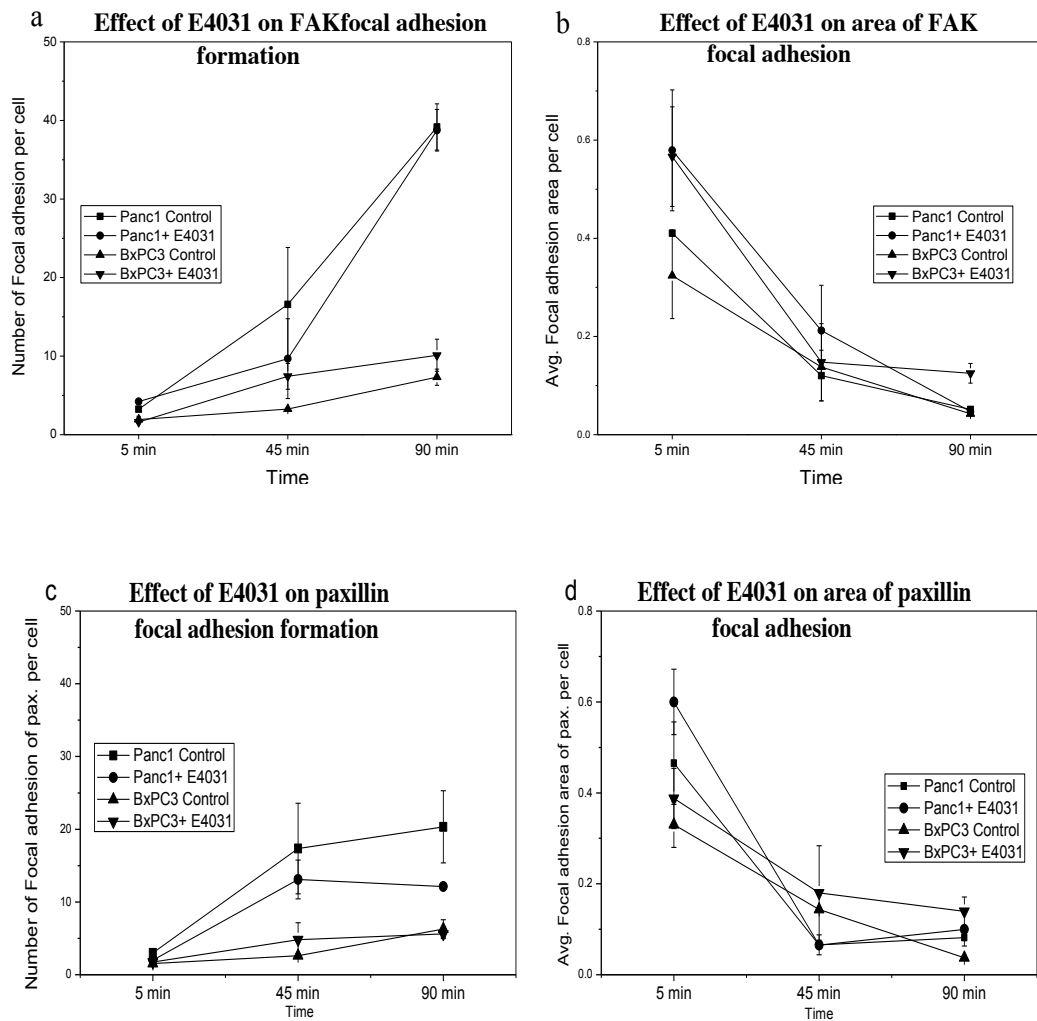
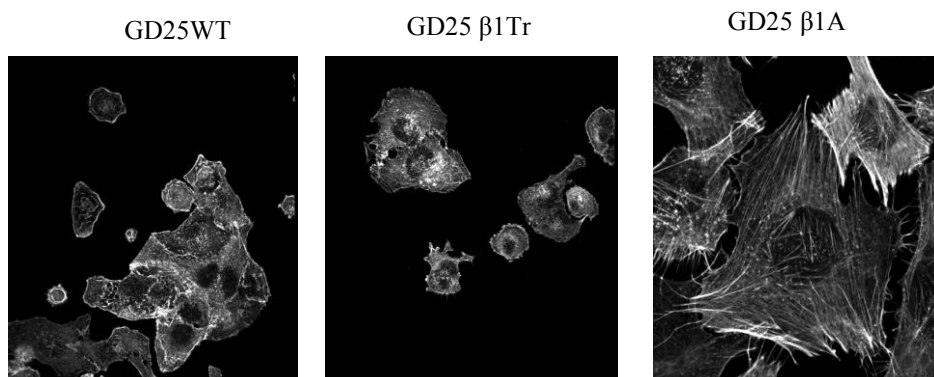


Figure 15: The effect of E4031 was further studied on its impact on focal adhesions of FAK and paxillin and the area of FAs. The number of FAs of FAK (a) and Paxillin (c and d) increased as cell adhesion matures, while the surface area of FAs of both FAK and paxillin decreased and formed more defined smaller FAs (b and e). The E4031 treatment did not show any impact on number of FAs and area of FAs.

Panc1 cells showed significantly higher number of FAs of FAK and paxillin than BxPC3 cells but similar area of per FA. The E4031 treatment, however, did not influence both number of FAs and area of FAs (figure 15).

4.4.5. HERG1 channels are involved in altering actin cytoskeleton organization mediated by $\beta 1$ integrins

As mentioned above the integrins-ECM engagement activates the integrins by changing the conformation from bent to upright position. This in turn leads to the recruitment of several proteins at the cytoplasmic tail of the integrins to further activate the integrins and form focal adhesions (FA). Thus both ECM binding domain at the extracellular and intracellular protein binding cytoplasmic domain are crucial for cell adhesion, signaling and provide structure to the cells. The stable structure to the attached cells is provided by number of cytoskeletal proteins like actin, tubulin etc. So we sought to study the (i) organization of the actin organization regulated by cytoplasmic tail of $\beta 1$ integrins and (ii) whether hERG1 channels also play a role cell adhesion and actin organization. To this purpose, mouse fibroblast GD25WT cells, that lack $\beta 1$ integrin, were stably transfected with plasmid coding for $\beta 1$ integrin truncated at cytoplasmic tail ($\beta 1$ Tr) and full-length $\beta 1$ A. These cells were seeded on FN to observe the differences in cell morphology and actin cytoskeleton organization. The f-actin staining by rhodamine conjugated phalloidin showed that both GD25 WT and GD25 $\beta 1$ Tr had more dispersed shorter f-actin that were localized near the cell membrane and cells exhibited round shape morphology Whereas GD25 $\beta 1$ A cells, that has full-length cytoplasmic tail, showed more organized longer f-actin that were spread along the cells providing more stable cell structure and spread morphology (figure 16 top panel). We then seeded Panc1 and BxPC3 cells on FN and PLL and observed that cells seeded on FN showed spread morphology and longer f-actin than cells on PLL (Figure 16 bottom panel).



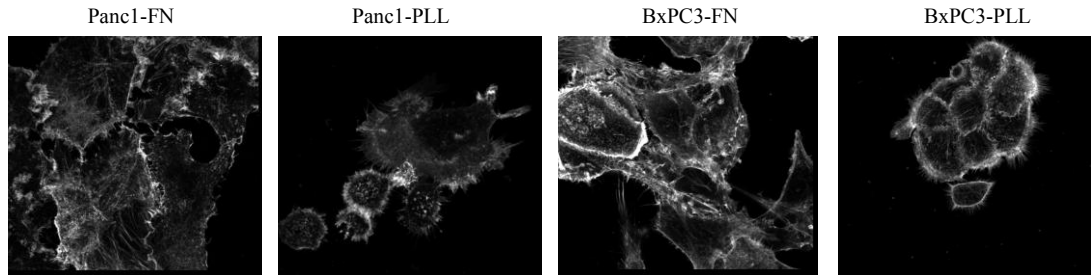


Figure 16. Filament-actin staining was performed with rhodamine-conjugated phalloidin in Panc1 and BxPC3 cells seeded on FN and PLL. The f-actin was highly localized in the cytoplasm when cells were seeded on FN and provided spread morphology to the cells as well as longer actin stress fibres. But on PLL, where the cell attachment is not mediated through engagement of integrins showed that f-actin is mostly localised near the membrane with much shorter length.

After establishing the study that full-length $\beta 1$ integrins as well as ECM are essential for cell spread morphology and cytoskeleton organization we investigated whether hERG1 channels are involved in modulating the cell adhesion and cytoskeleton organization. To study the role of hERG1-mediated changes in actin organization we used endogenous high and low hERG1 expressing Panc1 and BxPC3 cells, transiently transfected hERG1 gene in HEK293 and mouse fibroblast GD25 β 1A cells. Panc1 and BxPC3 cells were seeded on fibronectin and treated with hERG1 blocker E4031 for 6, 24 and 48hrs, fixed with 4% PFA and stained for actin using rhodamine-conjugated phalloidin as per the protocol. HERG1 activator NS1643 (50 μ M) was also tested on Panc1 cells. On the other hand non-hERG1 expressing HEK293 and GD25 β 1A cells were transiently transfected with hERG1-GFP plasmid, seeded on fibronectin and stained for actin. The raw images of the cells stained for f-actin were obtained from confocal microscopy and processed using MatLab codes to identify only the actin filaments (figure 17) (Balcioglu H.E et al., 2015).

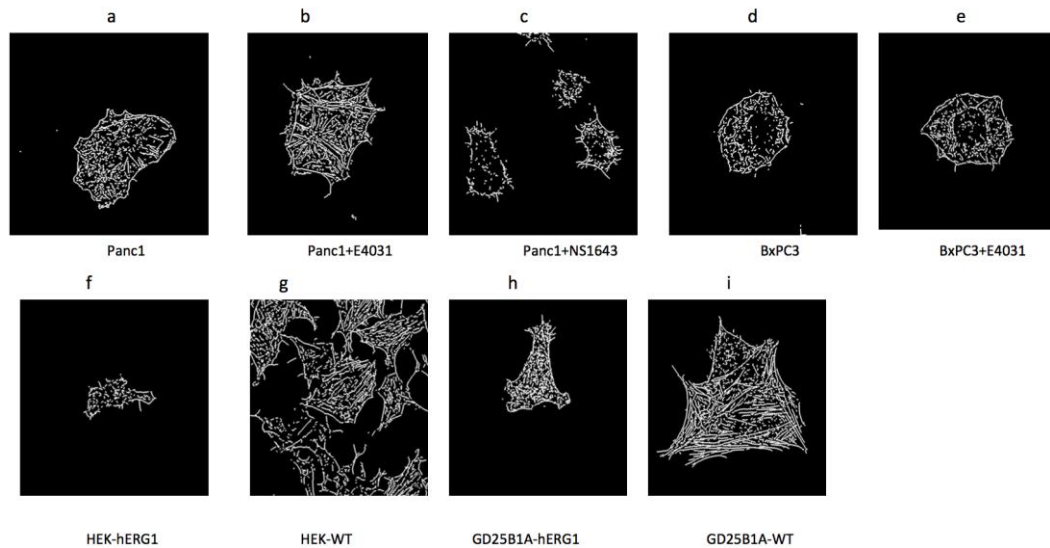


Figure 17. All the above cells were stained for f-actin and images were captured using confocal microscope. The images were further processed by MatLab program to detect only f-actin filaments. The functional hERG1 expressing cells show more scattered and shorter filaments that hERG1 non-expressing or hERG1 blocked cells.

The functional blocking of hERG1 channels by E4031 treatment for 24h induced longer and more organized f-actin stress fibres in Panc1 cells. On the other hand the hERG1 activator did not induce any changes compared to untreated cells (figure 17 a, b, c). We did not observe any changes in f-actin length and organization in BxPC3 cells (figure 17 d, e). This is consistent with the fact that BxPC3 cells express very low amount of hERG1 channels. The observation that f-actin organization was linked to hERG1 activity was further corroborated by experiments in which HEK293 and GD25 β 1A cells were transfected with functional hERG1 channels (figure 17 f-i). In fact, non-hERG1 expressing HEK293 (figure 17g) and GD25 β 1A (figure 17i) showed actin organization similar to that of functional blocking of the channels in Panc1. On the contrary, the f-actin organization in hERG1 positive HEK293 and GD25 β 1A was similar to that of Panc1 cells in control conditions. The alterations in the f-actin length were quantified using MatLab codes and expressed in μm . The average number of f-actin filaments varied between cells from 900 to 4000 filaments and the mean value of all the actin lengths, without setting the threshold, is represented below (figure 18). As can be observed from the

figure 18 the hERG1 gene transfection in GD25B1A and HEK293 cells decreased the actin filament length compared to un-transfected cells. On the contrary functional blocking of hERG1 in Panc1 cells increased the length of actin filaments. This observation is significant especially from cell migration point-of-view. Because for the cells to migrate, the lamellum, that has high density of actin filaments (100/ μm), must be pushed forward. Long and flexible actin filaments cannot sustain the pushing force hence; cells create dense nascent filaments that are short-branched filaments to push against the membrane and provide structural basis for polymerization-driven protrusion (Pollard T.D and Borisy G.G, 2003). Therefore we argue that blocking of hERG1 channels impair the cell migration by inducing changes in actin organization.

We further measured the cell-spread area and observed that E4031 treatment (in hERG1 expressing Panc1 cells) or non-hERG1 expressing cells showed more spread area and that untreated or hERG1 transfected cells (figure19). This observation was particularly evident in hERG1 transfected GD25 β 1A fibroblast cells that was significantly large cells. The control HEK293 cells, on the other hand, are much smaller in size and hence hERG1 transfection in these cells decreased the cell-spread area to lesser extent. However, surprisingly the hERG1 blocking in Panc1

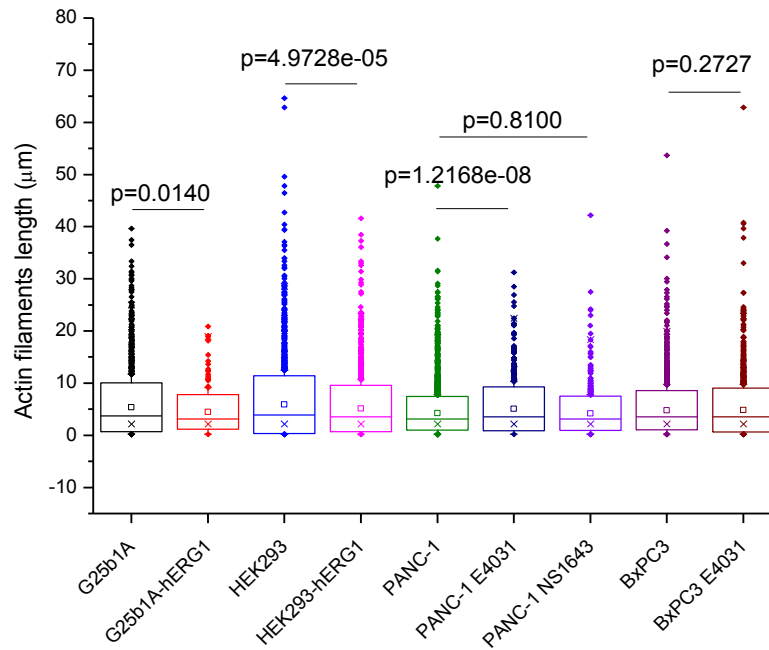


Figure 18. The histogram above is the average length of the actin filaments. The cells that are expressing functional hERG1 channels have shorter filaments compared to the cells that are either non-hERG1 expressing or hERG1 expressing cells that are treated with hERG1 channel blocker. The statistical significance was tested by Brown-Forsythe test and $<5\%$ is considered as statistically significant ($p \leq 0.01$).

cells did not change the surface area of the cells. This could be because of the fact that endogenous expression of hERG1 channels in Panc1 cells was much lower than in the cells transfected with hERG1 channels. At this point of time we could only speculate that the level of hERG1 expression in Panc1 cells was adequate to alter the actin organization but not adequate to cause hyper polarization that could have any impact on cell area (or volume) and hence further characterization of hERG1 in Panc1 cells is required. However, neither hERG1 blocking nor hERG1 expression altered the orientation of actin filaments (figure20). Thus we conclude here that hERG1 channels are involved actin filaments organization and cell-spread area but not on actin orientation that are mediated through interactions with $\beta 1$ integrins.

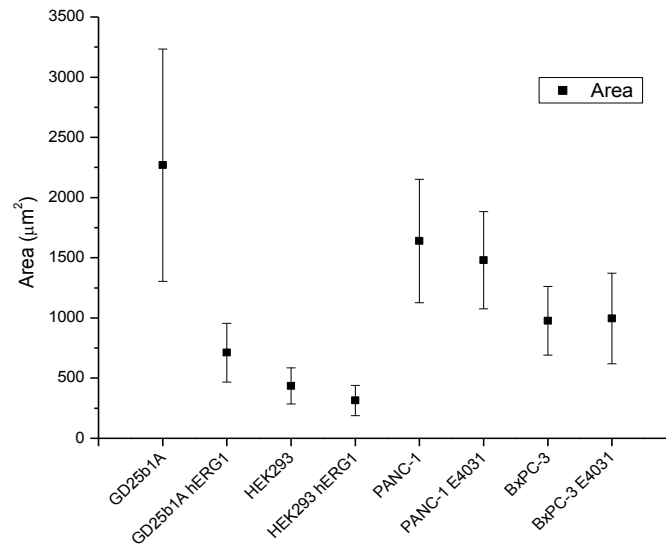


Figure19. The role of hERG1 expression in cell surface area was studied. The over expression of hERG1 channels in GD25 β 1A and HEK293 cells decreased the cell surface area compared to WT cells.

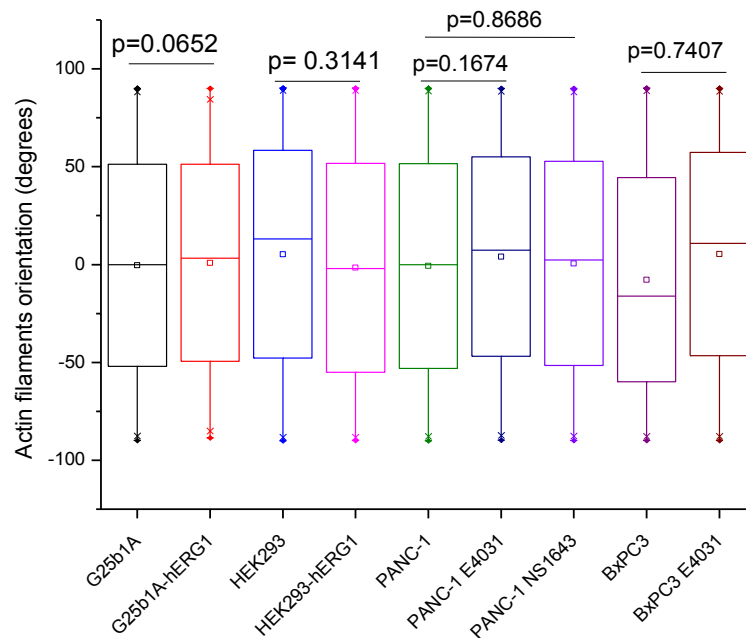


Figure20. The over expression of hERG1 channels or functional blocking of hERG1 channels (in Panc1) did not alter the actin orientation (angle).

4.5. HERG1 channels in PDAC cell migration stimulated by activated PSC through actin dynamics and altered calcium concentration

4.5.1. Functional blocking of hERG1 channels mitigate the PDAC cell migration through altered actin dynamics and decreased intracellular calcium concentration

Finally, we aimed to study the role of hERG1 channels in actin dynamics. This work was performed in the laboratory of Professor Albrecht Schwab, University of Munster, DE. Here we challenged the hERG1 role in more complex and dynamic experimental setup that is closer to physiological conditions of PDAC. The PDAC is characterized to be highly desmoplastic with excess deposition of collagen matrix around the tumor cells. The PDAC tumor microenvironment is also highly complex and dynamic. It includes pancreatic stellate cells (PSCs), immune cells, lymphocytes, endothelial cells and the secretomes of this individual cell types. The secretomes of one set of cells can stimulate other cells and vice-versa and trigger tumor progression. As tumor cells grow, the blood supply is hindered. This mainly occurs in central portion within the tumor mass that is hence deprived of oxygen called as hypoxia. It is worth noting that oxygen is essential to support tumor growth. This hypoxic condition in PDAC adds new dimension to the already complex disease. Due to the limitation of oxygen the tumor and stromal cells evolve to sustain the growth as tumor progresses. In addition, the hypoxic condition triggers the signaling pathways that directly induce the pro-invasive programming in cancer and stromal cells (Yuen A and Diaz B, 2014). Further, both *in vitro* and *in vivo* studies show that hypoxia activates PSCs and in turn increases fibrosis and angiogenesis (Masamune A et al., 2008). PSCs activation leads to increased secretion of various growth factors, ECMs, cytokines, interleukins etc. that increase the interaction with nearby PDAC cells (Eguchi D et al., 2013). There are more than 650 proteins that are secreted by activated PSCs, compared to ~45 proteins from quiescent PSCs, and >27% of these proteins are implicated in cellular processes, metabolism and human diseases (Wehr A.Y et al., 2011). Hence activated PSCs have been increasingly proven to play key

role in promoting as well as protecting the PDAC against the tumor targeting (McCarroll J.A et al., 2014) and perceived to be a potential target to control the tumor progression. We aimed to study the interactions between PDAC and stellate cells and whether hERG1 channels are involved in the interactions. Thus we first characterized the expression level of $\beta 1$ integrins and hERG1 channels in PSCs cells. Immunofluorescence experiments show that PSCs have high expression of $\beta 1$ integrins and no hERG1 expression (figure 21a and b). The patch clamp experiments were performed to study the presence of hERG1 current and observed that E4031 treatment decreased the hERG1 type current by meagre -10pA thus considered as insignificant (figure 21c).

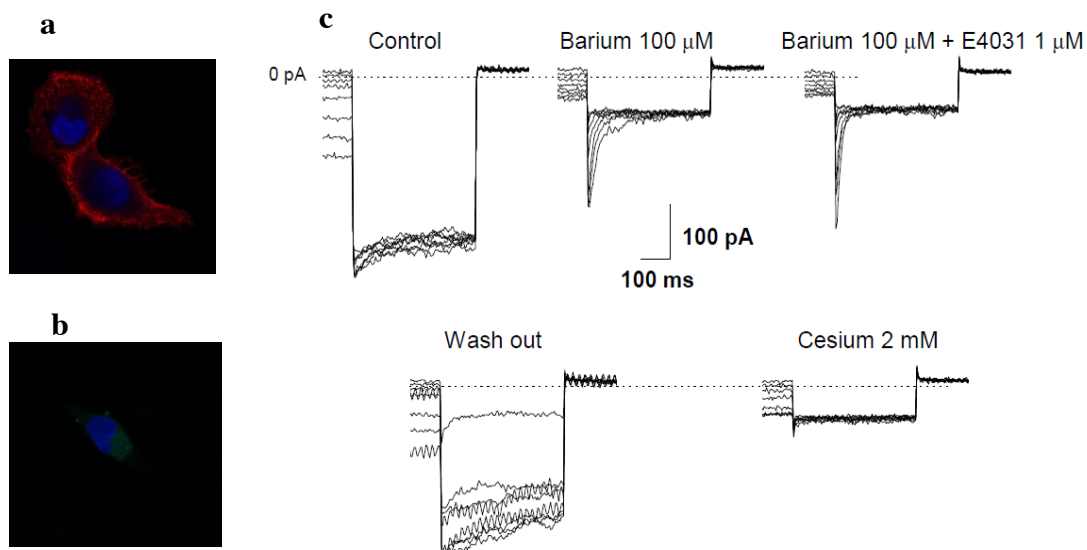


Figure 21: Immunofluorescence staining in PSC cells shows high surface expression for $\beta 1$ (a) and very low signal for hERG1 (b). Whole-cell patch clamp experiments confirm small traces of hERG1 current that was abolished when cells were treated with E4031 (c).

Then, we attempted to study the co-culture migration between PDAC and PSC cells on more closely to physiological matrix composition. We labelled the PDAC cell Panc1 with rhodamine-conjugated nanoparticles to differentiate from PSCs. Due to the lack of significant number of labelled cells within the microscopic field per experiments and unhealthy labelled cells we could not quantify co-culture migration and role of hERG1 channels in co-culture migration (data not shown). So

we switched to single cell migration of Panc1 cells stimulated by activated PSCs and the data are reported below.

4.5.2. HERG1 channel blocker E4031 decreases the Panc1 cells migration stimulated by hypoxia activated PSCs on desmoplastic matrix.

Here we studied whether blocking the hERG1 channels would impair, at least in partial, the PDAC cell migration on two-dimensional matrix. In order to mimic the physiological tissue composition that exist within the desmoplastic microenvironment the T-flasks (12cm²) were coated with ‘desmoplastic matrix (DM)’ containing ~89% of collagen-1, 4.5% each of fibronectin and laminin, 1% each of collagen-III and collagen-IV. The matrix were gently mixed in RPMI medium containing HEPES buffer (see materials and methods section for details) and coated overnight at 37C for the matrix to polymerize. The immortalized hPSCs were grown to ~ 90% confluent and growth medium was changed to serum free DMEM medium (10ml). The hPSCs were then incubated in hypoxia incubator (1% CO₂) for activation for not more than 18h and conditioned medium (filtered using 0.22µm filter) was used for the stimulation of Panc1 cells. Approximately 70,000 Panc1 cells were seeded on DM and allowed to attach and spread (~2h). The Panc1 cells were stimulated with conditioned medium, without dilution, of hPSCs (2.5ml). Immediately cells treated with hERG1 blocker E4031 and during the course of the experiments. In addition, two sets of medium were used as stimulant; (i) conditioned medium of hPSCs cells incubated in normoxia incubator and (ii) only serum free DMEM medium incubated in hypoxia incubator for 18hrs. The cell migration video was generated using time-lapse images with interval of 5mins for 6hrs. For the analysis of migration every second image (that is 10mins interval) between 2-6hrs was considered. The track of random cell migration show that both the conditioned medium from normoxia and hypoxia hPSCs increased the Panc1 cell migration significantly compared to unconditioned medium (figure 22 top panel). The increase in normoxia-conditioned media stimulated Panc1 cell migration could be reasoned that hPSCs are immortalized and activated cells that have characteristic features of lost Vitamin A droplet and expression of α -smooth muscle actin (α -sma) (Jesnowski R et al., 2005).

As mentioned above the activated hPSCs stimulate various soluble factors like GFs, ILKs etc. that stimulate the cells. Hence we reason that these immortalized and activated PSCs, though maintained in normoxia conditions, could stimulate cell migration. The E4031 treatment significantly decreased the cell migration in both non-stimulated and stimulated conditions (figure 22 bottom panel).

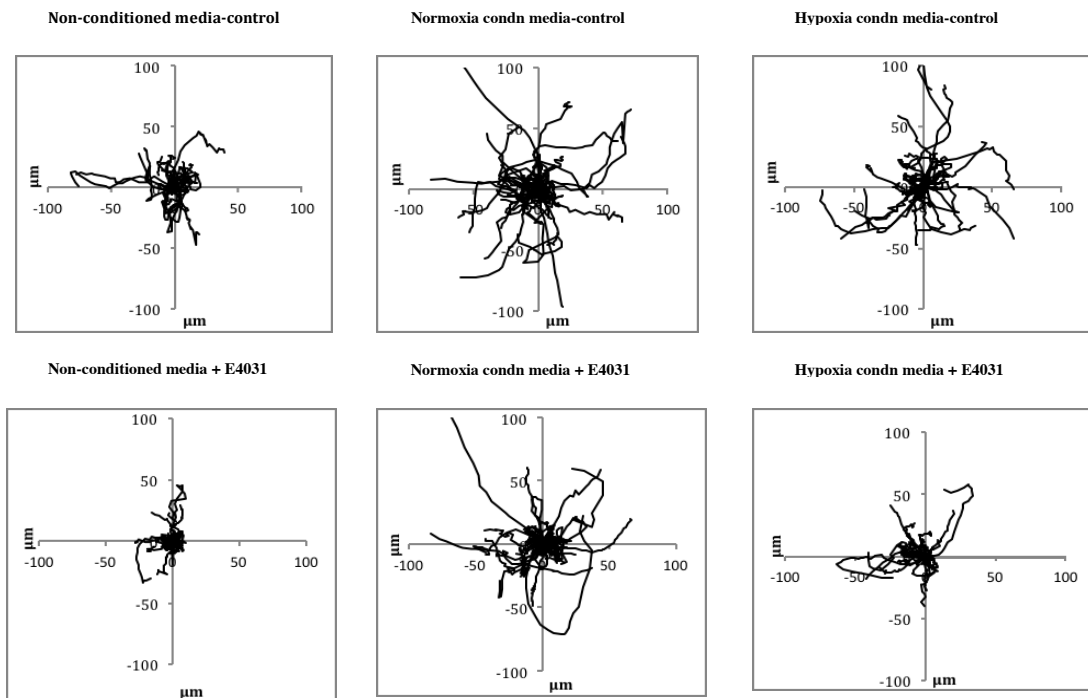


Figure 22. The position or location of each cell was normalized to origin. The direction of random cell migration was tracked using Amira software and represented on X and Y-axis.

We further quantified the translocation of the cells from starting point, the total distance, the speed at which the cells migrated, the directionality of the migration, structure index (SI) and surface area of the cells during the course of the experiments were quantified using the ImageJ software. The cell migration rate, translocation of the cells from the original point to end and total path of the cell migration are shown in figure 23. The non-stimulated cells migrated shorter distance and at slower speed than cells stimulated with conditioned medium from both normoxia and hypoxia activated hPSCs. Interestingly, the hERG1 blocker E4031 showed highest inhibition of cell migration rate and total path, by ~45% each, under

hypoxia conditioned media compared to both normoxia (25%) and non-conditioned (35%) medium.

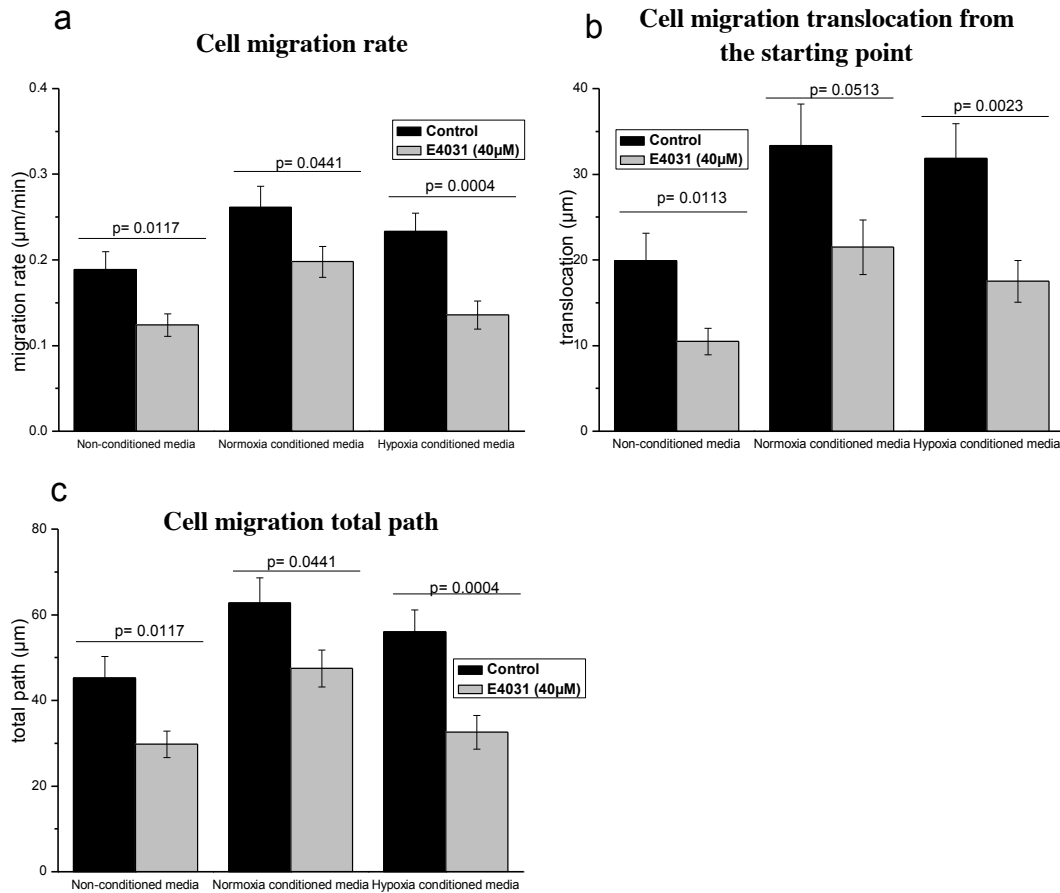


Figure 23. The quantification of Panc1 cell migration stimulated media conditioned media of activated hPSCs. Panc1 cells stimulated under normoxia and hypoxia conditioned medium showed higher cell migration rate (a), translocation of the cells from the origin point (b) and longer total path migrated than the cell stimulated with non-conditioned medium. The hERG1 blocker E4031 (40µM) decreased the migration of cells under all stimulation conditions.

As can be observed from the cell track in figure 22 the directionality of the cells were random and blocking the channel restricted the migration without altering the directionality. However, E4031 altered the morphology of the cells (represented as structure index, SI) in non-conditioned and hypoxia stimulation conditions and not in significantly enough in normoxia conditions (figure 24a) whereas E4031 showed inconsistent effect on the total surface area of cell in these conditions (figure 24b).

The SI close to 1 represents that cells are near round shaped while SI close to 0 represents more polarized or flattened structure.

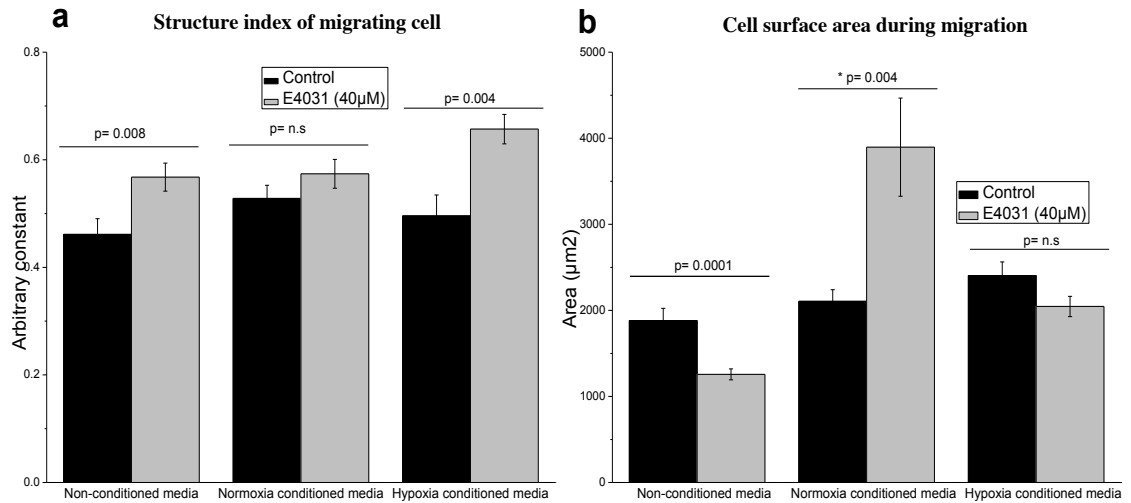


Figure 24. The changes in the structure index (S.I) (a) and surface area (b) of the migrating cells were calculated and represented here is the average during the four-hour migration. The S.I of cells were increased in E4031 treatment, but to a lesser extent in normoxic condition (n.s->non-significant statistically). The effect of E4031 on surface area was however inconsistent in each conditions.

The cell migration rate (and hence total path) was consistent during the course of the experiment. The cells treated with E4031 showed the inhibition effect on the migration that persisted throughout the experiment (figure 25).

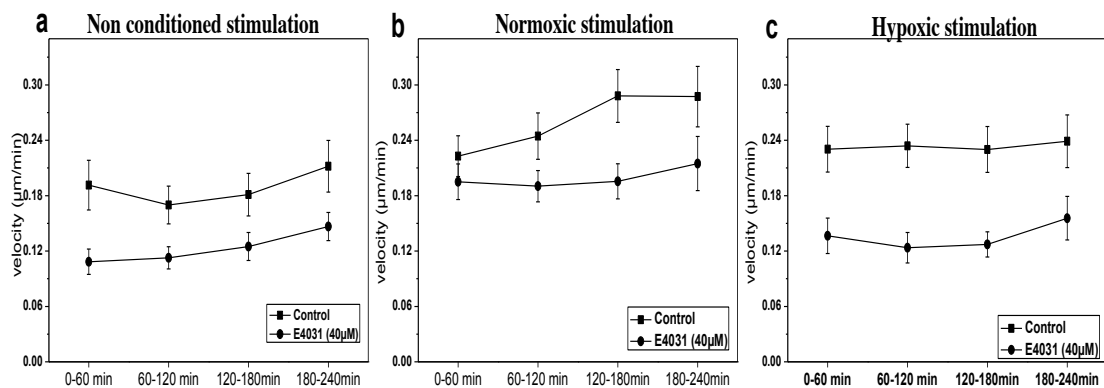


Figure 25. The time course of cell migration rate under the stimulation of in non-conditioned, normoxic and hypoxic conditioned media. The cell migration rate was constant throughout the migration (4hrs) and inhibitory effect of E4031 was immediate and persistent during the migration period.

4.5.3. HERG1 channel blocker E4031 alters the actin dynamics of the migrating Panc1 cells stimulated by conditioned medium of hypoxically activated PSCs.

The actin dynamics was studied by transfecting the Panc1 cells with plasmid harbouring lifeAct-GFP gene. The analysis of actin dynamics was performed in collaboration with Dr Stefano Coppola, University of Leiden, NL. The lifeAct-GFP stains for f-actin filaments without interfering with its dynamics (Riedl J et al., 2008). The lifeAct-GFP transfected Panc1 cells were seeded on thin coating of DM (1/10th of used in migration) with the same composition of migration set-up. When the cells were attached and spread they were stimulated with PSC conditioned media and immediately treated with E4031. The GFP stained actin filaments were visualised under TIRF microscope and images were acquired for two minutes with 1second interval. To assess the actin dynamics, the time series of images were analysed using the spatio-temporal image correlation spectroscopy (STICS) method (Hebert B et al., 2005). Below is the representative image of Panc1 cells that was analysed for the actin dynamics of flow map generated by STICS analysis (figure 26). Each arrow represents the velocity vector of the actin filaments.

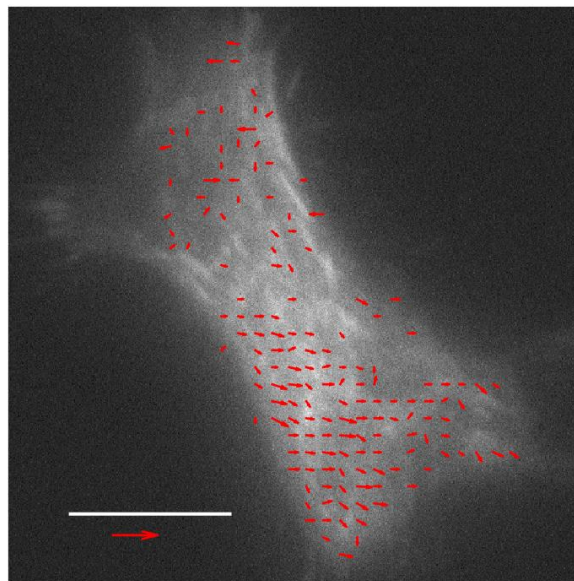


Figure 26. Representative image of the actin flow map in Panc1 cells used to study the actin dynamics/velocity stimulated by either PSCs conditioned medium. The red arrow represents the velocity vector within the corresponding region of interest (ROI). The scale bar is 10 μm and the red arrow below the scale bar represents the reference velocity of 0.05 $\mu\text{m/s}$.

Figure 27 shows the boxplot for the velocity of actin flow obtained from the STICS analysis. There is significant difference for the E4031 treatment with respect to the control. The PSC stimulation increases the actin dynamics by changing the flow magnitude. The actin filaments have two ends; barbed and pointed ends that are dynamically different with barbed end is 10 times more dynamic and fast growing end of the actin filaments (Blanchoin L et al., 2014). The formation of f-actin filaments (polymerization) is initiated by spontaneous nucleation of monomeric unit of actin (globular-actin or G-actin). Hence the growth of the f-actin depends on the concentration of the readily available G-actin for assembling called as critical concentration (C_c). When the f-actin is formed under steady state condition there is equilibrium between association and dissociation of G-actin from the filament actin. In the so-called treadmilling of actin filaments there is constant association and dissociation of G-actin. From the treadmilling point of view our analysis is no more than a flow (the association/disassociation of G monomers lengthens or shortens the actin filaments substantially mimicking a motion in a specific direction, i.e. a flow). The velocity of actin flow was estimated to be $0.008 \pm 0.003 \mu\text{m/s}$ and 0.0089 ± 0.0057 for 1h and 24h stimulation control conditions respectively. The E4031 treatment however, significantly (statistically) increased the velocity of actin flow to 0.0102 ± 0.0103 and 0.0102 ± 0.0113 for 1h and 24h treatment respectively. The diffusion co-efficient of actin was also increased in E4031 treatment compared to control conditions (figure 27 left panel).

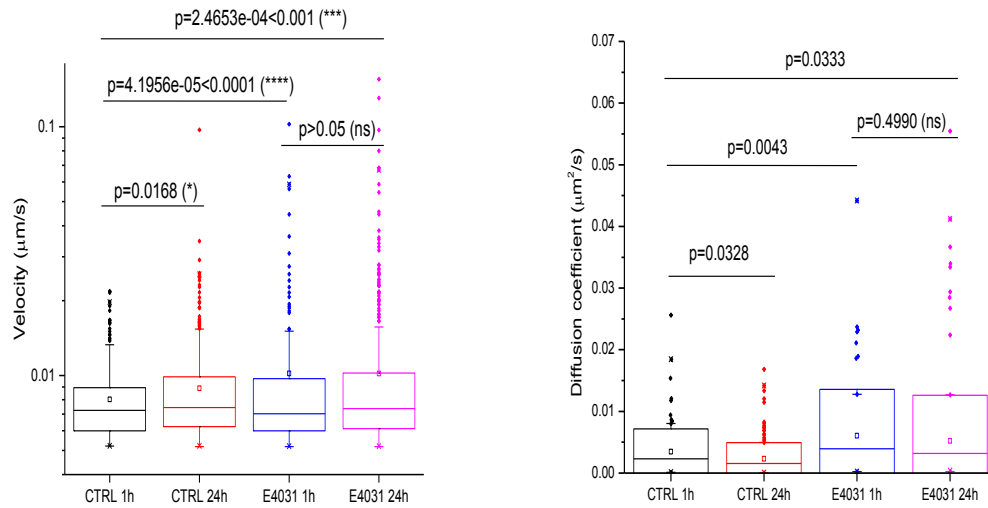
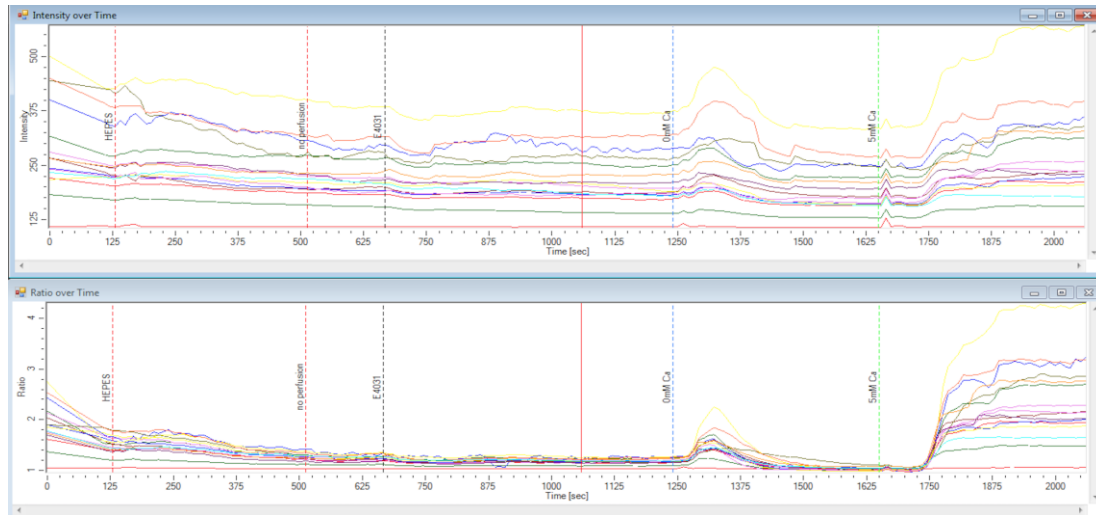


Figure 27. The velocity of actin dynamics or flow was analysed using STICS method. The conditioned medium of PSCs increases the actin dynamics by increasing the flow magnitude.

4.5.4. HERG1 channel blocker decreases the intracellular concentration of calcium and in Panc1 cells stimulated by PSC conditioned media.

In the previous sections, hERG1 channels are shown to be involved in Panc1 cell migration and actin dynamics. Panc1 cells were stimulated by PSC secretomes on DM and hERG1 blocker inhibited the cell migration and actin dynamics drastically. We further set to study the possible mechanism that is involved in the hERG1 mediated cell migration and cytoskeleton organization including actin dynamics. Calcium is one of the most essential chemical elements required for the human beings. While at the organismic level, Ca^{2+} with other compounds composes the bone to support the bodies, at the tissue level Ca^{2+} compartments regulate membrane potential in neuronal and cardiac activities and at the cellular level Ca^{2+} concentrations determine the cellular physiology including cell proliferation, death and migration (Tsai F.C et al., 2015). The intracellular Ca^{2+} concentrations are spatially and temporally regulated with precision. Within the migrating cells the Ca^{2+} concentration is gradient with higher concentrations at the cell rear and very low concentration at the cell front (Wei C et al., 2012). This global gradient of the Ca^{2+} concentration inside the cell could partly due to distribution of subcellular

Ca²⁺ storing organelles. Most of the migration machineries like actin, focal adhesion complexes and the regulatory components like small GTPases are all Ca²⁺ sensitive, hence the fluctuations in Ca²⁺ concentration, expectedly, will have an effect on cell migration. Most of the intracellular Ca²⁺ concentration is derived from the endoplasmic reticulum, however the changes in membrane potential can also drive Ca²⁺ influx for ex through transient receptor potential (TRP) channels or through store-operated Ca²⁺ entry (SOCE). The actin dynamics has shown to be regulated due to changes in Ca²⁺ influx. For ex, depolarization of neuron cells led to influx of Ca²⁺ that altered actin bundle and retrograde flow (Welnhof E.A et al., 1999). Although Ca²⁺ does not bind directly to actin bundles it affects the multiple actin regulators. Small Rho GTPases like Rac1, RhoA and Cdc42 are key regulators of actin dynamics in a spatially dependent manner; Rac1 is localized in lamellipodia, RhoA around FAs and Cdc42 in filopodia. These GTPases also regulate each other in cyclic manner and synchronised for the efficient cell migration (Tsai F.C et al., 2015). To this end we aimed to study the role of hERG1 channels in intracellular Ca²⁺ concentration as well as the activities of Rho GTPases that regulate actin dynamics. Panc1 cells were seeded on the DM matrix as mentioned in actin dynamics experimental setup (10% of total matrix composition in cell migration) and cells were stimulated for 1hr with conditioned media of hypoxically activated PSCs. The calcium measurement was performed as detailed in materials and methods section. Scheme 9 below shows the measurement events in the intracellular calcium measurement setup.



Scheme 9. A typical experimental scheme of intracellular calcium measurement in perfusion system that includes drug treatment and calibration buffers (0mM and 5mM).

The Panc1 cells that are seeded on DM and stimulated with PSC conditioned medium for 1hr showed the average $[Ca^{2+}]_i$ to be around 190nM. In the same setp when cells were treated with E4031 we observed the decrease in the final $[Ca^{2+}]_i$ by more than two-fold to 85nM. Interestingly when Panc1 cells were seeded on FN without stimulation the $[Ca^{2+}]_i$ was ~140nM which was decreased to ~65nM with E4031 treatment. To confirm these observations of the role of hERG1 channels on $[Ca^{2+}]_i$ we used hERG1 transfected HEK293-C5 and mock plasmid transfected HEK293-Mock cells. The Ca^{2+} concentration in HEK-C5 cells was around 170nM that was decreased to ~80nM while HEK-Mock cells showed the $[Ca^{2+}]_i$ around 90nM and E4031 treatment showed less significant decrease in concentration to ~63nM (figure 28). Hence we conclude that hERG1 channels regulate cell migration and actin cytoskeleton organization through interactions with $\beta 1$ integrins and this regulation could be due to the decreased $[Ca^{2+}]_i$. We speculate that there could perhaps be indirect interactions between hERG1 and calcium permitting channels like transient receptor potential (TRP) channels and therefore further investigation is necessary.

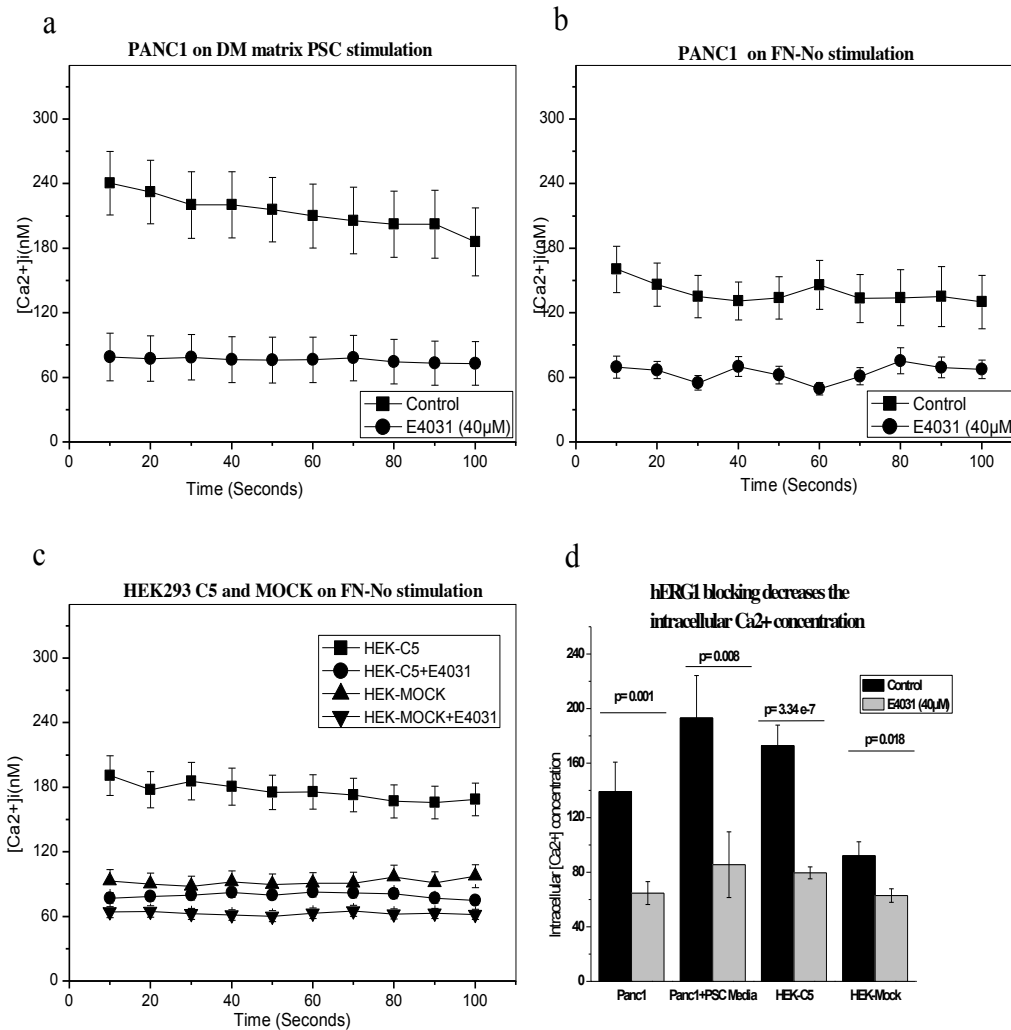


Figure 28. The intracellular Ca^{2+} concentration was measured using calibration buffer consisting of 0mM and 5mM Ca^{2+} . The time course of intracellular concentrations was measured at the end of treatment. The concentration was estimated for at least 10 time points over-a-period of 100 seconds. The hERG1 blocker E4031 decreased the intracellular concentration by more than 2 fold in both PSC stimulated Panc1 cells seeded on DM matrix (a) and non-stimulation on FN (b). The exogenous expression of hERG1 channels in HEK293 cells also showed drastic increase in intracellular Ca^{2+} compared to mock transfected HEK293 cells. The E4031 treatment decreased the elevated Ca^{2+} concentration to that of HEK-mock cells and E4031 has little effect on HEK-mock (c). The overall intracellular concentration of Ca^{2+} is at least 2 fold lower when cells expressing hERG1 were treated with E4031 (d).

5. CONCLUSION REMARKS

Cancer cell arises from the transformation of normal cell that has characteristic features of slow and limited proliferative capabilities. During the transformation normal cells acquire series of genetic mutations that eventually lead to becoming cancer cells that has ever-proliferating capabilities and at much faster rate. At the molecular level the cancer cell possesses the alterations in vast number genes that are otherwise tumor suppressor genes. More often the tumor suppressor genes are either mutated or deleted for ex. *TP53*, or tumor-enhancing gene (oncogenes) are constitutively activated for ex. *KRas* that ever induce cell proliferation. In addition there are many membrane proteins that are also highly expressed. This includes, among many other membrane proteins, epidermal growth factor receptors (EGFR), several integrin receptors, ion channels etc.

The roles of ion channels in regulating the cellular functions including cell cycle progression, cell-volume regulation and other physiological processes have been well studied. In addition there has been increasing evidence that ion channels are also implicated in all most all cancer besides other pathological conditions. The groups of pathological conditions in which ion channels are implicated are termed as channelopathies. In primary cancer or cancer cell lines ion channels' expression is generally up regulated although some ion channels are also down regulated. Potassium ion channels are the single largest class of ion channels that are expressed in cells. The voltage-gated potassium ion channels HERG1 also called as hERG1 is expressed by gene *KCNH2*. The hERG1 channels are aberrantly expressed in most of the cancers including pancreatic ductal adenocarcinoma (PDAC) and hence serve as a marker for diagnosis and potential targets for therapy.

Firstly, we studied the role of hERG1 channels in PDAC cell lines (Panc1, MiaPaCa2 and BxPC3). Our study shows that hERG1 channels are differently expressed in these cell lines and primary tumours in human. The functional blocking

of the channels by hERG1 specific small molecule drug E4031 showed inhibitory effect on cell proliferation and anchorage independent cell survival of PDAC cells. Further study demonstrates that the inhibitory effect on cell proliferation was mediated through MAPK/ERK signaling pathway in Panc1 cells (Lastraioli et al., 2015).

Secondly, we reasoned that hERG1 channels could be, in partial, regulating the cell proliferation through interactions with EGFRs and integrins. So we immediately characterized the expression levels of EGFRs and surface expression of integrins $\beta 1$ and $\alpha V\beta 5$ on various ECM proteins. The EGFR expression was very high in all cell lines. Interestingly, the surface expression of both $\beta 1$ and $\alpha V\beta 5$ was greatly enhanced when Panc1 cells were seeded on FN. The interactions between hERG1, EGFR and $\beta 1$ and $\alpha V\beta 5$ were studied through co-immunoprecipitation (co-IP) experiments. The experiments revealed that hERG1 makes macromolecular complex formation between EGFR, $\beta 1$ and $\alpha V\beta 5$ integrins. Interestingly, hERG1 strongly co-localizes with only $\beta 1$ integrins. However, complex formation (both co-IP and co-localization) between hERG1 and $\beta 1$ was conditional; that is hERG/ $\beta 1$ complex formation occurred only when $\beta 1$ integrin was activated by ECMs and hERG1 channel was functional. Hence we pursued our interests in understanding the mechanism involved in interactions between hERG1 and $\beta 1$ integrins. When Panc1 cells were seeded on PLL or when cells were treated with E4031 the hERG1/ $\beta 1$ complex formation was drastically reduced.

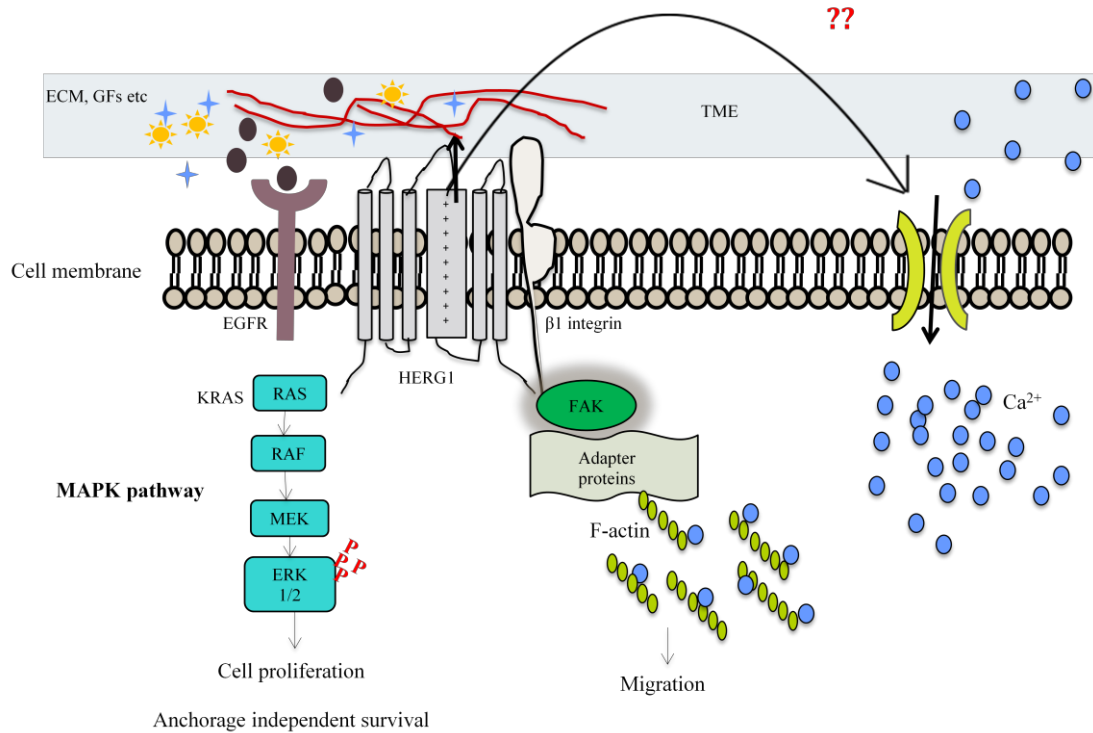
Thirdly, we attempted to study which domains in hERG1 and $\beta 1$ could be involved in complex formation. For this purpose we used non-hERG1 expressing HEK293 cells transfected with variants of hERG1 channels that do not harbour N or C-terminus domain. On the other hand we also used mouse fibroblast GD25WT cells that is negative for $\beta 1$ integrins. GD25WT cells were co-transfected with (i) $\beta 1$ integrin coding gene devoid of cytoplasmic tail and full-length hERG1 and (ii) full length $\beta 1$ and hERG1. Our co-IP findings suggest that cytoplasmic domains of both hERG1 and $\beta 1$ are not necessary for the interactions. Further characterization shows

that the closed state conformation of the hERG1 channel is more favourable for complex formation with $\beta 1$ integrins.

Fourthly, based on the above observations we hypothesized that hERG1 channels could modulate the integrin mediated functions like cell adhesion, migration and cytoskeleton organization. The time course of cell adhesion on FN was unaltered when Panc1 cells were treated with E4031 or hERG1 channels were transfected in HEK293 cells. This was also supported by the fact the number and area of focal adhesions of FAK and paxillin (two of the most important focal adhesion proteins that are recruited at the early stage of cell adhesion) was also unaffected with E4031 treatment. However, E4031 treatment reduced the migration of Panc1 cells (Lastraioli et al., 2015). This prompted us to hypothesize that hERG1 could be involved in modulating the migration machineries of cells most notably cytoskeleton proteins like actin. In deed Panc1 cells treated with E4031 altered the actin cytoskeleton organization in Panc1 cells. The functional blocking of hERG1 by E4031 treatment produced more organized and longer actin filaments that are spread along the cell body than control conditions where the actin filaments are significantly shorter and dispersed. This observation was further strengthened when HEK293 and GD25WT $\beta 1A$ were transfected with functional hERG1 channels. The over expression of hERG1 channels produced shorter and dispersed actin filaments similar to control Panc1 cells. In addition, due to the alterations in actin organization we observed the decrease in cell spread area especially in hERG1 over expressing HEK293 and GD25WT $\beta 1A$ cells. However, the orientation of actin filaments was constant. The overall functional role of hERG1 channels in Panc1 cells in interactions with EGFR and integrins has been summarized in the schematic representation above (scheme 9).

Finally, we challenged the role of hERG1 channels in regulating cell migration and actin cytoskeleton in more complex and multifactorial system. To this purpose we studied the role of hERG1 channels in Panc1 cells migration stimulated by hypoxically activated PSCs' conditioned medium. The Panc1 cells were plated on

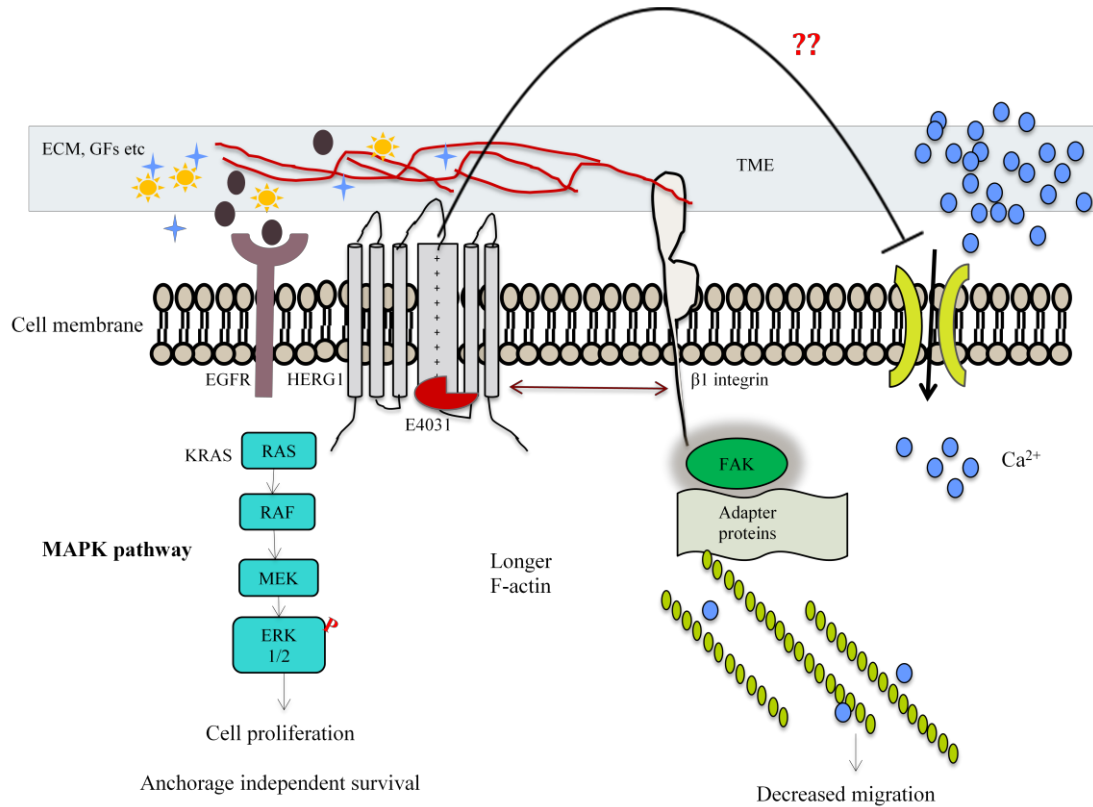
desmoplastic matrix (DM) coating and cells were stimulated with conditioned medium of PSCs.



Scheme 9: The above scheme represents the interactions of functionally active hERG1 channels with EGFR and $\beta 1$ integrins in tumor microenvironment mimicked in vitro. Functionally active hERG1 channels interact with EGFR and integrins and, modulate the intracellular signaling pathways that are implicated in cell proliferation, anchorage independent survival and cell migration. Functionally active hERG1 channels interact with EGFRs and increase pro-proliferative cell signaling through RAS/ERK pathway (increased phosphorylation of ERK1/2). HERG1 channels interact with $\beta 1$ integrins in more tightly and co-ordinated manner. In fact hERG1 and $\beta 1$ integrins are shown to be co-localized and regulate integrin mediated cell migration, signaling pathways as well as actin cytoskeleton organization. The functional hERG1 channels lead to increased cell migration and shorter and dispersed actin filaments. This could be due to the increase in $[Ca^{2+}]_i$, perhaps through TRPM8 cells and therefore further investigation is necessary.

The PSCs' conditioned media significantly increased the cell migration compared to non-conditioned medium. HERG1 blocking showed highest inhibition of cell migration stimulated by conditioned media. Further we attempted to study the changes in the dynamics of actin organization in the same set up. Spatio-temporal

image correlation spectroscopy (STICS) method reveals that E4031 treatment significantly increased the actin dynamics as well as diffusion coefficient of actin in contrast to control conditions. We reasoned that the changes in actin organization and dynamics due to blocking of hERG1 channels could be because of the shift in the calcium concentrations. Because hyperpolarization of breast cancer cells by activating the hERG1 channels has shown to increase the calcium influx, which was however completely reversed by generic calcium channel blocker CoCl₂ (Neut M.P et al., 2015). In addition, the cytoskeleton proteins are calcium sensitive proteins and therefore it was noteworthy to study role of hERG1 channel blocking in intracellular calcium concentrations. Hence we measured the intracellular calcium concentrations between control and E4031 treatment events and observed that $[Ca^{2+}]_i$ was decreased by more than two-fold when cells were E4031 treated. However, the exact mechanism through which the calcium entry was inhibited, due to hERG1 blocking, is not understood. We speculate that the calcium entry could be mediated through transient receptor potential cation channel, subfamily 8 (TRPM8), among many other calcium-permitting channels. The expression of TRPM8 channels is up regulated in Panc1 cells and hence further investigation for the establish the relation between hERG1 and TRPM8 channels is essential for better understanding of the underlying mechanism. The overall effect of functional blocking of hERG1 channels by E4031 on interactions with EGFR and integrins has been summarized in the schematic representation below (scheme 10).



*Scheme10. The above scheme represents the interactions of functionally blocked (by E4031) hERG1 channels with EGFR and $\beta 1$ integrins in tumor microenvironment mimicked in vitro. When hERG1 channels are functionally blocked we observed the decreased in phosphorylation of ERK1/2 (shown as single **P**) that lead to slower growth rate of cells. The E4031 showed the highest effect in the interactions between hERG1 and $\beta 1$ integrins. In fact, E4031 treatment impaired the co-localization between hERG1 and $\beta 1$. Further, E4031 treatment decreased the cell migration and produced longer and more organized actin filaments. The E4031 also decreased the $[Ca^{2+}]_i$.*

6. REFERENCES

- Altier C, Zamponi G. W. Analysis of GPCR/ion channel interactions. *Methods Mol Biol.* 2011; 756:215-25.
- Ames, B.N., and L.S. Gold. 1998. The causes and prevention of cancer: the role of environment. *Biotherapy (Dordrecht, Netherlands)*. 11:205–20.
- Andersen, A.P., J.M.M. Moreira, and S.F. Pedersen. 2014. Interactions of ion transporters and channels with cancer cell metabolism and the tumour microenvironment. *Philos. Trans. R. Soc. Lond., B, Biol. Sci.* 369:20130098. doi:10.1098/rstb.2013.0098.
- Apte, M.V., S. Park, P.A. Phillips, N. Santucci, D. Goldstein, R.K. Kumar, G.A. Ramm, M. Buchler, H. Friess, J.A. McCarroll, G. Keogh, N. Merrett, R. Pirola, and J.S. Wilson. 2004. Desmoplastic reaction in pancreatic cancer: role of pancreatic stellate cells. *Pancreas.* 29:179–87.
- Arcangeli, A., O. Crociani, E. Lastraioli, A. Masi, S. Pillozzi, and A. Becchetti. 2009. Targeting ion channels in cancer: a novel frontier in antineoplastic therapy. *Curr. Med. Chem.* 16:66–93.
- Arcangeli, A. 2011. Ion channels and transporters in cancer. 3. Ion channels in the tumor cell-microenvironment cross talk. *Am. J. Physiol., Cell Physiol.* 301:C762–71. doi:10.1152/ajpcell.00113.2011.
- Armstrong, T., G. Packham, L.B. Murphy, A.C. Bateman, J.A. Conti, D.R. Fine, C.D. Johnson, R.C. Benyon, and J.P. Iredale. 2004. Type I collagen promotes the malignant phenotype of pancreatic ductal adenocarcinoma. *Clinical cancer research : an official journal of the American Association for Cancer Research.* 10:7427–37. doi:10.1158/1078-0432.CCR-03-0825.
- Arthur, W.T., and K. Burridge. 2001. RhoA inactivation by p190RhoGAP regulates cell spreading and migration by promoting membrane protrusion and polarity. *Molecular biology of the cell.* 12:2711–20.
- Artym, V.V., and H.R. Petty. 2002. Molecular proximity of Kv1.3 voltage-gated potassium channels and beta(1)-integrins on the plasma membrane of melanoma cells: effects of cell adherence and channel blockers. *The Journal of general physiology.* 120:29–37.
- Asher, V., R. Khan, A. Warren, R. Shaw, G.V. Schalkwyk, A. Bali, and H.M. Sowter. 2010. The Eag potassium channel as a new prognostic marker in ovarian cancer. *Diagn Pathol.* 5:78. doi:10.1186/1746-1596-5-78.

- Balcioglu HE, van Hoorn H, Donato DM, Schmidt T, Danen EH. The integrin expression profile modulates orientation and dynamics of force transmission at cell-matrix adhesions. *J Cell Sci.* 2015 Apr 1; 128(7): 1316-26.
- Betapudi, V., V. Rai, J.R. Beach, and T. Egelhoff. 2010. Novel regulation and dynamics of myosin II activation during epidermal wound responses. *Exp. Cell Res.* 316:980–91. doi:10.1016/j.yexcr.2010.01.024.
- Binggeli, R., and I.L. Cameron. 1980. Cellular potentials of normal and cancerous fibroblasts and hepatocytes. *Cancer research.* 40:1830–5.
- Blackiston, D.J., K.A. McLaughlin, and M. Levin. 2009. Bioelectric controls of cell proliferation: ion channels, membrane voltage and the cell cycle. *Cell cycle (Georgetown, Tex.)*. 8:3527–36.
- Blanchoin, L., Boujemaa-Paterski, R., Sykes, C., Plastino, J. 2014. Actin dynamics, architecture and mechanics in cell motility. *Physiol Rev.* Jan; 94(1): 235-63. doi: 10.1152/physrev.00018.2013.
- Bose, T., A. Ciešlar-Pobuda, and E. Wiechec. 2015. Role of ion channels in regulating Ca²⁺ homeostasis during the interplay between immune and cancer cells. *Cell Death Dis.* 6:e1648. doi:10.1038/cddis.2015.23.
- Brundage, R.A., K.E. Fogarty, R.A. Tuft, and F.S. Fay. 1991. Calcium gradients underlying polarization and chemotaxis of eosinophils. *Science (New York, N.Y.)*. 254:703–6.
- Calderwood, D.A. 2004a. Integrin activation. *Journal of cell science.* 117:657–66. doi:10.1242/jcs.01014.
- Calderwood, D.A. 2004b. Talin controls integrin activation. *Biochemical Society transactions.* 32:434–7. doi:10.1042/BST0320434.
- Calderwood, D.A., I.D. Campbell, and D.R. Critchley. 2013. Talins and kindlins: partners in integrin-mediated adhesion. *Nature reviews. Molecular cell biology.* 14:503–17. doi:10.1038/nrm3624.
- Campbell, I.D., and M.J. Humphries. 2011. Integrin structure, activation, and interactions. *Cold Spring Harbor perspectives in biology.* 3. doi:10.1101/cshperspect.a004994.
- Campbell, P.J., S. Yachida, L.J. Mudie, P.J. Stephens, E.D. Pleasance, L.A. Stebbings, L.A. Morsberger, C. Latimer, S. McLaren, M.-L.L. Lin, D.J. McBride, I. Varela, S.A. Nik-Zainal, C. Leroy, M. Jia, A. Menzies, A.P. Butler, J.W. Teague, C.A. Griffin, J. Burton, H. Swerdlow, M.A. Quail, M.R. Stratton, C. Iacobuzio-

Donahue, and P.A. Futreal. 2010. The patterns and dynamics of genomic instability in metastatic pancreatic cancer. *Nature*. 467:1109–13. doi:10.1038/nature09460.

Cherubini, A., G. Hofmann, S. Pillozzi, L. Guasti, O. Crociani, E. Cilia, P. Di Stefano, S. Degani, M. Balzi, M. Olivotto, E. Wanke, A. Becchetti, P. Defilippi, R. Wymore, and A. Arcangeli. 2005. Human ether-a-go-go-related gene 1 channels are physically linked to beta1 integrins and modulate adhesion-dependent signaling. *Mol. Biol. Cell*. 16:2972–83. doi:10.1091/mbc.E04-10-0940.

Clare, J.J. 2010. Targeting ion channels for drug discovery. *Discov Med*. 9:253–60.

Clark, C.E., S.R. Hingorani, R. Mick, C. Combs, D.A. Tuveson, and R.H. Vonderheide. 2007. Dynamics of the immune reaction to pancreatic cancer from inception to invasion. *Cancer Res*. 67:9518–27. doi:10.1158/0008-5472.CAN-07-0175.

Cone, C.D., and C.M. Cone. 1976. Induction of mitosis in mature neurons in central nervous system by sustained depolarization. *Science (New York, N.Y.)*. 192:155–8.

Crociani, O., F. Zanieri, S. Pillozzi, E. Lastraioli, M. Stefanini, A. Fiore, A. Fortunato, M. D'Amico, M. Masselli, E. De Lorenzo, L. Gasparoli, M. Chiu, O. Bussolati, A. Becchetti, and A. Arcangeli. 2013. hERG1 channels modulate integrin signaling to trigger angiogenesis and tumor progression in colorectal cancer. *Scientific reports*. 3:3308. doi:10.1038/srep03308.

Cubilla, A.L., and P.J. Fitzgerald. 1976. Morphological lesions associated with human primary invasive nonendocrine pancreas cancer. *Cancer research*. 36:2690–8.

Dang, C.V. 2012. Links between metabolism and cancer. *Genes Dev*. 26:877–90. doi:10.1101/gad.189365.112.

Deer, E., J. González-Hernández, J. Coursen, J. Shea, J. Ngatia, C. Scaife, M. Firpo, and S. Mulvihill. 2010. Phenotype and Genotype of Pancreatic Cancer Cell Lines. *Pancreas*. 39:425. doi:10.1097/MPA.0b013e3181c15963.

Desgrosellier, J.S., L.A. Barnes, D.J. Shields, M. Huang, S.K. Lau, N. Prévost, D. Tarin, S.J. Shattil, and D.A. Cheresh. 2009. An integrin alpha(v)beta(3)-c-Src oncogenic unit promotes anchorage-independence and tumor progression. *Nat. Med*. 15:1163–9. doi:10.1038/nm.2009.

Desgrosellier, J.S., and D.A. Cheresh. 2010. Integrins in cancer: biological implications and therapeutic opportunities. *Nat. Rev. Cancer*. 10:9–22. doi:10.1038/nrc2748.

Duronio, R. J., Xiong Y. 2013. Signaling pathways that control cell proliferation. *Cold Spring Harb Perspect Biol*. 2013 Mar 1; 5(3).

- Dworakowska, B., and K. Dołowy. 2000. Ion channels-related diseases. *Acta Biochim. Pol.* 47:685–703.
- Ebrahimi, B., S.L. Tucker, D. Li, J.L. Abbruzzese, and R. Kurzrock. 2004. Cytokines in pancreatic carcinoma: correlation with phenotypic characteristics and prognosis. *Cancer*. 101:2727–36. doi:10.1002/cncr.20672.
- Ellenrieder, V., B. Alber, U. Lacher, S.F. Hendler, A. Menke, W. Boeck, M. Wagner, M. Wilda, H. Friess, M. Büchler, G. Adler, and T.M. Gress. 2000. Role of MT-MMPs and MMP-2 in pancreatic cancer progression. *Int. J. Cancer*. 85:14–20.
- Eguchi D, Ikenaga N, Ohuchida K, Kozono S, Cui L, Fujiwara K, Fujino M, Ohtsuka T, Mizumoto K, Tanaka M. Hypoxia enhances the interaction between pancreatic stellate cells and cancer cells via increased secretion of connective tissue growth factor. *J Surg Res*. 2013 May; 181(2): 225-33.
- Fässler R, Pfaff M, Murphy J, Noegel AA, Johansson S, Timpl R, Albrecht R. Lack of beta 1 integrin gene in embryonic stem cells affects morphology, adhesion, and migration but not integration into the inner cell mass of blastocysts. *J Cell Biol*. 1995 Mar; 128(5): 979-88.
- Feng, J., J. Yu, X. Pan, Z. Li, Z. Chen, W. Zhang, B. Wang, L. Yang, H. Xu, G. Zhang, and Z. Xu. 2014a. HERG1 functions as an oncogene in pancreatic cancer and is downregulated by miR-96. *Oncotarget*. 5:5832–44.
- Froeling, F.E., C. Feig, C. Chelala, R. Dobson, C.E. Mein, D.A. Tuveson, H. Clevers, I.R. Hart, and H.M. Kocher. 2011. Retinoic acid-induced pancreatic stellate cell quiescence reduces paracrine Wnt- β -catenin signaling to slow tumor progression. *Gastroenterology*. 141:1486–97, 1497.e1–14. doi:10.1053/j.gastro.2011.06.047.
- Fuchs, C.S., G.A. Colditz, M.J. Stampfer, E.L. Giovannucci, D.J. Hunter, E.B. Rimm, W.C. Willett, and F.E. Speizer. 1996. A prospective study of cigarette smoking and the risk of pancreatic cancer. *Arch. Intern. Med.* 156:2255–60.
- Giannone, G., P. Rondé, M. Gaire, J. Haiech, and K. Takeda. 2002. Calcium oscillations trigger focal adhesion disassembly in human U87 astrocytoma cells. *J. Biol. Chem.* 277:26364–71. doi:10.1074/jbc.M203952200.
- Gnoni, A., A. Licchetta, A. Scarpa, A. Azzariti, A.E. Brunetti, G. Simone, P. Nardulli, D. Santini, M. Aieta, S. Delcuratolo, and N. Silvestris. 2013. Carcinogenesis of pancreatic adenocarcinoma: precursor lesions. *International journal of molecular sciences*. 14:19731–62. doi:10.3390/ijms141019731.
- Grzesiak, J.J., and M. Bouvet. 2006. The alpha2beta1 integrin mediates the malignant phenotype on type I collagen in pancreatic cancer cell lines. *Br. J. Cancer*. 94:1311–

9. doi:10.1038/sj.bjc.6603088.

Grzesiak, J.J., J.C. Ho, A.R. Moossa, and M. Bouvet. 2007. The integrin-extracellular matrix axis in pancreatic cancer. *Pancreas*. 35:293–301. doi:10.1097/mpa.0b013e31811f4526.

Grzesiak, J.J., H.S. Tran Cao, D.W. Burton, S. Kaushal, F. Vargas, P. Clopton, C.S. Snyder, L.J. Deftos, R.M. Hoffman, and M. Bouvet. 2011. Knockdown of the $\beta(1)$ integrin subunit reduces primary tumor growth and inhibits pancreatic cancer metastasis. *Int. J. Cancer*. 129:2905–15. doi:10.1002/ijc.25942.

Guerra, C., A.J. Schuhmacher, M. Cañamero, P.J. Grippo, L. Verdaguer, L. Pérez-Gallego, P. Dubus, E.P. Sandgren, and M. Barbacid. 2007. Chronic pancreatitis is essential for induction of pancreatic ductal adenocarcinoma by K-Ras oncogenes in adult mice. *Cancer Cell*. 11:291–302. doi:10.1016/j.ccr.2007.01.012.

Guo W, Giancotti FG. Integrin signalling during tumour progression. *Nat Rev Mol Cell Biol*. 2004 Oct; 5(10): 816-26.

Haeno, H., M. Gonen, M.B. Davis, J.M. Herman, C.A. Iacobuzio-Donahue, and F. Michor. 2012. Computational modeling of pancreatic cancer reveals kinetics of metastasis suggesting optimum treatment strategies. *Cell*. 148:362–75. doi:10.1016/j.cell.2011.11.060.

Hall, P.A., P. Coates, N.R. Lemoine, and M.A. Horton. 1991. Characterization of integrin chains in normal and neoplastic human pancreas. *J. Pathol*. 165:33–41. doi:10.1002/path.1711650107.

Hanahan, D., and R.A. Weinberg. 2011. Hallmarks of cancer: the next generation. *Cell*. 144:646–74. doi:10.1016/j.cell.2011.02.013.

Hannigan GE, Leung-Hagesteijn C, Fitz-Gibbon L, Coppolino MG, Radeva G, Filmus J, Bell JC, Dedhar S. Regulation of cell adhesion and anchorage-dependent growth by a new beta 1-integrin-linked protein kinase. *Nature*. 1996 Jan 4; 379(6560): 91-6.

Hansen, S.B. 2015. Lipid agonism: The PIP2 paradigm of ligand-gated ion channels. *Biochimica et biophysica acta*. 1851:620–8. doi:10.1016/j.bbalip.2015.01.011.

Harburger, D., and D. Calderwood. 2009. Integrin signalling at a glance. *J. Cell Sci*. 122:159–163. doi:10.1242/jcs.018093.

Hartung, F., W. Stühmer, and L.A. Pardo. 2011. Tumor cell-selective apoptosis induction through targeting of K(V)10.1 via bifunctional TRAIL antibody. *Molecular cancer*. 10:109. doi:10.1186/1476-4598-10-109.

- Hebert B, Costantino S, Wiseman PW. Spatiotemporal image correlation spectroscopy (STICS) theory, verification, and application to protein velocity mapping in living CHO cells. *Biophys J*. 2005 May; 88(5): 3601-14. Epub 2005 Feb 18.
- Heek, N.T. van, A.K. Meeker, S.E. Kern, C.J. Yeo, K.D. Lillemoe, J.L. Cameron, G.J. Offerhaus, J.L. Hicks, R.E. Wilentz, M.G. Goggins, A.M. De Marzo, R.H. Hruban, and A. Maitra. 2002. Telomere shortening is nearly universal in pancreatic intraepithelial neoplasia. *The American journal of pathology*. 161:1541–7. doi:10.1016/S0002-9440(10)64432-X.
- Heldin, C.-H.H. 2013. Targeting the PDGF signaling pathway in tumor treatment. *Cell Commun. Signal*. 11:97. doi:10.1186/1478-811X-11-97.
- Hezel, A.F., A.C. Kimmelman, B.Z. Stanger, N. Bardeesy, and R.A. Depinho. 2006. Genetics and biology of pancreatic ductal adenocarcinoma. *Genes Dev*. 20:1218–49. doi:10.1101/gad.1415606.
- Horzum U, Ozdil B, Pesen-Okvur D. Step-by-step quantitative analysis of focal adhesions. *MethodsX*. 2014 Jul 7; 1: 56-9.
- Huang, X., and L.Y. Jan. 2014. Targeting potassium channels in cancer. *The Journal of cell biology*. 206:151–62. doi:10.1083/jcb.201404136.
- Hübner, C.A., and T.J. Jentsch. 2002. Ion channel diseases. *Hum. Mol. Genet*. 11:2435–45.
- Huttenlocher, A., M.H. Ginsberg, and A.F. Horwitz. 1996. Modulation of cell migration by integrin-mediated cytoskeletal linkages and ligand-binding affinity. *The Journal of cell biology*. 134:1551–62.
- Huttenlocher, A., and A.R. Horwitz. 2011. Integrins in cell migration. *Cold Spring Harbor perspectives in biology*. 3:a005074. doi:10.1101/cshperspect.a005074.
- Huveneers, S., and E.H. Danen. 2009. Adhesion signaling - crosstalk between integrins, Src and Rho. *Journal of cell science*. 122:1059–69. doi:10.1242/jcs.039446.
- Hwang, R.F., T. Moore, T. Arumugam, V. Ramachandran, K.D. Amos, A. Rivera, B. Ji, D.B. Evans, and C.D. Logsdon. 2008. Cancer-associated stromal fibroblasts promote pancreatic tumor progression. *Cancer Res*. 68:918–26. doi:10.1158/0008-5472.CAN-07-5714.
- Iacobuzio-Donahue, C.A. 2012. Genetic evolution of pancreatic cancer: lessons learnt from the pancreatic cancer genome sequencing project. *Gut*. 61:1085–94. doi:10.1136/gut.2010.236026.

Iacobuzio-Donahue, C.A., B. Fu, S. Yachida, M. Luo, H. Abe, C.M. Henderson, F. Vilardell, Z. Wang, J.W. Keller, P. Banerjee, J.M. Herman, J.L. Cameron, C.J. Yeo, M.K. Halushka, J.R. Eshleman, M. Raben, A.P. Klein, R.H. Hruban, M. Hidalgo, and D. Laheru. 2009. DPC4 gene status of the primary carcinoma correlates with patterns of failure in patients with pancreatic cancer. *Journal of clinical oncology: official journal of the American Society of Clinical Oncology*. 27:1806–13. doi:10.1200/JCO.2008.17.7188.

Iacobuzio-Donahue, C.A., V.E. Velculescu, C.L. Wolfgang, and R.H. Hruban. 2012. Genetic basis of pancreas cancer development and progression: insights from whole-exome and whole-genome sequencing. *Clin. Cancer Res.* 18:4257–65. doi:10.1158/1078-0432.CCR-12-0315.

Ino, Y., R. Yamazaki-Itoh, K. Shimada, M. Iwasaki, T. Kosuge, Y. Kanai, and N. Hiraoka. 2013. Immune cell infiltration as an indicator of the immune microenvironment of pancreatic cancer. *Br. J. Cancer*. 108:914–23. doi:10.1038/bjc.2013.32.

Jäger, H., T. Dreker, A. Buck, K. Giehl, T. Gress, and S. Grissmer. 2004. Blockage of intermediate-conductance Ca²⁺-activated K⁺ channels inhibit human pancreatic cancer cell growth in vitro. *Molecular pharmacology*. 65:630–8. doi:10.1124/mol.65.3.630.

Jehle, J., P.A. Schweizer, H.A. Katus, and D. Thomas. 2011. Novel roles for hERG K(+) channels in cell proliferation and apoptosis. *Cell Death Dis.* 2:e193. doi:10.1038/cddis.2011.77.

Jentsch, T.J., C.A. Hübner, and J.C. Fuhrmann. 2004. Ion channels: function unravelled by dysfunction. *Nat. Cell Biol.* 6:1039–47. doi:10.1038/ncb1104-1039.

Jesnowski R, Fürst D, Ringel J, Chen Y, Schrödel A, Kleeff J, Kolb A, Schareck WD, Löhr M. Immortalization of pancreatic stellate cells as an in vitro model of pancreatic fibrosis: deactivation is induced by matrigel and N-acetylcysteine. *Lab Invest*. 2005 Oct; 85(10): 1276-91.

Jones, S., X. Zhang, D.W. Parsons, J.C. Lin, R.J. Leary, P. Angenendt, P. Mankoo, H. Carter, H. Kamiyama, A. Jimeno, S.-M.M. Hong, B. Fu, M.-T.T. Lin, E.S. Calhoun, M. Kamiyama, K. Walter, T. Nikolskaya, Y. Nikolsky, J. Hartigan, D.R. Smith, M. Hidalgo, S.D. Leach, A.P. Klein, E.M. Jaffee, M. Goggins, A. Maitra, C. Iacobuzio-Donahue, J.R. Eshleman, S.E. Kern, R.H. Hruban, R. Karchin, N. Papadopoulos, G. Parmigiani, B. Vogelstein, V.E. Velculescu, and K.W. Kinzler. 2008. Core signaling pathways in human pancreatic cancers revealed by global genomic analyses. *Science*. 321:1801–6. doi:10.1126/science.1164368.

Kaczorowski, G.J., O.B. McManus, B.T. Priest, and M.L. Garcia. 2008. Ion channels

as drug targets: the next GPCRs. *J. Gen. Physiol.* 131:399–405. doi:10.1085/jgp.200709946.

Kanda, M., H. Matthaei, J. Wu, S.-M.M. Hong, J. Yu, M. Borges, R.H. Hruban, A. Maitra, K. Kinzler, B. Vogelstein, and M. Goggins. 2012. Presence of somatic mutations in most early-stage pancreatic intraepithelial neoplasia. *Gastroenterology*. 142:730–733.e9. doi:10.1053/j.gastro.2011.12.042.

Kim, C., F. Ye, and M.H. Ginsberg. 2011. Regulation of integrin activation. *Annual review of cell and developmental biology*. 27:321–45. doi:10.1146/annurev-cellbio-100109-104104.

Ko, J.-H.H., E.A. Ko, W. Gu, I. Lim, H. Bang, and T. Zhou. 2013. Expression profiling of ion channel genes predicts clinical outcome in breast cancer. *Mol. Cancer*. 12:106. doi:10.1186/1476-4598-12-106.

Kumar, C. 1998. Signaling by integrin receptors. *Oncogene*. 17:-. doi:10.1038/sj.onc.1202172.

Kupersmidt S, Snyders DJ, Raes A, Roden DM. A K⁺ channel splice variant common in human heart lacks a C-terminal domain required for expression of rapidly activating delayed rectifier current. *J Biol Chem*. 1998 Oct 16; 273(42): 27231-5.

Lallet-Daher, H., C. Wiel, D. Gitenay, N. Navaratnam, A. Augert, B. Le Calvé, S. Verbeke, D. Carling, S. Aubert, D. Vindrieux, and D. Bernard. 2013. Potassium channel KCNA1 modulates oncogene-induced senescence and transformation. *Cancer Res*. 73:5253–65. doi:10.1158/0008-5472.CAN-12-3690.

Lang, F., M. Föllner, K. Lang, P. Lang, M. Ritter, A. Vereninov, I. Szabo, S.M. Huber, and E. Gulbins. 2007. Cell volume regulatory ion channels in cell proliferation and cell death. *Methods in enzymology*. 428:209–25. doi:10.1016/S0076-6879(07)28011-5.

Lang, F., M. Föllner, K.S. Lang, P.A. Lang, M. Ritter, E. Gulbins, A. Vereninov, and S.M. Huber. 2005. Ion channels in cell proliferation and apoptotic cell death. *The Journal of membrane biology*. 205:147–57. doi:10.1007/s00232-005-0780-5.

Lansu, and Gentile. 2013. Potassium channel activation inhibits proliferation of breast cancer cells by activating a senescence program. *Cell Death & Disease*. 4:e652. doi:10.1038/cddis.2013.174.

Lastraioli, E., G. Perrone, A. Sette, A. Fiore, O. Crociani, S. Manoli, M. D'Amico, M. Masselli, J. Iorio, M. Callea, D. Borzomati, G. Nappo, F. Bartolozzi, D. Santini, L. Bencini, M. Farsi, L. Boni, F. Di Costanzo, A. Schwab, A. Onetti Muda, R. Coppola, and A. Arcangeli. 2015. hERG1 channels drive tumour malignancy and may serve as prognostic factor in pancreatic ductal adenocarcinoma. *Br. J. Cancer*.

112:1076–87. doi:10.1038/bjc.2015.28.

Lawson, C., S.-T.T. Lim, S. Uryu, X.L. Chen, D.A. Calderwood, and D.D. Schlaepfer. 2012. FAK promotes recruitment of talin to nascent adhesions to control cell motility. *The Journal of cell biology*. 196:223–32. doi:10.1083/jcb.201108078.

Legate, K.R., S.A. Wickström, and R. Fässler. 2009. Genetic and cell biological analysis of integrin outside-in signaling. *Genes & development*. 23:397–418. doi:10.1101/gad.1758709.

Levite, M., L. Cahalon, A. Peretz, R. HersHKoviz, A. Sobko, A. Ariel, R. Desai, B. Attali, and O. Lider. 2000. Extracellular K(+) and opening of voltage-gated potassium channels activate T cell integrin function: physical and functional association between Kv1.3 channels and beta1 integrins. *The Journal of experimental medicine*. 191:1167–76.

Lowenfels, A.B., P. Maisonneuve, G. Cavallini, R.W. Ammann, P.G. Lankisch, J.R. Andersen, E.P. Dimagno, A. Andrén-Sandberg, and L. Domellöf. 1993. Pancreatitis and the risk of pancreatic cancer. International Pancreatitis Study Group. *N. Engl. J. Med.* 328:1433–7. doi:10.1056/NEJM199305203282001.

Lu P, Weaver VM, Werb Z. The extracellular matrix: a dynamic niche in cancer progression. *J Cell Biol*. 2012 Feb 20; 196(4):395-406.

Lu, J., S. Zhou, M. Siech, H. Habisch, T. Seufferlein, and M.G. Bachem. 2014. Pancreatic stellate cells promote haptotaxis of cancer cells through collagen I-mediated signalling pathway. *Br. J. Cancer*. 110:409–20. doi:10.1038/bjc.2013.706.

Mantoni, T.S., S. Lunardi, O. Al-Assar, A. Masamune, and T.B. Brunner. 2011. Pancreatic stellate cells radioprotect pancreatic cancer cells through β 1-integrin signaling. *Cancer Res*. 71:3453–8. doi:10.1158/0008-5472.CAN-10-1633.

Masamune A, Kikuta K, Watanabe T, Satoh K, Hirota M, Shimosegawa T. Hypoxia stimulates pancreatic stellate cells to induce fibrosis and angiogenesis in pancreatic cancer. *Am J Physiol Gastrointest Liver Physiol*. 2008 Oct; 295(4): G709-17.

McCarroll JA, Naim S, Sharbeen G, Russia N, Lee J, Kavallaris M, Goldstein D, Phillips PA. Role of pancreatic stellate cells in chemoresistance in pancreatic cancer. *Front Physiol*. 2014 Apr 9; 5:141

Mitra, S.K., D.A. Hanson, and D.D. Schlaepfer. 2005. Focal adhesion kinase: in command and control of cell motility. *Nature reviews. Molecular cell biology*. 6:56–68. doi:10.1038/nrm1549.

Mizejewski, G.J. 1999. Role of integrins in cancer: survey of expression patterns. *Proc. Soc. Exp. Biol. Med.* 222:124–38.

Morello V, Cabodi S, Sigismund S, Camacho-Leal MP, Repetto D, Volante M, Papotti M, Turco E, Defilippi P. β 1 integrin controls EGFR signaling and tumorigenic properties of lung cancer cells. *Oncogene*. 2011 Sep 29; 30(39): 4087-96.

Mould, A.P., J.A. Askari, and M.J. Humphries. 2000. Molecular basis of ligand recognition by integrin alpha 5beta 1. I. Specificity of ligand binding is determined by amino acid sequences in the second and third NH2-terminal repeats of the alpha subunit. *The Journal of biological chemistry*. 275:20324-36. doi:10.1074/jbc.M000572200.

Nagano, M., D. Hoshino, N. Koshikawa, T. Akizawa, and M. Seiki. 2012. Turnover of focal adhesions and cancer cell migration. *International journal of cell biology*. 2012:310616. doi:10.1155/2012/310616.

Nandy, D., and D. Mukhopadhyay. 2011. Growth factor mediated signaling in pancreatic pathogenesis. *Cancers*. 3:841-71. doi:10.3390/cancers3010841.

Nechyporuk-Zloy V, Dieterich P, Oberleithner H, Stock C, Schwab A. Dynamics of single potassium channel proteins in the plasma membrane of migrating cells. *Am J Physiol Cell Physiol*. 2008 Apr; 294(4): C1096-102

Perez-Neut, M., Shum, A., Cuevas, B.D., Miller, R., Gentile, S. 2015. Stimulation of hERG1 channel activity promotes a calcium-dependent degradation of cyclin E2, but not cyclin E1, in breast cancer cells. *Oncotarget*. 2015 Jan 30; 6(3): 1631-9.

Owens, D.M., and F.M. Watt. 2001. Influence of beta1 integrins on epidermal squamous cell carcinoma formation in a transgenic mouse model: alpha3beta1, but not alpha2beta1, suppresses malignant conversion. *Cancer Res*. 61:5248-54.

Pardo, L.A., D. del Camino, A. Sánchez, F. Alves, A. Brüggemann, S. Beckh, and W. Stühmer. 1999. Oncogenic potential of EAG K(+) channels. *EMBO J*. 18:5540-7. doi:10.1093/emboj/18.20.5540.

Parsons, J.T., A.R. Horwitz, and M.A. Schwartz. 2010. Cell adhesion: integrating cytoskeletal dynamics and cellular tension. *Nature reviews. Molecular cell biology*. 11:633-43. doi:10.1038/nrm2957.

Phillips, P.A., J.A. McCarroll, S. Park, M.-J.J. Wu, R. Pirola, M. Korsten, J.S. Wilson, and M.V. Apte. 2003. Rat pancreatic stellate cells secrete matrix metalloproteinases: implications for extracellular matrix turnover. *Gut*. 52:275-82.

Pillozzi, S., M.F. Brizzi, P.A. Bernabei, B. Bartolozzi, R. Caporale, V. Basile, V. Boddi, L. Pegoraro, A. Becchetti, and A. Arcangeli. 2007. VEGFR-1 (FLT-1), beta1 integrin, and hERG K+ channel for a macromolecular signaling complex in acute myeloid leukemia: role in cell migration and clinical outcome. *Blood*. 110:1238-50.

doi:10.1182/blood-2006-02-003772.

Pollard TD, Borisy GG. Cellular motility driven by assembly and disassembly of actin filaments. *Cell*. 2003 Feb 21; 112(4): 453-65.

Prevarskaya, N., R. Skryma, and Y. Shuba. 2010. Ion channels and the hallmarks of cancer. *Trends Mol Med*. 16:107–21. doi:10.1016/j.molmed.2010.01.005.

Ricono, J.M., M. Huang, L.A. Barnes, S.K. Lau, S.M. Weis, D.D. Schlaepfer, S.K. Hanks, and D.A. Cheresh. 2009. Specific cross-talk between epidermal growth factor receptor and integrin alphavbeta5 promotes carcinoma cell invasion and metastasis. *Cancer Res*. 69:1383–91. doi:10.1158/0008-5472.CAN-08-3612.

Riedl J, Crevenna AH, Kessenbrock K, Yu JH, Neukirchen D, Bista M, Bradke F, Jenne D, Holak TA, Werb Z, Sixt M, Wedlich-Soldner R. Lifeact: a versatile marker to visualize F-actin. *Nat Methods*. 2008 Jul; 5(7): 605-7.

Roshani, R., F. McCarthy, and T. Hagemann. 2014. Inflammatory cytokines in human pancreatic cancer. *Cancer Lett*. 345:157–63. doi:10.1016/j.canlet.2013.07.014.

Rosen LB, Greenberg ME. Stimulation of growth factor receptor signal transduction by activation of voltage-sensitive calcium channels. *Proc Natl Acad Sci U S A*. 1996 Feb 6; 93(3): 1113-8.

Ross RS. Molecular and mechanical synergy: cross-talk between integrins and growth factor receptors. *Cardiovasc Res*. 2004 Aug 15; 63(3): 381-90.

Ruoslahti, E. 1996. RGD and other recognition sequences for integrins. *Annual review of cell and developmental biology*. 12:697–715. doi:10.1146/annurev.cellbio.12.1.697.

Schneiderhan, W., F. Diaz, M. Fundel, S. Zhou, M. Siech, C. Hasel, P. Möller, J.E.E. Gschwend, T. Seufferlein, T. Gress, G. Adler, and M.G. Bachem. 2007. Pancreatic stellate cells are an important source of MMP-2 in human pancreatic cancer and accelerate tumor progression in a murine xenograft model and CAM assay. *J. Cell. Sci*. 120:512–9. doi:10.1242/jcs.03347.

Schwab, A., A. Fabian, P.J. Hanley, and C. Stock. 2012. Role of ion channels and transporters in cell migration. *Physiological reviews*. 92:1865–913. doi:10.1152/physrev.00018.2011.

Schwab, A., and C. Stock. 2014. Ion channels and transporters in tumour cell migration and invasion. *Philos. Trans. R. Soc. Lond., B, Biol. Sci*. 369:20130102. doi:10.1098/rstb.2013.0102.

Serrels, B., and M.C. Frame. 2012. FAK and talin: who is taking whom to the integrin engagement party? *The Journal of cell biology*. 196:185–7. doi:10.1083/jcb.201112128.

Shattil, S.J., C. Kim, and M.H. Ginsberg. 2010. The final steps of integrin activation: the end game. *Nature reviews. Molecular cell biology*. 11:288–300. doi:10.1038/nrm2871.

Shen, B., M.K. Delaney, and X. Du. 2012. Inside-out, outside-in, and inside-outside-in: G protein signaling in integrin-mediated cell adhesion, spreading, and retraction. *Current opinion in cell biology*. 24:600–6. doi:10.1016/j.ccb.2012.08.011.

Sheetz MP, Felsenfeld D, Galbraith CG, Choquet D. Cell migration as a five-step cycle. *Biochem Soc Symp*. 1999; 65: 233-43.

Srichai M B and Zent R. Integrin Structure and Function. *Cell-Extracellular Matrix Interactions in Cancer. Chapter 2*.

Szászi, K., G. Sirokmány, C. Di Ciano-Oliveira, O.D. Rotstein, and A. Kapus. 2005. Depolarization induces Rho-Rho kinase-mediated myosin light chain phosphorylation in kidney tubular cells. *American journal of physiology. Cell physiology*. 289:C673–85. doi:10.1152/ajpcell.00481.2004.

Takagi, J. 2004. Structural basis for ligand recognition by RGD (Arg-Gly-Asp)-dependent integrins. *Biochemical Society transactions*. 32:403–6. doi:10.1042/BST0320403.

Tang, D., D. Wang, Z. Yuan, X. Xue, Y. Zhang, Y. An, J. Chen, M. Tu, Z. Lu, J. Wei, K. Jiang, and Y. Miao. 2013. Persistent activation of pancreatic stellate cells creates a microenvironment favorable for the malignant behavior of pancreatic ductal adenocarcinoma. *Int. J. Cancer*. 132:993–1003. doi:10.1002/ijc.27715.

Than, B.L., J.A. Goos, A.L. Sarver, M.G. O’Sullivan, A. Rod, T.K. Starr, R.J. Fijneman, G.A. Meijer, L. Zhao, Y. Zhang, D.A. Largaespada, P.M. Scott, and R.T. Cormier. 2014. The role of KCNQ1 in mouse and human gastrointestinal cancers. *Oncogene*. 33:3861–8. doi:10.1038/onc.2013.350.

Tsai, F.-C.C., and T. Meyer. 2012. Ca²⁺ pulses control local cycles of lamellipodia retraction and adhesion along the front of migrating cells. *Curr. Biol*. 22:837–42. doi:10.1016/j.cub.2012.03.037.

Tsai FC, Kuo GH, Chang SW, Tsai PJ. Ca²⁺ signaling in cytoskeletal reorganization, cell migration, and cancer metastasis. *Biomed Res Int*. 2015; 2015:409245

Urrego, D., A.P. Tomczak, F. Zahed, W. Stühmer, and L.A. Pardo. 2014. Potassium channels in cell cycle and cell proliferation. *Philos. Trans. R. Soc. Lond., B, Biol. Sci*.

369:20130094. doi:10.1098/rstb.2013.0094.

Vicente-Manzanares, M., C.K. Choi, and A.R. Horwitz. 2009. Integrins in cell migration--the actin connection. *Journal of cell science*. 122:199–206. doi:10.1242/jcs.018564.

Viloria CG, Barros F, Giráldez T, Gómez-Varela D, de la Peña P. Differential effects of amino-terminal distal and proximal domains in the regulation of human erg K(+) channel gating. *Biophys J*. 2000 Jul; 79(1): 231-46.

Vonlaufen, A., S. Joshi, C. Qu, P.A. Phillips, Z. Xu, N.R. Parker, C.S. Toi, R.C. Pirola, J.S. Wilson, D. Goldstein, and M.V. Apte. 2008. Pancreatic stellate cells: partners in crime with pancreatic cancer cells. *Cancer Res*. 68:2085–93. doi:10.1158/0008-5472.CAN-07-2477.

Waddell, N., M. Pajic, A.-M.M. Patch, D.K. Chang, K.S. Kassahn, P. Bailey, A.L. Johns, D. Miller, K. Nones, K. Quek, M.C. Quinn, A.J. Robertson, M.Z. Fadlullah, T.J. Bruxner, A.N. Christ, I. Harliwong, S. Idrisoglu, S. Manning, C. Nourse, E. Nourbakhsh, S. Wani, P.J. Wilson, E. Markham, N. Cloonan, M.J. Anderson, J.L. Fink, O. Holmes, S.H. Kazakoff, C. Leonard, F. Newell, B. Poudel, S. Song, D. Taylor, N. Waddell, S. Wood, Q. Xu, J. Wu, M. Pinese, M.J. Cowley, H.C. Lee, M.D. Jones, A.M. Nagrial, J. Humphris, L.A. Chantrill, V. Chin, A.M. Steinmann, A. Mawson, E.S. Humphrey, E.K. Colvin, A. Chou, C.J. Scarlett, A.V. Pinho, M. Giry-Laterriere, I. Rooman, J.S. Samra, J.G. Kench, J.A. Pettitt, N.D. Merrett, C. Toon, K. Epari, N.Q. Nguyen, A. Barbour, N. Zeps, N.B. Jamieson, J.S. Graham, S.P. Niclou, R. Bjerkgvig, R. Grützmann, D. Aust, R.H. Hruban, A. Maitra, C.A. Iacobuzio-Donahue, C.L. Wolfgang, R.A. Morgan, R.T. Lawlor, V. Corbo, C. Bassi, M. Falconi, G. Zamboni, G. Tortora, M.A. Tempero, A.J. Gill, J.R. Eshleman, C. Pilarsky, A. Scarpa, E.A. Musgrove, J.V. Pearson, A.V. Biankin, and S.M. Grimmond. 2015. Whole genomes redefine the mutational landscape of pancreatic cancer. *Nature*. 518:495–501. doi:10.1038/nature14169.

Wang, R., C.I. Gurguis, W. Gu, E.A. Ko, I. Lim, H. Bang, T. Zhou, and J.-H.H. Ko. 2015. Ion channel gene expression predicts survival in glioma patients. *Sci Rep*. 5:11593. doi:10.1038/srep11593.

Wang, Z., D. Kong, S. Banerjee, Y. Li, N.V. Adsay, J. Abbruzzese, and F.H. Sarkar. 2007. Down-regulation of platelet-derived growth factor-D inhibits cell growth and angiogenesis through inactivation of Notch-1 and nuclear factor-kappaB signaling. *Cancer Res*. 67:11377–85. doi:10.1158/0008-5472.CAN-07-2803.

Watnick RS. The role of the tumor microenvironment in regulating angiogenesis. *Cold Spring Harb Perspect Med*. 2012 Dec 1; 2(12)

Wehr, A.Y., E.E. Furth, V. Sangar, I.A. Blair, and K.H. Yu. 2011. Analysis of the human pancreatic stellate cell secreted proteome. *Pancreas*. 40:557–66. doi:10.1097/MPA.0b013e318214efaf.

Wei, C., X. Wang, M. Chen, K. Ouyang, L.-S.S. Song, and H. Cheng. 2009. Calcium flickers steer cell migration. *Nature*. 457:901–5. doi:10.1038/nature07577.

Wei C, Wang X, Zheng M, Cheng H. Calcium gradients underlying cell migration. *Curr Opin Cell Biol*. 2012 Apr; 24(2): 254-61

Welnhof EA, Zhao L, Cohan CS. Calcium influx alters actin bundle dynamics and retrograde flow in *Helisoma* growth cones. *J Neurosci*. 1999 Sep 15; 19(18): 7971-82.

Whiteside, T.L. 2008. The tumor microenvironment and its role in promoting tumor growth. *Oncogene*. 27:5904–12. doi:10.1038/onc.2008.271.

Wu, J., H. Matthaei, A. Maitra, M. Dal Molin, L.D. Wood, J.R. Eshleman, M. Goggins, M.I. Canto, R.D. Schulick, B.H. Edil, C.L. Wolfgang, A.P. Klein, L.A. Diaz, P.J. Allen, C.M. Schmidt, K.W. Kinzler, N. Papadopoulos, R.H. Hruban, and B. Vogelstein. 2011. Recurrent GNAS mutations define an unexpected pathway for pancreatic cyst development. *Sci Transl Med*. 3:92ra66. doi:10.1126/scitranslmed.3002543.

Xie, C., J. Zhu, X. Chen, L. Mi, N. Nishida, and T.A. Springer. 2010. Structure of an integrin with an alpha domain, complement receptor type 4. *The EMBO journal*. 29:666–79. doi:10.1038/emboj.2009.367.

Xiong, J.P., T. Stehle, B. Diefenbach, R. Zhang, R. Dunker, D.L. Scott, A. Joachimiak, S.L. Goodman, and M.A. Arnaout. 2001. Crystal structure of the extracellular segment of integrin alpha Vbeta3. *Science (New York, N.Y.)*. 294:339–45. doi:10.1126/science.1064535.

Xu, S.-Z.Z., F. Zeng, M. Lei, J. Li, B. Gao, C. Xiong, A. Sivaprasadarao, and D.J. Beech. 2005. Generation of functional ion-channel tools by E3 targeting. *Nat. Biotechnol*. 23:1289–93. doi:10.1038/nbt1148.

Yachida, S., S. Jones, I. Bozic, T. Antal, R. Leary, B. Fu, M. Kamiyama, R.H. Hruban, J.R. Eshleman, M.A. Nowak, V.E. Velculescu, K.W. Kinzler, B. Vogelstein, and C.A. Iacobuzio-Donahue. 2010. Distant metastasis occurs late during the genetic evolution of pancreatic cancer. *Nature*. 467:1114–7. doi:10.1038/nature09515.

Yachida, S., C.M. White, Y. Naito, Y. Zhong, J.A. Brosnan, A.M. Macgregor-Das, R.A. Morgan, T. Saunders, D.A. Laheru, J.M. Herman, R.H. Hruban, A.P. Klein, S. Jones, V. Velculescu, C.L. Wolfgang, and C.A. Iacobuzio-Donahue. 2012. Clinical significance of the genetic landscape of pancreatic cancer and implications for

- identification of potential long-term survivors. *Clin. Cancer Res.* 18:6339–47. doi:10.1158/1078-0432.CCR-12-1215.
- Yang, M., and W.J. Brackenbury. 2013. Membrane potential and cancer progression. *Frontiers in physiology.* 4:185. doi:10.3389/fphys.2013.00185.
- Yuen A, Díaz B. The impact of hypoxia in pancreatic cancer invasion and metastasis. *DOVE.* 2014. Volume 2014:2 Pages 91—106
- Zhou B, Irwanto A, Guo YM, Bei JX, Wu Q, Chen G, Zhang TP, Lei JJ, Feng QS, Chen LZ, Liu J, Zhao YP. Exome sequencing and digital PCR analyses reveal novel mutated genes related to the metastasis of pancreatic ductal adenocarcinoma. *Cancer Biol Ther.* 2012 Aug; 13(10): 871-9.
- Zhang M, Liu J, Tseng GN. Gating charges in the activation and inactivation processes of the HERG channel. *J Gen Physiol.* 2004 Dec; 124(6): 703-18. Epub 2004 Nov 15.
- Zhou, Y., C.-O. Wong, K. Cho, D. van der Hoeven, H. Liang, D. Thakur, J. Luo, M. Babic, K. Zinsmaier, M. Zhu, H. Hu, K. Venkatachalam, and J. Hancock. 2015. Membrane potential modulates plasma membrane phospholipid dynamics and K-Ras signaling. *Science.* 349:873–6. doi:10.1126/science.aaa5619.
- Zhu, J., C.V. Carman, M. Kim, M. Shimaoka, T.A. Springer, and B.-H.H. Luo. 2007. Requirement of alpha and beta subunit transmembrane helix separation for integrin outside-in signaling. *Blood.* 110:2475–83. doi:10.1182/blood-2007-03-080077.
- Zutter, M.M., S.A. Santoro, W.D. Staatz, and Y.L. Tsung. 1995. Re-expression of the alpha 2 beta 1 integrin abrogates the malignant phenotype of breast carcinoma cells. *Proc. Natl. Acad. Sci. U.S.A.* 92:7411–5.